



JACOBS
UNIVERSITY

Antibiotic Permeation through Bacterial Membrane Porins

by

Pratik Raj Singh

A thesis submitted in partial fulfillment
of the requirements for the degree of

**Doctor of Philosophy
in Biochemical Engineering**

Approved Dissertation Committee

Prof. Dr. Mathias Winterhalter

Prof. Dr. Roland Benz

Prof. Dr. Matteo Ceccarelli

Prof. Dr. Ulrich Kleinekathöfer

Date of Defense: 19/09/2014

School of Engineering and Science

To my beloved Mom and Dad

Table of Content

<i>Abstract</i>	<i>vii</i>
<i>Acknowledgements</i>	<i>ix</i>

Chapter 1: General Introduction

1.1 Antibiotic resistance: Global problem.....	2
1.2 Antibiotic resistance mechanisms in bacteria.....	3
1.3 Bacterial cell envelope	5
1.4 Porin	8
1.5 Antibiotic diffusion through porins	14
1.6 Motivation	17
1.7 Scope of my thesis.....	18
1.8 References	20

Chapter 2: Molecular transport across the porin from Gram-positive bacteria: *Nocardia farcinica*

2.1 Pulling Peptides through nanochannels: resolving peptide binding and translocation through the hetero-oligomeric channel from <i>Nocardia farcinica</i>	34
2.2 Transport across the outer membrane porin of mycolic acid containing actinomycetales: <i>Nocardia farcinica</i>	49

Chapter 3: Modulation of antibiotic permeation across OmpF channel in presence of Magnesium

3.1 Antibiotic permeation across the OmpF channel: modulation of the affinity site in the presence of magnesium.....	77
--	----

Chapter 4: Slowing down antibiotic permeation using Ionic Liquids

4.1 Permeation through nanochannels: revealing fast kinetics	88
4.2 Probing the transport of ionic liquids in aqueous solution through nanopores	97
4.3 Combining the effect of temperature and Ionic liquid in antibiotic permeation ..	104

Chapter 5: Antibiotic permeation across the outer membrane porins of *Enterobacter aerogenes*

5.1 Antibiotic permeation across outer membrane porins of *Enterobacter aerogenes* 110

Chapter 6: Summary and future outlook

6.1 Summary of the thesis 131

6.2 *Nocardia farcinica*: Tool for DNA sequencing 132

Abstract

Bacterial cell envelope acts as a first line of defense against various antibacterial compounds. Antibacterial compounds such as antibiotics and antimicrobial peptides need to penetrate the outer membrane barrier of the cell envelope to reach their target site. Hydrophilic antibiotics such as penicillins and carbapenems are known to utilize water-filled protein channels in the outer-membrane to diffuse inside the cell periplasm. Down-regulation in expression of channel proteins and mutations in important amino acid residues of the proteins channels are often induced to limit the permeation of penetrating antibiotics.

This thesis highlights an interdisciplinary approach to comprehend the mechanisms of antibiotics translocation through the bacterial cell envelope. *In vitro* single channel electrophysiology experiments, *in vivo* biological assays and molecular dynamics simulation studies are combined together to obtain an atomistic and molecular detail of antibiotic permeation through the outer membrane protein channels. Antibiotics interaction with the outer-membrane proteins channels from Gram-negative bacteria such as *Escherichia coli* and *Enterobacter aerogenes* and Gram-positive bacteria *Nocardia farcinica* have been characterized in detail.

Here, we present two fascinating aspects that could alter the interaction of antibiotic with the protein channels. First, the biophysical characteristics of membrane proteins play a significant role in determining the translocation of antibiotics. For example, we have shown how the negatively charged *N. farcinica* porin allow the permeation of positively charged antibiotics; however neutralizing the negatively charged residues of the pore showed a depleted interaction of positively charged antibiotics. Second, the external conditions can also drastically change the kinetics of antibiotic interaction with the channel protein. For instance, we have shown that the presence of magnesium ion in the solution can modulate the kinetics of enrofloxacin interaction with the *E. coli* OmpF porin. Similarly, changing the external electrolyte solution from potassium chloride to bulky ionic liquid solution can drastically slow down the kinetics of antibiotic with the channel protein.

Overall, we have explored various aspects involved in understanding the permeation of hydrophilic antibiotics through the outer-membrane protein channels.

Acknowledgements

I would like to thank and acknowledge all the people who have journeyed with me, supported me and motivated me during my PhD period. This rollercoaster ride would not have been possible without you all.

Firstly, I would like to express my sincere gratitude to Prof. Mathias Winterhalter for giving me an opportunity to work as a PhD student in his research group. I am extremely grateful for his continuous guidance and support as well as encouraging ideas and motivations. I am highly indebted to him for helping me develop my career as an independent research scientist (and a bartender).

I would like to thank Prof. Roland Benz for giving me an opportunity to work in his research group. I am very happy to have you as my supervisor, collaborator and my thesis committee member. I am extremely grateful for your advices and suggestions which has been an important aspect for my PhD dissertation.

I would also like to thank Prof. Matteo Ceccarelli for being my external PhD committee member. I am very grateful for your collaboration and assistance with my OmpF-enrofloxacin project.

I would also like to thank Prof. Ulrich Kleinekathöfer for his collaboration in the *Nocardia farcinica* and ionic liquid project and also being in my thesis committee defense.

I am very grateful to Dr. Mahendran Kozhinjampara for being a mentor, supervisor and a friend all along my PhD period. From introducing me to the electrophysiology techniques to helping me write scientific papers, I thank you for all your support during my PhD.

My PhD thesis has been successful because of the opportunity to work and collaborate with different scientific groups. I would like to thank Dr. Niraj Modi for their collaboration in the *Nocardia farcinica* and Ionic liquid project. I would also like to thank Prof. Jean-Marie Pagès and Dr. Muriel Masi for their collaboration with the *Enterobacter aerogenes* project.

I am extremely grateful to all the lab members of the Winterhalter and Benz group. I would like to thank Dr. Ivan Barcena and Harsha Bajaj for helping me in my *Nocardia farcinica* project. I would like to thank Usha Lamichanne for her help and discussions both scientific and non-scientific. I still remember the time when we two were the only students in our research group. Recently our lab has grown in number and is livelier in atmosphere. I would like to thank Eva, Yann, Melinda, Alex, Tatiana, Samaneh, Naresh, Satya, Watcharin, Daniel, Yvonne, Helge, Farhan and Sonalli for all the good times we shared together. And finally, to

all those who have been involved in bilayer measurements, thank you for sharing the frustration with me.

Professional and personal life work hand in hand and I would like to thank all my friends and family for your support and love. I would like to especially thank Nivedita Yumnam for being a significant part of my life. Your love has always given me strength, joy and encouragement. I would like to thank Kanchan and Garima for supporting me like a family from the day I entered Germany up until now. I would like to thank, Sidhant, Richa, Sushil, Sabrina, Rosalba, Martha, Sunil, Abhinandan, Amuz and Anup for all the memorable time, good and the bad, that we encountered together. Time may have separated us apart but I shall always cherish the memories we spent together.

Finally, I would like to thank my family back home for their blessings have helped me become the person I am today. I am grateful to my mom and my brother for their constant love and care and also their support at the darkest of times. I would like to thank my sister Annada, who has been like a friend and an advisor to me throughout my life. I am heavily thankful to my grandparents who have become the cornerstone of my existence. And lastly, I dedicate my thesis in the memory of my dad who I am sure would have been proud of me today.

Chapter 1

General Introduction

We should be taught not to wait for inspiration to start a thing. Action always generates inspiration. Inspiration seldom generates action.
- Frank Tibolt

1.1 Antibiotic resistance: Global problem

“It is time to close the book on infectious diseases, and declare the war against pestilence won”. A famous US surgeon Dr. William H. Stewart made this statement in the 1960s, which was considered the golden age of antibiotics, where major improvements in health care accompanied by newly developed antibiotics drastically reduced the mortality rates of patients suffering from infectious diseases [1]. However, half a century later, the rapid increase in the emergence of multidrug resistance superbugs such as methicillin resistant *Staphylococcus aureus*, multidrug resistant *Mycobacterium tuberculosis*, *Pseudomonas aeruginosa*, and *Acinetobacter baumannii*, has clearly defied the above statement [2–5]. The constant rise of antibiotic resistant bacteria accompanied by the rapid decline in new antibiotic discovery implies the possible apocalyptic post-antibiotic era. In short, “**Antibiotic resistance has become a global problem**”.

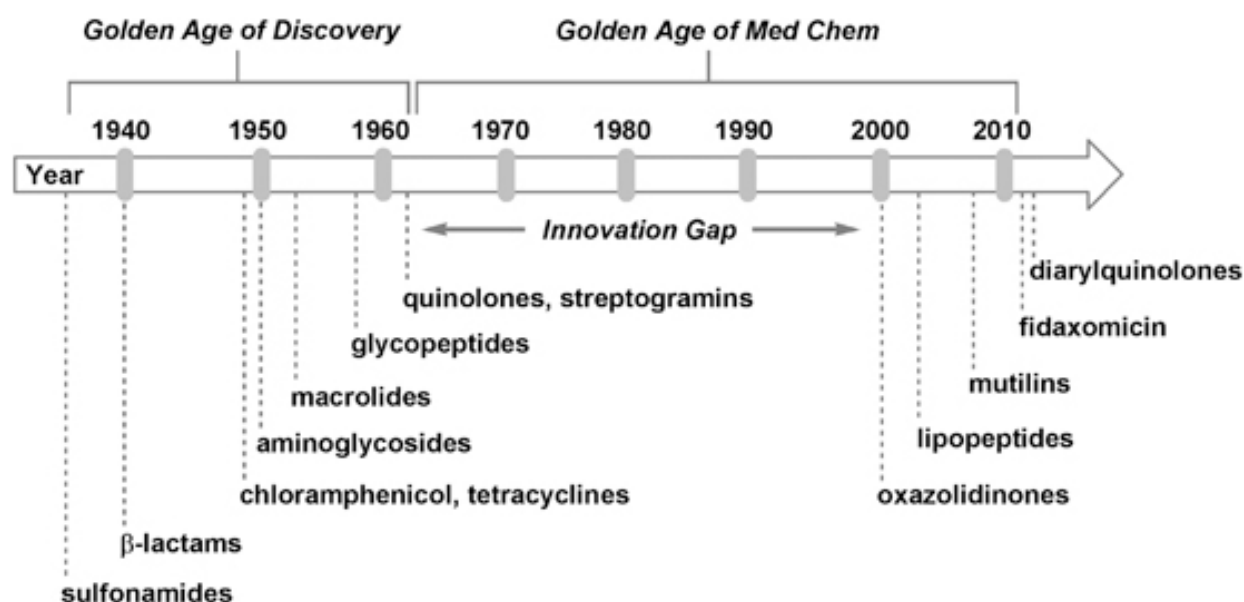


Figure 1: Timeline of antibiotic introduction in the market. (Re-used by permission from Nature publishing group, License number: 3451341158269)

A panacea for infectious diseases started with the discovery of penicillin and sulfa drugs during the 1940s [6]. Antibiotics were considered as a medical miracle saving countless lives all around the world. Soon after, during the 1950s and the 1960s, new researches on antibiotic discovery led to the introduction of new classes of antibiotics in the market, such as aminoglycosides, macrolides and tetracyclines [6,7]. **Figure 1** shows the timeline of antibiotic discovery. However, by the nature of evolution, bacteria have learned to adapt themselves to different antibiotics by numerous resistant mechanisms [7–10]. The emergence of resistant bacteria started mainly in the hospitals, soon after the antibiotics were used to treat infected patients [11]. The sulfonamide and penicillin-resistant *Staphylococcus aureus* and *Neisseria*

gonorrhoeae were the first resistant strains identified in 1940s [12,13], followed by the β -lactamase producing *Haemophilus influenza* in 1970s [14], and the streptomycin resistant *Mycobacterium tuberculosis* [15] and methicillin resistant *Staphylococcus aureus* in 1980s [16,17]. However, multidrug resistant strain was initially only detected in the enteric bacteria such as *E. coli* and *Salmonella* [18–20], which later was found in different other classes of bacteria such as *Pseudomonas aeruginosa*, *Acinetobacter baumannii* and even multidrug resistant *Mycobacterium tuberculosis* [10,19,21]. With the emergence of multidrug resistant bacteria, the need for new antibiotics is greater than ever. Even so, the newly developed antibiotics are rather only modifications of existing antibiotics [22]. Since the 1970s, only two new classes of antibiotics, oxazolidinones and cyclic lipopeptides have been introduced in the market [6,23]. In this everlasting combat between bacteria and antibiotics, the bacteria will always evolve with newer resistance mechanisms. Therefore, the only way possible is to constantly develop new antibiotics.

The advancement of genomics in the 1990s induced new hope in genome based antibiotic discovery [24]. The full genomic sequence of bacteria allowed us to obtain several target genes within the bacteria that were essential for their growth and sustainability. Meanwhile, numerous tools for high throughput technologies were developed that could screen a wide range of synthetic and natural compounds present in the database to obtain prospective compounds that could be the next antibiotic in the pipeline [25]. However, most of the potential compounds that worked wonderfully *in vitro*, were less effective *in vivo*. Using genomics, Glaxo-Smith-Kline spent 7 years identifying more than 300 potential bacterial target sites and performed 70 high throughput screening campaigns for each target site with no fruitful result [24]. New approaches and tools to antibiotic discovery along with understanding the mechanism of bacterial resistance is one of the most important tasks at hand. The various different classes of antibiotics, their target sites and the resistance mechanism of bacteria against different antibiotics are discussed below.

1.2 Antibiotic resistance mechanisms in bacteria

Bacteria have developed resistance mechanisms against different classes of antibiotics based on their target site [26]. Table 1 shows all the different classes of antibiotics developed and the target site of these antibiotics inside the bacteria.

Table 1: Target site of different classes of antibiotics [19]

Antibiotic Class	Target Site
β -lactams (penicillins, cephalosporins, carbapenems, monobactams)	Inhibits cell wall synthesis
Fluoroquinolones	Inhibits DNA synthesis
Aminoglycosides, Tetracyclines	Inhibits protein synthesis
Sulfonamides, trimethoprim	Inhibits folic acid synthesis
Polymyxins	Disrupt cell membrane
Rifampin	Inhibits RNA synthesis

The resistance mechanisms of bacteria are usually genomic, implying that the alterations in the genetic code of bacteria make the susceptible bacteria turn resistant [19,27]. The acquired resistance can be due to genetic mutations or through gene transfer via plasmids and transposons from another resistant bacterial strain [27]. **Figure 2** depicts different mechanisms that the bacteria employ to gain resistance [26]. For instance, some bacteria are able to produce enzymes like β -lactamases and metallo- β -lactamases that degrade the penetrating β -lactam antibiotics such as penicillins, carbapenems and cephalosporins [28,29]. Resistance against antibiotics can be obtained by either altering the antibiotic molecule or altering the antibiotic target site inside the bacteria [30]. For example, resistance against aminoglycosides is usually obtained by altering the structure of the antibiotic molecule by enzymes such as N-acetyltransferases and O-adenyltransferases [31]. Similarly, resistance to fluoroquinolones is obtained by modification of the target sites, DNA Gyrase A and Topoisomerase IV [32]. All these enzymatic reactions are rather specific to a certain class of antibiotics depending on their sites of action.

Another important mechanism favored to gain resistance to almost all the antibiotic classes is by altering the permeation of the antibiotics through the cell membrane [30,33,34]. Previous studies have outlined porins as the major pathway of antibiotic uptake through the outer-membrane of the bacteria [34]. The bacteria are able to either lower the expression of porins or bring mutations in them to limit antibiotic transport [8,35,36]. Similarly, multidrug-efflux pumps such as AcrAB-TolC complex present in the cell envelope are able to actively pump the incoming antibiotics out of the cell making the compound inactive [37,38]. The cell membrane, acting as the first line of defense, plays a major role in reducing the permeation of

antibiotics into the cell. Hence, understanding permeation of antibiotics through the complex cell envelope of the bacteria is not only an interesting topic for research but quiet essential to win the race against antibiotic resistance.

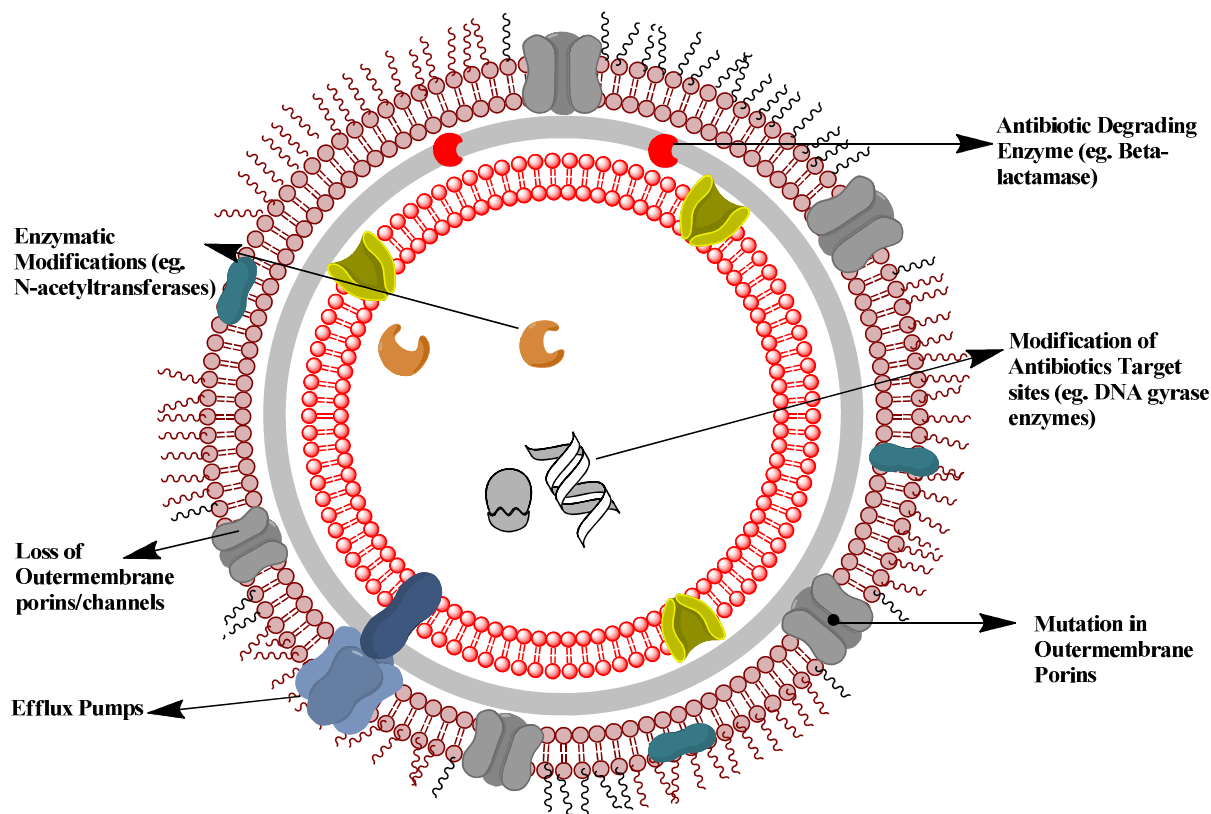


Figure 2: Various mechanisms of antibiotic resistance utilized by bacteria

The major part of my thesis focuses in understanding the molecular details of antibiotics transport through the outer-membrane of the bacterial cell envelope, with particular interest in obtaining the kinetics of antibiotics interaction with the outer-membrane porins. In this chapter, I will begin by describing the complex bacterial cell envelope and introduce different types of porins present in the outer-membrane, followed by literature review on antibiotic transport through the cell membrane.

1.3 Bacterial cell envelope

The cell membrane of bacteria is an intricate multilayered assembly responsible for both structural and functional roles in the cell [39]. The cell membrane acts as a first line of defense protecting the cell against various hostile environments, yet ensuring its survival by selectively allowing a passage of nutrients into the cell cytoplasm [40,41]. The presence of

hydrophobic lipid bilayer and the water-filled outer membrane porins allow the permeation of both hydrophobic and hydrophilic compounds into the cell [42,43]. However, the selectivity factor of permeation is more complicated, and the assembly of cell envelope plays a vital role in regulating selectivity.

The bacterial cells are divided into two major groups according to the structure of their cell envelope: a) Gram-positive bacteria and b) Gram-negative bacteria. The nomenclature of classification comes from a scientist Christian Gram, who devised the method to differentiate bacteria based on a staining technique. The staining technique was based on the differentiated cell envelope of the two class of bacteria mainly staining the peptidoglycan layer [41]. The multilayered structure of the cell envelope of these two bacteria is shown below in **Figure 3**.

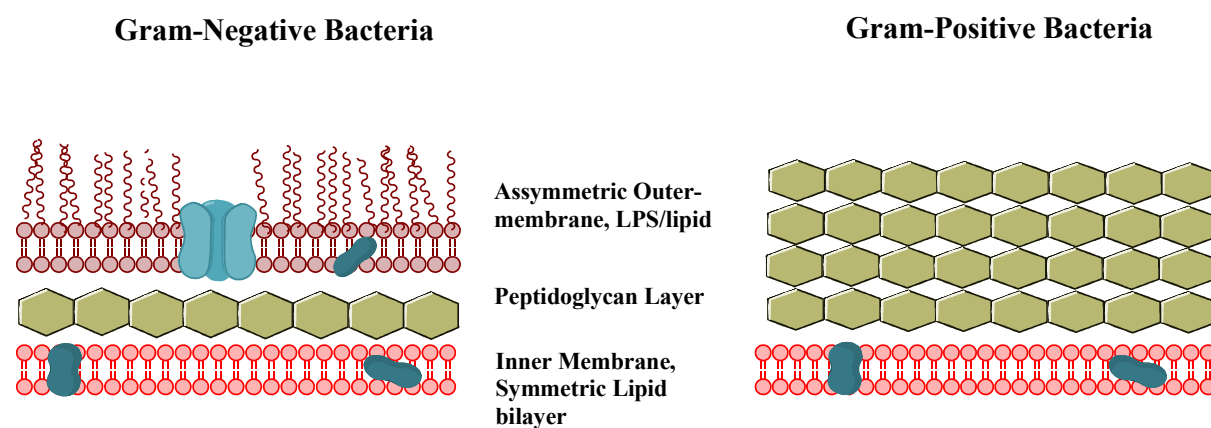


Figure 3: Schematic representation of the cell envelope of Gram-negative and Gram-positive bacteria

The cell envelope of Gram-negative bacteria is a two membrane envelope separated by a thin peptidoglycan layer. The outer-membrane is asymmetric in nature, with the outer-leaflet composed of Lipopolysaccharides (LPS) and the inner leaflet composed of phospholipids, whereas the inner-membrane is symmetric and composed solely of phospholipids [41,43]. The LPS leaflet consists of a hydrophobic glucosamine-based phospholipid (lipid A), negatively charged short core oligosaccharide and long O-antigen polysaccharides [44]. The repulsive force between the negatively charged regions in the two LPS molecules is neutralized by the presence of divalent cations such as Mg^{2+} in the leaflet [45]. The LPS molecules can significantly lower the permeability of lipophilic molecules across the cell envelope and thus protect the cell from hydrophobic antibiotics and detergents [39,46]. The inner leaflet, similar to inner membrane, is composed of 80% phosphatidylethanolamine, 15% phosphatidylglycerol and 5% cardiolipin [40]. The peptidoglycan layer separating the two membranes is a polymer composed of repeating disaccharide N-acetylglucosamine and N-acetylmuramic acid [47]. They provide rigidity to the cell and protect the cell to collapse from

osmotic pressure [41]. The presence of lipids in the cell membrane provides a strong barrier for the permeation of hydrophilic molecules. Thus, cells contain water filled protein channels, called porins, which allow selective permeation of hydrophilic compounds into the cell, which will be discussed later in detail [39].

In contrast, the cell envelope of Gram-positive bacteria is solely composed of a single membrane with a thick peptidoglycan layer facing the cell exterior. Comparatively speaking, the peptidoglycan layer of Gram-positive bacteria is around 30-100 nm in length, significantly larger than the Gram-negative bacteria that contain a peptidoglycan layer of only a few nanometers [41]. The thick peptidoglycan layer is composed of repeating disaccharide units covalently attached to other anionic polymers like teichoic acids and lipoteichoic acids [48]. Overall, the peptidoglycan layer is a mesh-like exoskeleton giving structure to the cell; however, the layer is porous enough to allow diffusion of different hydrophilic metabolites into the plasma membrane [34,49]. Thus, unlike Gram-negative bacteria, Gram-positive bacteria do not require porins for permeation of hydrophilic molecules.

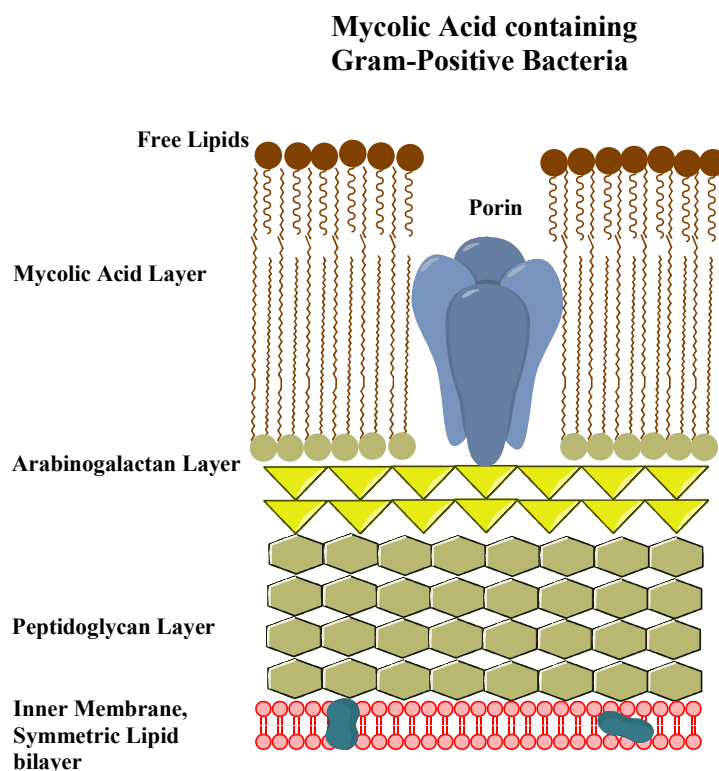


Figure 4: Schematic representation of the cell envelope of mycolic acid containing actinomycetes

Within the Gram-positive bacterial family, lies a specific group of bacteria that contains a rather unique cell envelope. Accordingly, these bacteria are classified as mycolata, or mycolic acid containing actinomycetes [50] (**Figure 4**). Even though the exact organization of the cell envelope is still unclear, the mycolata are known to contain an outer-membrane of mycolic

acid similar in function to that of the outer-membrane of Gram-negative bacteria [51,52]. The cell envelope contains a peptidoglycan layer which is covalently attached to the arabinogalactan layer which is then covalently attached to the mycolic acid layer [53,54]. The mycolic acids are long alkyl chain fatty acids (60-90 in mycobacteria, 40-60 in nocardia and 20-30 in corynebacteria) that can contain various functional groups such as methoxy, keto, epoxy ester groups or cyclopropane rings [52,55–57]. The mycolic acid layer acts as a barrier for the permeation of hydrophilic compounds and thus porins have been identified in the mycolata family of bacteria such as mycobacteria and nocardia [58–61].

1.4 Porins

Porins are water-filled protein channels present in the cell membrane that allow permeation of hydrophilic molecules [39,42]. They are present in the outer-membrane of Gram-negative bacteria, the mycolic acid containing actinomycetes, and even the outer-membrane of cell organelles such as mitochondria and chloroplast [39]. The number of porins in the outer membrane lies in the range of 10^5 porins per cell covering at least $\frac{1}{4}$ of the total surface area, making them one of the most abundant proteins in cells [62]. The structure and functional characteristics of these porins have been widely studied in last 40 years using various techniques. The functional studies of solute transport through porins have been determined using liposome swelling assay and planar lipid bilayer electrophysiology [63–74]. The crystal structure of different porins have been solved using crystallography which illustrates that except for few, most of the porins from Gram-negative bacteria have a beta-barrel motif and are either monomeric or trimeric in nature [75–77]. Similarly, computational studies have been performed extensively to understand the molecular details of ion and substrate transport through the porins [78–82]. The rigid structure, different substrate specificities, varying sizes and possibility of easy modification make porins an ideal candidate to different biological applications. Novel methods of research to study transport across porins have become quite popular since the last decade where porins are used as biological nanopores for biosensing [83]. A short description of different types of porins found in the bacteria is presented below.

1.4.1 Gram-negative bacterial porins

Gram-negative bacterial porins are usually differentiated by their substrate selectivity and are divided into two general classes; *i*) general diffusion porins or non-specific porins and *ii*)

specific porins [39,40,42]. For example, general diffusion porins such as *E. coli* OmpF/OmpC allow permeation of wide range of solute molecules including sugars, ions and amino acids, while specific porins such as *E. coli* LamB/ScrY allow permeation of only maltose and sucrose respectively [64,66,84–87]. The general diffusion porins such as OmpF also allow the permeation of maltose; however the rate of diffusion of maltose through OmpF is highly dependent on the concentration gradient across the membrane. In case of very low concentration (mM ranges) the diffusion of maltose through the OmpF porin is insignificant which is why specific channels such as LamB, that have an affinity site to maltose, are needed for higher rate of permeation [39].

i) General diffusion porins

The *E. coli* general porins, OmpF, OmpC and PhoE are the three most extensively studied porins, and are appropriately termed as “classical porins”. All the three porins allow diffusion of wide range of substrate yet have a selective filter based on charge and size [39,88,89]. The constriction region of OmpF (largest of three porins) is around 0.9 nM and has a molecular weight cut off filter of 600 Da [75,90,91]. OmpF and OmpC are both cation selective channels whereas; PhoE is an anion selective channel [67,92,93]. Interestingly, it has been observed that high salt concentration promotes the over-expression of OmpC compared to OmpF. Studies have shown that the selectivity of OmpF to cation decreases at high salt concentration whereas the selectivity of OmpC to cation is always higher compared to that of OmpF. This could mean that to preserve the selectivity filter, there is an increase in OmpC production [39,94]. Other bacterial species such as *Enterobacter aerogenes*, *Klebsiella pneumoniae*, *Providencia stuartii* and many more also have similar diffusion porins. OmpF/OmpC homologues in each of these species have been identified, such as Omp35/Omp36 in *Enterobacter aerogenes*, OmpK35/OmpK36 in *Klebsiella pneumoniae*, and Ompst1/Ompst2 in *Providencia stuartii* [95–99].

As mentioned earlier, most of the general diffusion porins and its homologues are structurally similar and have a structure based on a beta-barrel motif. The beta-barrel can have strands ranging from 8 beta-strands (OmpA) to 22 beta- strands (BtuB) [100]. However, most of the general diffusion porins have 16 beta-strands and are trimeric or monomeric. The beta barrel is aligned in such a way that the hydrophobic amino acids face outwards into the lipid membrane and the hydrophilic amino acids face inwards into the pore [100]. The *E. coli*

OmpF was one of the first porin whose crystal structure was resolved by Cowan et al. and is shown below in **Figure 5** [75].

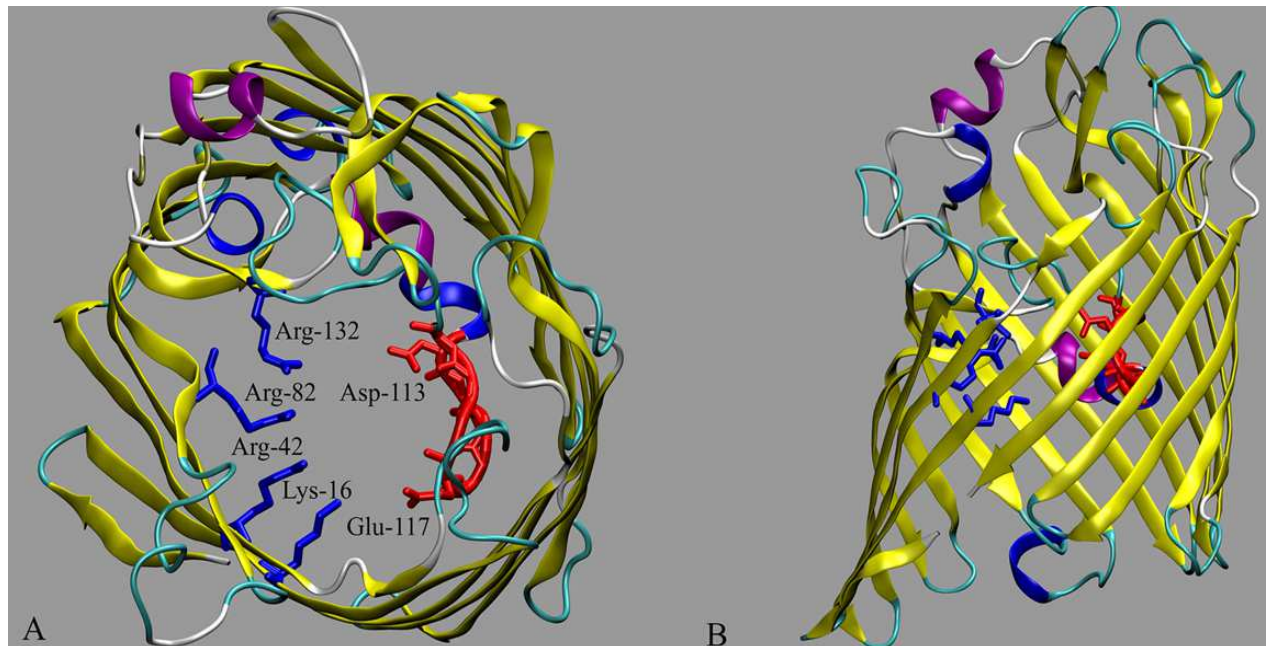


Figure 5: Crystal structure of single monomer of *E. coli* OmpF porin (Re-used by permission from *Frontiers in Bioscience*) [101]

The OmpF channel forms a homotrimer with each monomer consisting of 16 anti-parallel beta strands forming a beta-barrel $7 \times 10 \text{ \AA}$ in diameter. The beta barrel spans the outer membrane with long loops on the extra cellular side and short loops on periplasmic side. Each monomer is stabilized by the internal loop structures whereas the strong hydrophobic interaction between the monomer barrels stabilizes the trimer porins. The loop 2 also plays a major role in trimer stability, as it folds into the adjacent monomer pore and interacts with the loops 2, 3 and 4 of the adjacent monomer. The most significant aspect of the channel is the L3 loop present in the protein, which folds back into the channel forming a constriction zone of around 9 \AA at half the height of the channel giving it an hour glass like shape. This folding of the L3 loops plays an important role by acting as a steric barrier and introducing strong electrostatic interactions inside the pore. The two negatively charged residues D113 and E117 in the L3 loops and cluster of positive charge residues, R42, R82 and R132 in the opposite barrel wall create a strong transverse electric field inside the channel [75,76]. The importance of these residues in the constriction region has been shown in various mutational studies [102,103]. Mutating the D113 residue changes the selectivity of the channel and the rate of sugar transport through the OmpF channel [104,105]. Increased interaction of ampicillin antibiotic has also been observed in D133N mutant compared to the WT OmpF channel [106].

ii) Specific porins

Different types of substrate-specific porins have been identified in *E. coli* and other *Enterobacteriaceae*. The maltose specific LamB [84,85], sucrose specific ScrY [87], nucleotide specific Tsx [107], fatty acid specific FadL [108,109], water specific aquaporin [110], and cyclodextrin specific CymA [111] are some few examples of substrate specific porins. These channels have a strong binding affinity to their respective substrate with the dissociation constant K_D in μM concentrations[39]. The structure of both LamB and ScrY channels are similar to that of OmpF channel, except that both of these are 18 beta-stranded barrels. Structure of LamB channel bound with the maltose sugar is shown below in **Figure 6** [112,113]. Both the channels have loop 3 folding in the center of the pore forming a constriction, however the constriction region of LamB is smaller than OmpF while ScrY has a larger constriction region than that of OmpF. The larger size of the substrate of ScrY channel could be the reason for the larger pore size [39]. Another interesting channel is the CymA from *Klebsiella oxytoca* that allows the permeation of cyclodextrin molecules that have a mass of around 1 kDa. The half saturation constant of cyclodextrins to CymA, has been measured to be around 28 μM by titration experiments [114,115]. However, the crystal structure of the protein is still unknown and it would be really interesting to understand how a porin is able to transport such a huge molecule across the membrane.

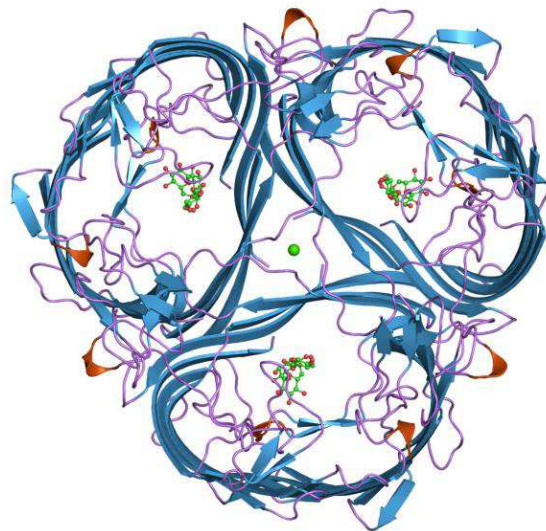


Figure 6: Crystal Structure of *E. coli* LamB with maltose bound in the constriction region (Creative Commons rights, displayed on <http://www.ebi.ac.uk/>)

Apart from *Enterobacteriaceae* species, various other specific channels have been identified in different Gram-negative bacteria. For example, *Pseudomonas aeruginosa* is a multidrug resistance bacterium that is known to have numerous specific channels [63]. Furthermore,

Pseudomonas aeruginosa does not contain any general diffusion porin in their outer-membrane, which is why it has a rather low permeability and high intrinsic resistance. The glucose selective OprB [116], phosphate selective OprO and OprP [117], and amino acid selective OprD [118] are a few examples of substrate specific porins. Electrophysiology measurements on channel conductance have shown that these specific channels are usually very small and mostly remain in a closed conformation [119].

1.4.2 Porins from Gram-positive actinomycetes

The mycolic acid containing actinomycetes (mycobacteria, nocardia, corynebacteria), have a highly complex hydrophobic cell exterior [53,120]. Similar to their Gram-negative counterparts, it was initially expected that these group of bacteria contain porins in their outer-membrane for the transport of hydrophilic solutes. In 1992, Trias and Benz identified the first channel forming protein in the cell wall of mycobacteria [61]. Soon after, porins in the cell wall of *Mycobacterium chelonae* [61], *Mycobacterium smegmatis* [121], *Mycobacterium tuberculosis* [122], *Nocardia farcinica* [59], *Nocardia corynebacterioides* [123], and *Corynebacterium glutamicum* [124], were identified and biophysical characterizations such as conductance, selectivity, voltage dependence were performed. MspA porin from *Mycobacterium smegmatis* is one of the most studied porin in this group of mycolata and the crystal structure of the porin has been determined as shown in **Figure 7** [125]. The structure of the pore is completely different from the usual beta-barrel porins of Gram-negative bacteria.

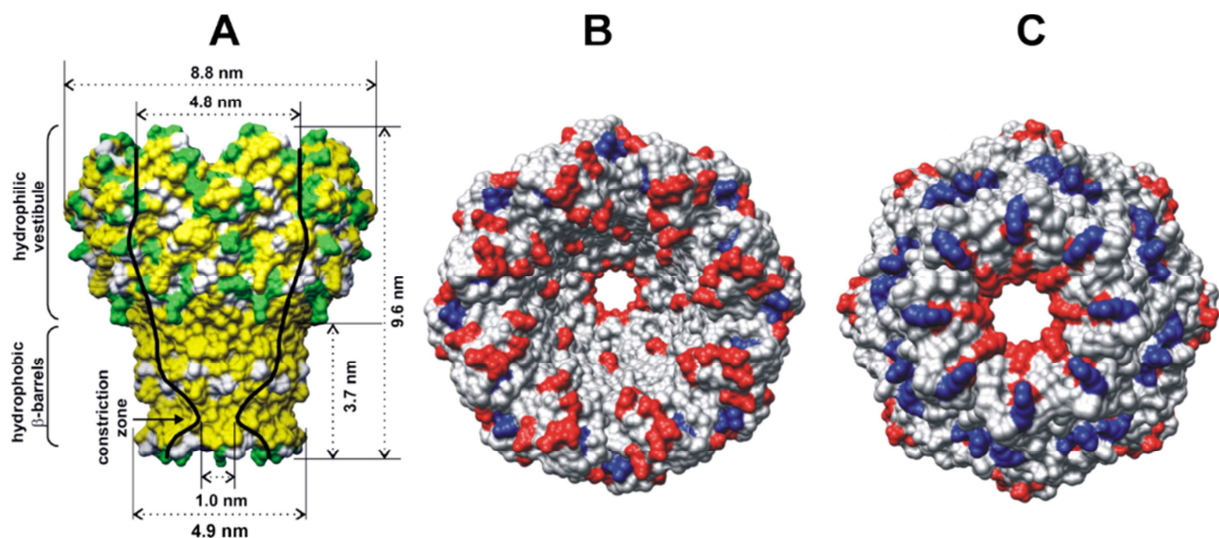


Figure 7: Crystal structure of MspA porin from *Mycobacterium smegmatis* (Creative Commons, Re used with article published in Beilstein Journal of Nanotechnology [126])

The MspA porin is a goblet shaped homo-octameric channel that forms a single functional pore. The MspA channel is 9.6 nm in length and 8.8 nm in width, and contains a hydrophobic domain of 3.7 nm and a hydrophilic vestibule of 5.9 nm. The periplasmic loop, L6 of MspA is longer than the extracellular loops and forms a constriction region of 1 nm in the periplasmic entry. The shorter extracellular loops are present in the vestibular opening forming a 4.8 nm wide pore. The constriction zone of the octameric MspA channel consists of 16 aspartate residues creating a high density of negative charges. Overall, the MspA channel consists of 160 negatively charged amino acids and 64 positively charged amino acids, making the channel highly cation selective [125]. Using liposome swelling assay and mutational studies, MspA has been shown to be the pathway of permeation of various hydrophilic solutes [127–129]. Furthermore, MspA porin is garnering interest as a tool in nanotechnology to perform next generation DNA sequencing [83].

1.4.3 Porins from Chloroplast and Mitochondria

The mitochondria and chloroplast are doubled membrane cell organelles. The exchange of hydrophilic molecules from the cell cytoplasm into the mitochondria and chloroplast is performed using general diffusion porins [130]. Channel forming proteins have been identified in the mitochondria of *Paramecium* [131,132], *Saccharomyces cerevisiae* [133], human [134] and *Neurospora crassa* [135]. However, most of these porins are highly voltage dependent and anion selective (VDAC), such that it remains in closed state at voltages higher than 20-40 mV [130,132]. The structure of mitochondrial VDAC channel is similar to that of OmpF channel, whereby a beta-barrel is formed by 19 odd beta strands [136].

Interestingly, TOM/TIM complex machinery has also been identified in the mitochondrial membrane of different organisms, which is known to contain a pore forming complex [137]. The machinery has been characterized in detail and peptide translocation studies have been performed identifying the machinery to be involved in protein translocation across the membrane [138,139].

Overall, the importance of porins in translocation of various essential hydrophilic compounds such as sugars, amino acids and proteins has been illustrated above. However, porins have also been recognized as the major pathway of antibiotic translocation into the cell. The next section contains some of the past studies highlighting porins as the pathway of antibiotics, and how porin regulation can play a major role in determining bacterial resistance.

1.5 Antibiotic diffusion through porins

Antibiotics need to permeate through the outer-membrane of the cell envelope to reach their target sites. Depending on the antibiotic structure and properties, three major pathways of antibiotic permeation exist (**Figure 8**), *i*) lipid Bilayer, *ii*) water-filled porins and *iii*) self-promoted uptake [33,39,140]. Most of the hydrophobic antibiotics such as macrolides and rifamycin slowly diffuse across the lipid bilayer [40,141], while hydrophilic antibiotics such as β -lactams, fluoroquinolones and chloramphenicols mainly use the general diffusion porins pathway for penetration [66,70–72]. Previous studies have shown that some antibiotics such as aminoglycosides utilize polymyxin B like self-promoted pathway, which is still not properly understood [39,142].

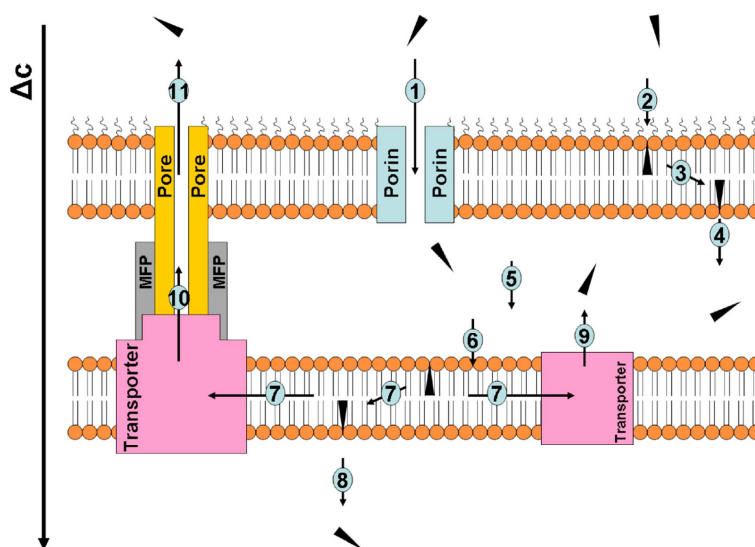


Figure 8: Diffusion mechanisms of different antibiotics through the bacterial cell envelope. Re-used by permission from Bentham Science Publishers, license no: 3434710773130

Porins have been identified to serve as pathways of hydrophilic antibiotics through the cell membrane [8,70]. Translocation of different β -lactam antibiotics such as penicillins and cephalosporins through porins has been demonstrated using liposome swelling assay and antibiotic flux assay [70,143]. These studies indicate that the rate of permeation of zwitterionic antibiotics is accelerated by general diffusion porins as opposed to the anionic antibiotics.

Different *in vivo* studies based on Minimum inhibitory concentration (MIC) assays and antibiotic killing assays have also highlighted porins as the major pathway of antibiotics permeation [144]. Loss of porins OmpF/OmpC in *E. coli* displayed increased resistance of *E. coli* to different cephalosporin and beta-lactams antibiotics [145]. In a study carried out by Pages *et al.*, the outer-membrane porin compositions of different β -lactam resistant clinical

Enterobacter aerogenes strains were studied. It showed that almost half of these highly resistant clinical isolates had little or no porins in their outer membrane [146]. Additionally, studies on *Enterobacter aerogenes* Omp36 porin have shown that a single mutation in the loop 3 region (Glycine > Aspartate) reduced the conductance of the pore and increased cephalosporin resistance [147]. In *Klebsiella pneumoniae*, the loss of OmpK35/36 porins in its outer-membrane demonstrated increased resistance to cephalosporin [98]. Similar studies have been performed on other Gram-negative bacteria; loss of OprD porin in *Pseudomonas aeruginosa* and loss of CarO porin from *Acinetobacter baumannii* increased their resistant to carbapenem antibiotics [148–150]. Knockout mutations of MspA porin from *Mycobacterium smegmatis*, a mycolata, have also shown to increase resistance to various hydrophilic antibiotics [151].

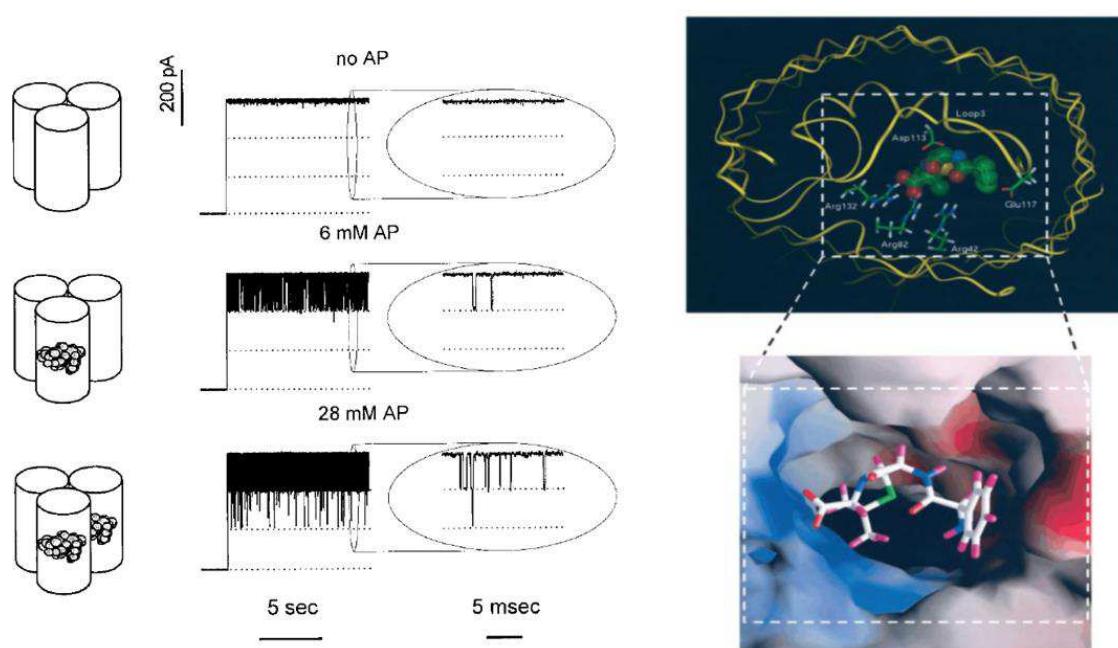


Figure 9: Electrophysiology recordings and Molecular dynamics simulations of ampicillin interaction with *E. coli* OmpF porin [72]. Re-used by permission from PNAS publishing group, Copyright (2002) National Academy of Sciences, U.S.A

Bezrukhov et al. first identified the molecular detail of antibiotic translocation through the porins by combining single channel electrophysiology and molecular dynamic simulation experiments [72]. The translocation of zwitterionic ampicillin antibiotic was studied with *E. coli* OmpF channel, where ampicillin molecules block the ion current through OmpF in transient manner. Computational studies performed on OmpF and ampicillin depict that the molecule at its zwitterionic form has a strong interaction at the constriction region with the negatively charged residues in the loop3 and the positively charged residue in the opposite

barrel. The specific interaction of the ampicillin molecule with the OmpF porin is shown below in **Figure 9**. It was hypothesized that the antibiotic molecule utilizes this affinity site inside to pore to increase the rate of penetration [72].

Similarly, single channel electrophysiology and computational study on antibiotic interaction through the porins have now been carried out with different classes of hydrophilic antibiotics and porins. Electrophysiological studies on OmpF porin with antibiotics from penicillin family- zwitterionic amoxicillin and anionic carbenicillin and piperacillin - further demonstrated the presence of strong interaction between amoxicillin and OmpF, while no such interactions were displayed for anionic antibiotics [152]. These observations were in accordance with the liposome swelling measurements, whereby zwitterionic compounds permeated faster through OmpF [70].

Rate of permeation of carbapenems, cephalosporins and penicillins with the Omp36 porins from *Enterobacter aerogenes* have also been studied using single channel electrophysiology and compared with the *in vivo* antibiotic killing assay [96]. The *Enterobacter* ATCC 13048 strain is known to express only Omp36 as a major diffusion porin in its outer-membrane. *In vivo* studies performed by over-expressing Omp36 porins in the outer-membrane showed an increased sensitivity to ertapenem and cefepime. Combining *in vivo* results with single channel electrophysiology studies, where strong interaction of ertapenem and cefepime with the Omp36 porin was observed, Omp36 was identified as a major pathway for antibiotic uptake.

Mutational studies performed on the different amino acids residues inside the constriction region of the OmpF pore affect the solute permeation and selectivity of the channel. An increased rate of permeation of ampicillin was observed for the D113N OmpF mutant using electrophysiology and liposome swelling assay [106]. Molecular docking of ampicillin in OmpF D113N mutant demonstrated an increased space in the constriction region which enhanced the flux of ampicillin in the D113N mutant. However, in case of R132A OmpF mutant, liposome swelling assay displayed a higher ampicillin flux while electrophysiology displayed reduced or little ampicillin blockage. Computational simulation estimated an increase in the size of the constriction region by a factor of 3 allowing higher diffusion of ampicillin molecule through the R132A mutant. However, due to the increased space complete blocking of ampicillin was not visible using electrophysiology as there was enough space for the ions to pass through even in the presence of ampicillin inside the channel. Therefore, interdisciplinary approaches are necessary to obtain a better understanding of transport processes of antibiotics through porins.

1.6 Motivation

The overuse of antibiotics in hospitals and agriculture farms has created a selective pressure for bacteria to evolve against the antibiotics and gain resistance [7,153]. The ever-growing need of new antibiotics against the rapidly emerging multi-drug resistance bacteria has been highlighted. Yet, various approaches such as genomic, combinatorial chemistry and drug screening to develop “New Drugs for Bad Bugs” have only led to disappointments [24]. Furthermore, the antibiotic discovery and development projects are economically unattractive for big pharmaceutical companies and more and more big companies are closing down their infectious diseases department. The total cost of antibiotic discovery to development calculated in 1991 by Center of Study of Drug Development in Tufts University was estimated around \$231 million, whereas the same study performed in 2000 showed the increase in cost to \$802 million dollar [154]. Another significant factor is the timeline of antibiotic development, which is around 10-14 years from discovery to trial phases until it comes out to the market [155]. The constant inflation in antibiotic discovery, long timeframe from discovery to market and the lower economic return to investment make antibiotic discovery unfavorable and thus, pharmaceutical companies opt out for financially rewarding diseases such as cancer and cardiovascular diseases. However, the social pressure exerted on big pharmaceutical companies on infectious diseases has prevented a complete shutdown of antibiotic discovery. Various collaborations between pharmaceutical companies, governments and research institutes now exist to continue antibiotic development and make it economically favorable.

Traditional methodology in antibiotic discovery has not yielded any results, which is why it is important to approach this problem in a different perspective [10]. Rather than screening different natural and synthetic compounds to obtain the perfect drug, an alternative approach is to first understand how and why the pre-existing drugs are ineffective. Initial studies have already pointed out that one of the major challenge lies in the delivery of the drug into the cell. Therefore, understanding the molecular mechanisms of influx and efflux of drug molecules through the cell membrane can be one way to overcome the problem of antibiotic resistance.

Using electrophysiology measurements, where a single outer-membrane porin is inserted into a planar lipid bilayer, one can measure the ion current passing through the channel. In presence of penetrating antibiotics, a change/fluctuation in the ion current is visible which represents the passage of a single antibiotic through a single porin. Performing statistical

analysis of channel blocking and unblocking, kinetic rates of antibiotic interaction with the channel can be obtained. Combining it with *in vivo* biological assay and molecular dynamics study, we can get a clear idea on various chemical and structural features important for enhancing permeation. However, there are limiting factor to this approach.

Electrophysiology techniques are still relatively new and time resolution of instruments can be considered one of the drawbacks for antibiotic interaction measurements. The time resolution of the current instrument is around 100 μ s when measured at the filter frequency of 10 kHz. Antibiotic permeation events are usually facilitated diffusion processes and if these events are smaller than the resolution of the instrument, we have a higher probability to miss these events. Also, screening of hundreds of antibiotic compounds is still a challenging task and new instrumentation and technology need to be developed. Molecular dynamic simulation has become an important tool to understand the atomistic detail of antibiotic interaction with the channel. However, high computational cost of this technique and the very short time frame (nano-seconds) of the experiment does not allow us to have a complete visualization of antibiotic transport through the porin. Nonetheless, improvements in the technology and methodology are being developed constantly and antibiotic resistance should be dealt giving priority to the problem of “**Translocation**”.

1.7 Scope of my thesis

Biophysical characterization of pores from Gram-negative bacteria such as OmpF, OmpC and its homologues has been studied extensively. However, limited research has been performed with respect to the pores from mycolic acid containing Gram-positive bacteria. Even though these porins act functionally similar, they are structurally distinct. Gram-positive bacterial porin such as MspA are larger and more robust in nature which is why they have been highly favorable for other applications such as biosensing. Understanding and characterizing other porins of similar nature was one of the major motivations to start this project. **Chapter 2** deals with biophysical characterization of porins from mycolic acid containing *Nocardia farcinica*. Sequentially similar to the MspA porin, *N. farcinica* porin is a hetero-oligomeric channel. Channel characterization and solute transport (sugars, peptide and antibiotics) through wild type and mutant *N. farcinica* porin was studied extensively using liposome swelling assay and electrophysiology.

Chapter 3 of my thesis discusses the modulation of antibiotic permeation through the *E. coli* OmpF porin in presence of divalent cations. Single channel electrophysiology experiments were performed to obtain antibiotic rate kinetics and were compared with molecular dynamics

simulation to obtain atomistic details of the variation of antibiotic interaction in presence and absence of magnesium ion.

In **Chapter 4**, we deal with the time resolution problem of the technique. As mentioned earlier, the resolution of the method does not allow us to observe antibiotic interaction faster than 100 μ s. Thus, we either need to develop newer technology and instruments or find a way to slow down the antibiotic interaction for detection. Our work deals with using Ionic Liquids salt solutions as a replacement to commonly used potassium chloride to slow down antibiotic permeation. Molecular dynamics simulation was performed to understand the ion transport of such bulky ionic liquids.

Finally, **Chapter 5** of my thesis comes under the European Union IMI translocation project. This project is a collaborative approach between industries and academic to apprehend the problem of antibiotic resistance with putting perspective on translocation. Major part of my work was to perform single channel electrophysiology measurements and screen the interaction of different classes of antibiotics through the Omp35/36/37 porins from *Enterobacter aerogenes*. *In vitro* results of antibiotic kinetics were later compared with *in vivo* experiments by obtaining antibiotic MIC assays and killing rates of cell with highly expressed outer membrane porins.

1.8 References

- [1] M.L. Cohen, Changing patterns of infectious disease., *Nature*. 406 (2000) 762–7. doi:10.1038/35021206.
- [2] B. Spellberg, R. Guidos, D. Gilbert, J. Bradley, H.W. Boucher, W.M. Scheld, et al., The epidemic of antibiotic-resistant infections: a call to action for the medical community from the Infectious Diseases Society of America., *Clin. Infect. Dis.* 46 (2008) 155–64. doi:10.1086/524891.
- [3] I. Chopra, C. Schofield, M. Everett, A. O’Neill, K. Miller, M. Wilcox, et al., Treatment of health-care-associated infections caused by Gram-negative bacteria: a consensus statement., *Lancet Infect. Dis.* 8 (2008) 133–9. doi:10.1016/S1473-3099(08)70018-5.
- [4] M. Barber, M. Rozwadowska-Dowzenko, INFECTION BY PENICILLIN-RESISTANT STAPHYLOCOCCI, *Lancet*. 252 (1948) 641–644. doi:10.1016/S0140-6736(48)92166-7.
- [5] J. CROFTON, D.A. MITCHISON, Streptomycin resistance in pulmonary tuberculosis., *Br. Med. J.* 2 (1948) 1009–15.
- [6] M.A. Fischbach, C.T. Walsh, Antibiotics for emerging pathogens., *Science*. 325 (2009) 1089–93. doi:10.1126/science.1176667.
- [7] J. Davies, D. Davies, Origins and evolution of antibiotic resistance., *Microbiol. Mol. Biol. Rev.* 74 (2010) 417–33. doi:10.1128/MMBR.00016-10.
- [8] K. Poole, Outer membranes and efflux: the path to multidrug resistance in Gram-negative bacteria., *Curr. Pharm. Biotechnol.* 3 (2002) 77–98.
- [9] B.H. Normark, S. Normark, Evolution and spread of antibiotic resistance., *J. Intern. Med.* 252 (2002) 91–106.
- [10] H. Yoneyama, R. Katsumata, Antibiotic resistance in bacteria and its future for novel antibiotic development., *Biosci. Biotechnol. Biochem.* 70 (2006) 1060–75. doi:10.1271/bbb.70.1060.
- [11] S.B. Levy, The challenge of antibiotic resistance., *Sci. Am.* 278 (1998) 46–53.
- [12] C.H. Rammelkamp, T. Maxon, Resistance of *Staphylococcus aureus* to the Action of Penicillin., *Exp. Biol. Med.* 51 (1942) 386–389. doi:10.3181/00379727-51-13986.
- [13] I. Lind, Epidemiology of antibiotic resistant *Neisseria gonorrhoeae* in industrialized and developing countries., *Scand. J. Infect. Dis. Suppl.* 69 (1990) 77–82.
- [14] J.D. Williams, F. Moosdeen, Antibiotic Resistance in *Haemophilus influenzae*: Epidemiology, Mechanisms, and Therapeutic Possibilities, *Rev. Infect. Dis.* 8 (1986) S555–S561. doi:10.2307/4454013.

- [15] A. Pablos-Méndez, M.C. Raviglione, A. Laszlo, N. Binkin, H.L. Rieder, F. Bustreo, et al., Global Surveillance for Antituberculosis-Drug Resistance, 1994–1997, *N. Engl. J. Med.* 338 (1998) 1641–1649. doi:10.1056/NEJM199806043382301.
- [16] S. Deresinski, Methicillin-resistant *Staphylococcus aureus*: an evolutionary, epidemiologic, and therapeutic odyssey., *Clin. Infect. Dis.* 40 (2005) 562–73. doi:10.1086/427701.
- [17] T.J. Foster, The *Staphylococcus aureus* “superbug”., *J. Clin. Invest.* 114 (2004) 1693–6. doi:10.1172/JCI23825.
- [18] T. WATANABE, Infective heredity of multiple drug resistance in bacteria., *Bacteriol. Rev.* 27 (1963) 87–115.
- [19] S.B. Levy, B. Marshall, Antibacterial resistance worldwide: causes, challenges and responses., *Nat. Med.* 10 (2004) S122–9. doi:10.1038/nm1145.
- [20] M.E. Rupp, P.D. Fey, Extended spectrum beta-lactamase (ESBL)-producing Enterobacteriaceae: considerations for diagnosis, prevention and drug treatment., *Drugs.* 63 (2003) 353–65.
- [21] F.M. Walsh, S.G.B. Amyes, Microbiology and drug resistance mechanisms of fully resistant pathogens., *Curr. Opin. Microbiol.* 7 (2004) 439–44. doi:10.1016/j.mib.2004.08.007.
- [22] D.J. Newman, G.M. Cragg, Natural products as sources of new drugs over the last 25 years., *J. Nat. Prod.* 70 (2007) 461–77. doi:10.1021/np068054v.
- [23] K.J. Simmons, I. Chopra, C.W.G. Fishwick, Structure-based discovery of antibacterial drugs., *Nat. Rev. Microbiol.* 8 (2010) 501–10. doi:10.1038/nrmicro2349.
- [24] D.J. Payne, M.N. Gwynn, D.J. Holmes, D.L. Pompliano, Drugs for bad bugs: confronting the challenges of antibacterial discovery., *Nat. Rev. Drug Discov.* 6 (2007) 29–40. doi:10.1038/nrd2201.
- [25] P.F. Chan, D.J. Holmes, D.J. Payne, Finding the gems using genomic discovery: antibacterial drug discovery strategies – the successes and the challenges, *Drug Discov. Today Ther. Strateg.* 1 (2004) 519–527. doi:10.1016/j.ddstr.2004.11.003.
- [26] A.J. Alanis, Resistance to antibiotics: are we in the post-antibiotic era?, *Arch. Med. Res.* 36 (n.d.) 697–705. doi:10.1016/j.arcmed.2005.06.009.
- [27] A.M. Sefton, Mechanisms of antimicrobial resistance: their clinical relevance in the new millennium., *Drugs.* 62 (2002) 557–66.
- [28] D.M. Livermore, beta-Lactamases in laboratory and clinical resistance., *Clin. Microbiol. Rev.* 8 (1995) 557–84.
- [29] K.S. Thomson, E. Smith Moland, Version 2000: the new beta-lactamases of Gram-negative bacteria at the dawn of the new millennium., *Microbes Infect.* 2 (2000) 1225–35.

- [30] K. Poole, Mechanisms of bacterial biocide and antibiotic resistance, *J. Appl. Microbiol.* 92 (2002) 55S–64S. doi:10.1046/j.1365-2672.92.5s1.8.x.
- [31] G.D. Wright, Aminoglycoside-modifying enzymes., *Curr. Opin. Microbiol.* 2 (1999) 499–503.
- [32] D.C. Hooper, Mechanisms of action and resistance of older and newer fluoroquinolones., *Clin. Infect. Dis.* 31 Suppl 2 (2000) S24–8. doi:10.1086/314056.
- [33] R.E. Hancock, The bacterial outer membrane as a drug barrier., *Trends Microbiol.* 5 (1997) 37–42. doi:10.1016/S0966-842X(97)81773-8.
- [34] H. Nikaido, Prevention of drug access to bacterial targets: permeability barriers and active efflux., *Science.* 264 (1994) 382–8.
- [35] W. Achouak, T. Heulin, J.-M. Pagès, Multiple facets of bacterial porins, *FEMS Microbiol. Lett.* 199 (2001) 1–7. doi:10.1111/j.1574-6968.2001.tb10642.x.
- [36] H.Y. Chen, D.M. Livermore, Activity of cefepime and other beta-lactam antibiotics against permeability mutants of *Escherichia coli* and *Klebsiella pneumoniae*., *J. Antimicrob. Chemother.* 32 Suppl B (1993) 63–74.
- [37] D. Ma, D.N. Cook, M. Alberti, N.G. Pon, H. Nikaido, J.E. Hearst, Molecular cloning and characterization of *acrA* and *acrE* genes of *Escherichia coli*., *J. Bacteriol.* 175 (1993) 6299–313.
- [38] J.A. Fralick, Evidence that TolC is required for functioning of the Mar/AcrAB efflux pump of *Escherichia coli*., *J. Bacteriol.* 178 (1996) 5803–5.
- [39] H. Nikaido, Molecular basis of bacterial outer membrane permeability revisited., *Microbiol. Mol. Biol. Rev.* 67 (2003) 593–656.
- [40] A.H. Delcour, Outer membrane permeability and antibiotic resistance., *Biochim. Biophys. Acta.* 1794 (2009) 808–16. doi:10.1016/j.bbapap.2008.11.005.
- [41] T.J. Silhavy, D. Kahne, S. Walker, The bacterial cell envelope., *Cold Spring Harb. Perspect. Biol.* 2 (2010) a000414. doi:10.1101/cshperspect.a000414.
- [42] A.H. Delcour, Solute uptake through general porins., *Front. Biosci.* 8 (2003) d1055–71.
- [43] E. Haber, ed., *The Cell Membrane*, Springer US, Boston, MA, 1985. doi:10.1007/978-1-4684-1215-4.
- [44] C.R.H. Raetz, C. Whitfield, Lipopolysaccharide endotoxins., *Annu. Rev. Biochem.* 71 (2002) 635–700. doi:10.1146/annurev.biochem.71.110601.135414.
- [45] R.T. Coughlin, S. Tonsager, E.J. McGroarty, Quantitation of metal cations bound to membranes and extracted lipopolysaccharide of *Escherichia coli*, *Biochemistry.* 22 (1983) 2002–2007. doi:10.1021/bi00277a041.

- [46] Y. Kamio, H. Nikaido, Outer membrane of *Salmonella typhimurium*: accessibility of phospholipid head groups to phospholipase C and cyanogen bromide activated dextran in the external medium, *Biochemistry*. 15 (1976) 2561–2570. doi:10.1021/bi00657a012.
- [47] W. Vollmer, Structural variation in the glycan strands of bacterial peptidoglycan., *FEMS Microbiol. Rev.* 32 (2008) 287–306. doi:10.1111/j.1574-6976.2007.00088.x.
- [48] F.C. Neuhaus, J. Baddiley, A continuum of anionic charge: structures and functions of D-alanyl-teichoic acids in gram-positive bacteria., *Microbiol. Mol. Biol. Rev.* 67 (2003) 686–723.
- [49] F.G. Riess, T. Lichtinger, A.F. Yassin, K.P. Schaal, R. Benz, The cell wall porin of the gram-positive bacterium *Nocardia asteroides* forms cation-selective channels that exhibit asymmetric voltage dependence., *Arch. Microbiol.* 171 (1999) 173–82.
- [50] E. STACKEBRANDT, F.A. RAINEY, N.L. WARD-RAINEY, Proposal for a New Hierarchic Classification System, *Actinobacteria classis nov.*, *Int. J. Syst. Bacteriol.* 47 (1997) 479–491. doi:10.1099/00207713-47-2-479.
- [51] M. Goodfellow, M.D. Collins, D.E. Minnikin, Thin-layer chromatographic analysis of mycolic acid and other long-chain components in whole-organism methanolysates of coryneform and related taxa., *J. Gen. Microbiol.* 96 (1976) 351–8.
- [52] J. Liu, C.E. Barry, G.S. Besra, H. Nikaido, Mycolic Acid Structure Determines the Fluidity of the Mycobacterial Cell Wall, *J. Biol. Chem.* 271 (1996) 29545–29551. doi:10.1074/jbc.271.47.29545.
- [53] D.E. Minnikin, Chemical principles in the organization of lipid components in the mycobacterial cell envelope., *Res. Microbiol.* 142 (1991) 423–7.
- [54] D. Chatterjee, C.M. Bozic, M. McNeil, P.J. Brennan, Structural features of the arabinan component of the lipoarabinomannan of *Mycobacterium tuberculosis*., *J. Biol. Chem.* 266 (1991) 9652–60.
- [55] I. Yano, K. Saito, Gas chromatographic and mass spectrometric analysis of molecular species of corynomycolic acids from *Corynebacterium ulcerans*., *FEBS Lett.* 23 (1972) 352–356.
- [56] L. ALSHAMAONY, M. GOODFELLOW, D.E. MINNIKIN, Free Mycolic Acids as Criteria in the Classification of *Nocardia* and the “rhodochrous” Complex, *J. Gen. Microbiol.* 92 (1976) 188–199. doi:10.1099/00221287-92-1-188.
- [57] M. Daffe, P.J. Brennan, M. McNeil, Predominant structural features of the cell wall arabinogalactan of *Mycobacterium tuberculosis* as revealed through characterization of oligoglycosyl alditol fragments by gas chromatography/mass spectrometry and by ¹H and ¹³C NMR analyses., *J. Biol. Chem.* 265 (1990) 6734–43.
- [58] J. Trias, R. Benz, Characterization of the channel formed by the mycobacterial porin in lipid bilayer membranes. Demonstration of voltage gating and of negative point charges at the channel mouth., *J. Biol. Chem.* 268 (1993) 6234–6240.

- [59] F.G. Riess, T. Lichtinger, R. Cseh, A.F. Yassin, K.P. Schaal, R. Benz, The cell wall porin of *Nocardia farcinica*: Biochemical identification of the channel-forming protein and biophysical characterization of the channel properties, *Mol. Microbiol.* 29 (1998) 139–150. doi:10.1046/j.1365-2958.1998.00914.x.
- [60] T. Lichtinger, A. Burkovski, M. Niederweis, R. Krämer, R. Benz, Biochemical and biophysical characterization of the cell wall porin of *Corynebacterium glutamicum*: The channel is formed by a low molecular mass polypeptide, *Biochemistry.* 37 (1998) 15024–15032. doi:10.1021/bi980961e.
- [61] J. Trias, V. Jarlier, R. Benz, Porins in the cell wall of mycobacteria., *Science.* 258 (1992) 1479–1481. doi:10.1126/science.1279810.
- [62] J. Smit, Y. Kamio, H. Nikaido, Outer membrane of *Salmonella typhimurium*: chemical analysis and freeze-fracture studies with lipopolysaccharide mutants., *J. Bacteriol.* 124 (1975) 942–58.
- [63] R. Benz, ed., *Bacterial and Eukaryotic Porins*, Wiley-VCH Verlag GmbH & Co. KGaA, Weinheim, FRG, 2004. doi:10.1002/3527603875.
- [64] H. Nikaido, E.Y. Rosenberg, Effect on solute size on diffusion rates through the transmembrane pores of the outer membrane of *Escherichia coli.*, *J. Gen. Physiol.* 77 (1981) 121–35.
- [65] T. Nakae, Outer membrane of *Salmonella typhimurium*: Reconstitution of sucrose-permeable membrane vesicles, *Biochem. Biophys. Res. Commun.* 64 (1975) 1224–1230. doi:10.1016/0006-291X(75)90823-2.
- [66] H. Nikaido, E.Y. Rosenberg, Porin channels in *Escherichia coli*: studies with liposomes reconstituted from purified proteins., *J. Bacteriol.* 153 (1983) 241–252.
- [67] R. Benz, A. Schmid, R.E. Hancock, Ion selectivity of gram-negative bacterial porins., *J. Bacteriol.* 162 (1985) 722–7.
- [68] R. Benz, K. Janko, P. Läger, Ionic selectivity of pores formed by the matrix protein (porin) of *Escherichia coli.*, *Biochim. Biophys. Acta.* 551 (1979) 238–47.
- [69] R. Benz, K. Janko, W. Boos, P. Läger, Formation of large, ion-permeable membrane channels by the matrix protein (porin) of *Escherichia coli.*, *Biochim. Biophys. Acta.* 511 (1978) 305–19.
- [70] Y. Kobayashi, I. Takahashi, T. Nakae, Diffusion of beta-lactam antibiotics through liposome membranes containing purified porins., *Antimicrob. Agents Chemother.* 22 (1982) 775–80.
- [71] F. Yoshimura, H. Nikaido, Diffusion of beta-lactam antibiotics through the porin channels of *Escherichia coli* K-12., *Antimicrob. Agents Chemother.* 27 (1985) 84–92.
- [72] E.M. Nestorovich, C. Danelon, M. Winterhalter, S.M. Bezrukov, Designed to penetrate: time-resolved interaction of single antibiotic molecules with bacterial pores., *Proc. Natl. Acad. Sci. U. S. A.* 99 (2002) 9789–94. doi:10.1073/pnas.152206799.

- [73] J. Bredin, N. Saint, M. Malléa, E. Dé, G. Molle, J.-M. Pagès, et al., Alteration of pore properties of *Escherichia coli* OmpF induced by mutation of key residues in anti-loop 3 region., *Biochem. J.* 363 (2002) 521–8.
- [74] A. Alcaraz, E.M. Nestorovich, M. Aguilera-Arzo, V.M. Aguilera, S.M. Bezrukov, Salting out the ionic selectivity of a wide channel: the asymmetry of OmpF., *Biophys. J.* 87 (2004) 943–57. doi:10.1529/biophysj.104/043414.
- [75] S.W. Cowan, R.M. Garavito, J.N. Jansonius, J.A. Jenkins, R. Karlsson, N. König, et al., The structure of OmpF porin in a tetragonal crystal form., *Structure.* 3 (1995) 1041–50.
- [76] S.W. Cowan, T. Schirmer, G. Rummel, M. Steiert, R. Ghosh, R.A. Paupit, et al., Crystal structures explain functional properties of two *E. coli* porins., *Nature.* 358 (1992) 727–33. doi:10.1038/358727a0.
- [77] A. Baslé, G. Rummel, P. Storici, J.P. Rosenbusch, T. Schirmer, Crystal structure of osmoporin OmpC from *E. coli* at 2.0 Å., *J. Mol. Biol.* 362 (2006) 933–42. doi:10.1016/j.jmb.2006.08.002.
- [78] P.R. Singh, M. Ceccarelli, M. Lovelle, M. Winterhalter, K.R. Mahendran, Antibiotic permeation across the OmpF channel: modulation of the affinity site in the presence of magnesium., *J. Phys. Chem. B.* 116 (2012) 4433–8. doi:10.1021/jp2123136.
- [79] K.R. Mahendran, E. Hajjar, T. Mach, M. Lovelle, A. Kumar, I. Sousa, et al., Molecular basis of enrofloxacin translocation through OmpF, an outer membrane channel of *Escherichia coli*—when binding does not imply translocation., *J. Phys. Chem. B.* 114 (2010) 5170–9. doi:10.1021/jp911485k.
- [80] E. Hajjar, A. Bessonov, A. Molitor, A. Kumar, K.R. Mahendran, M. Winterhalter, et al., Toward screening for antibiotics with enhanced permeation properties through bacterial porins., *Biochemistry.* 49 (2010) 6928–35. doi:10.1021/bi100845x.
- [81] A. Kumar, E. Hajjar, P. Ruggerone, M. Ceccarelli, Structural and dynamical properties of the porins OmpF and OmpC: insights from molecular simulations., *J. Phys. Condens. Matter.* 22 (2010) 454125. doi:10.1088/0953-8984/22/45/454125.
- [82] W. Im, B. Roux, Ions and counterions in a biological channel: a molecular dynamics simulation of OmpF porin from *Escherichia coli* in an explicit membrane with 1 M KCl aqueous salt solution., *J. Mol. Biol.* 319 (2002) 1177–97. doi:10.1016/S0022-2836(02)00380-7.
- [83] M. Wanunu, Nanopores: A journey towards DNA sequencing., *Phys. Life Rev.* 9 (2012) 125–58. doi:10.1016/j.pprev.2012.05.010.
- [84] R. Benz, A. Schmid, G.H. Vos-Scheperkeuter, Mechanism of sugar transport through the sugar-specific LamB channel of *Escherichia coli* outer membrane., *J. Membr. Biol.* 100 (1987) 21–9.

- [85] C. Andersen, M. Jordy, R. Benz, Evaluation of the rate constants of sugar transport through maltoporin (LamB) of *Escherichia coli* from the sugar-induced current noise., *J. Gen. Physiol.* 105 (1995) 385–401.
- [86] C. Hardesty, C. Ferran, J.M. DiRienzo, Plasmid-mediated sucrose metabolism in *Escherichia coli*: characterization of *scrY*, the structural gene for a phosphoenolpyruvate-dependent sucrose phosphotransferase system outer membrane porin., *J. Bacteriol.* 173 (1991) 449–56.
<http://www.pubmedcentral.nih.gov/articlerender.fcgi?artid=207032&tool=pmcentrez&rendertype=abstract> (accessed July 17, 2014).
- [87] C. Andersen, R. Cseh, K. Schülein, R. Benz, Study of sugar binding to the sucrose-specific ScrY channel of enteric bacteria using current noise analysis., *J. Membr. Biol.* 164 (1998) 263–74.
- [88] G.E. Schulz, Bacterial porins: structure and function, *Curr. Opin. Cell Biol.* 5 (1993) 701–707. doi:10.1016/0955-0674(93)90143-E.
- [89] H. Nikaido, Porins and specific channels of bacterial outer membranes., *Mol. Microbiol.* 6 (1992) 435–42.
- [90] B.K. Jap, P.J. Walian, Biophysics of the structure and function of porins, *Q. Rev. Biophys.* 23 (2009) 367. doi:10.1017/S003358350000559X.
- [91] R. Benz, K. Bauer, Permeation of hydrophilic molecules through the outer membrane of gram-negative bacteria. Review on bacterial porins., *Eur. J. Biochem.* 176 (1988) 1–19.
- [92] Y. KOBAYASHI, T. NAKAE, The mechanism of ion selectivity of OmpF-porin pores of *Escherichia coli*, *Eur. J. Biochem.* 151 (1985) 231–236. doi:10.1111/j.1432-1033.1985.tb09093.x.
- [93] R. Benz, A. Schmid, P. Van der Ley, J. Tommassen, Molecular basis of porin selectivity: membrane experiments with OmpC-PhoE and OmpF-PhoE hybrid proteins of *Escherichia coli* K-12., *Biochim. Biophys. Acta.* 981 (1989) 8–14.
- [94] L.A. Pratt, W. Hsing, K.E. Gibson, T.J. Silhavy, From acids to *osmZ*: multiple factors influence synthesis of the OmpF and OmpC porins in *Escherichia coli*, *Mol. Microbiol.* 20 (1996) 911–917. doi:10.1111/j.1365-2958.1996.tb02532.x.
- [95] Q.-T. Tran, K.R. Mahendran, E. Hajjar, M. Ceccarelli, A. Davin-Regli, M. Winterhalter, et al., Implication of porins in beta-lactam resistance of *Providencia stuartii*., *J. Biol. Chem.* 285 (2010) 32273–81. doi:10.1074/jbc.M110.143305.
- [96] C.E. James, K.R. Mahendran, A. Molitor, J.-M. Bolla, A.N. Bessonov, M. Winterhalter, et al., How beta-lactam antibiotics enter bacteria: a dialogue with the porins., *PLoS One.* 4 (2009) e5453. doi:10.1371/journal.pone.0005453.
- [97] C. Bornet, N. Saint, L. Fetnaci, M. Dupont, A. Davin-Régli, C. Bollet, et al., Omp35, a new *Enterobacter aerogenes* porin involved in selective susceptibility to

- cephalosporins., *Antimicrob. Agents Chemother.* 48 (2004) 2153–8.
doi:10.1128/AAC.48.6.2153-2158.2004.
- [98] A. Doménech-Sánchez, L. Martínez-Martínez, S. Hernández-Allés, M. del Carmen Conejo, A. Pascual, J.M. Tomás, et al., Role of *Klebsiella pneumoniae* OmpK35 porin in antimicrobial resistance., *Antimicrob. Agents Chemother.* 47 (2003) 3332–5.
- [99] S. Albertí, F. Rodríguez-Quñones, T. Schirmer, G. Rummel, J.M. Tomás, J.P. Rosenbusch, et al., A porin from *Klebsiella pneumoniae*: sequence homology, three-dimensional model, and complement binding., *Infect. Immun.* 63 (1995) 903–10.
- [100] L.K. Tamm, H. Hong, B. Liang, Folding and assembly of beta-barrel membrane proteins., *Biochim. Biophys. Acta.* 1666 (2004) 250–263.
doi:10.1016/j.bbamem.2004.06.011.
- [101] M. Ceccarelli, Simulating transport properties through bacterial channels., *Front. Biosci.* 14 (2009) 3222–3238. doi:10.2741/3446.
- [102] S.A. Benson, J.L. Occi, B.A. Sampson, Mutations that alter the pore function of the OmpF porin of *Escherichia coli* K12., *J. Mol. Biol.* 203 (1988) 961–70.
- [103] R. Misra, S.A. Benson, Genetic identification of the pore domain of the OmpC porin of *Escherichia coli* K-12., *J. Bacteriol.* 170 (1988) 3611–7.
- [104] P.S. Phale, A. Philippsen, C. Widmer, V.P. Phale, J.P. Rosenbusch, T. Schirmer, Role of charged residues at the OmpF porin channel constriction probed by mutagenesis and simulation., *Biochemistry.* 40 (2001) 6319–25.
- [105] K.L. Lou, N. Saint, A. Prilipov, G. Rummel, S.A. Benson, J.P. Rosenbusch, et al., Structural and functional characterization of OmpF porin mutants selected for larger pore size. I. Crystallographic analysis., *J. Biol. Chem.* 271 (1996) 20669–75.
- [106] E. Hajjar, K.R. Mahendran, A. Kumar, A. Bessonov, M. Petrescu, H. Weingart, et al., Bridging timescales and length scales: from macroscopic flux to the molecular mechanism of antibiotic diffusion through porins., *Biophys. J.* 98 (2010) 569–75.
doi:10.1016/j.bpj.2009.10.045.
- [107] K. Hantke, Phage T6--colicin K receptor and nucleoside transport in *Escherichia coli*., *FEBS Lett.* 70 (1976) 109–12.
- [108] P.N. Black, C.C. DiRusso, Molecular and biochemical analyses of fatty acid transport, metabolism, and gene regulation in *Escherichia coli*., *Biochim. Biophys. Acta.* 1210 (1994) 123–45. <http://www.ncbi.nlm.nih.gov/pubmed/8280762> (accessed July 17, 2014).
- [109] P.N. Black, Primary sequence of the *Escherichia coli* fadL gene encoding an outer membrane protein required for long-chain fatty acid transport., *J. Bacteriol.* 173 (1991) 435–42.
- [110] G. Calamita, The *Escherichia coli* aquaporin-Z water channel, *Mol. Microbiol.* 37 (2000) 254–262. doi:10.1046/j.1365-2958.2000.02016.x.

- [111] G. Fiedler, M. Pajatsch, A. Böck, Genetics of a novel starch utilisation pathway present in *Klebsiella oxytoca*., *J. Mol. Biol.* 256 (1996) 279–91. doi:10.1006/jmbi.1996.0085.
- [112] T. Schirmer, T.A. Keller, Y.F. Wang, J.P. Rosenbusch, Structural basis for sugar translocation through maltoporin channels at 3.1 Å resolution., *Science*. 267 (1995) 512–4.
- [113] J. Michels, A. Geyer, V. Mocanu, W. Welte, A.L. Burlingame, M. Przybylski, Structure and functional characterization of the periplasmic N-terminal polypeptide domain of the sugar-specific ion channel protein (ScrY porin)., *Protein Sci.* 11 (2002) 1565–74. doi:10.1110/ps.2760102.
- [114] F. Orlik, C. Andersen, C. Danelon, M. Winterhalter, M. Pajatsch, A. Böck, et al., CymA of *Klebsiella oxytoca* outer membrane: binding of cyclodextrins and study of the current noise of the open channel., *Biophys. J.* 85 (2003) 876–85. doi:10.1016/S0006-3495(03)74527-5.
- [115] M. Pajatsch, C. Andersen, A. Mathes, A. Böck, R. Benz, H. Engelhardt, Properties of a cyclodextrin-specific, unusual porin from *Klebsiella oxytoca*., *J. Biol. Chem.* 274 (1999) 25159–66.
- [116] J. Trias, E.Y. Rosenberg, H. Nikaido, Specificity of the glucose channel formed by protein D1 of *Pseudomonas aeruginosa*., *Biochim. Biophys. Acta.* 938 (1988) 493–6.
- [117] R.J. Siehnel, C. Egli, R.E. Hancock, Polyphosphate-selective porin OprO of *Pseudomonas aeruginosa*: expression, purification and sequence., *Mol. Microbiol.* 6 (1992) 2319–26.
- [118] R.E.W. Hancock, F.S.L. Brinkman, Function of pseudomonas porins in uptake and efflux., *Annu. Rev. Microbiol.* 56 (2002) 17–38. doi:10.1146/annurev.micro.56.012302.160310.
- [119] J. Liu, E. Eren, J. Vijayaraghavan, B.R. Cheneke, M. Indic, B. van den Berg, et al., OccK channels from *Pseudomonas aeruginosa* exhibit diverse single-channel electrical signatures but conserved anion selectivity., *Biochemistry.* 51 (2012) 2319–30. doi:10.1021/bi300066w.
- [120] D.E. Minnikin, Chemical principles in the organization of lipid components in the mycobacterial cell envelope, *Res. Microbiol.* 142 (1991) 423–427. doi:http://dx.doi.org/10.1016/0923-2508(91)90114-P.
- [121] J. Trias, R. Benz, Permeability of the cell wall of *Mycobacterium smegmatis*, *Mol. Microbiol.* 14 (1994) 283–290. doi:10.1111/j.1365-2958.1994.tb01289.x.
- [122] B. Kartmann, S. Stenger, M. Niederweis, S. Stengler, Porins in the cell wall of *Mycobacterium tuberculosis*., *J. Bacteriol.* 181 (1999) 6543–6.
- [123] F.G. Riess, R. Benz, Discovery of a novel channel-forming protein in the cell wall of the non-pathogenic *Nocardia corynebacteroides*., *Biochim. Biophys. Acta.* 1509 (2000) 485–95.

- [124] K. Ziegler, R. Benz, G.E. Schulz, A putative alpha-helical porin from *Corynebacterium glutamicum*., *J. Mol. Biol.* 379 (2008) 482–91. doi:10.1016/j.jmb.2008.04.017.
- [125] M. Faller, M. Niederweis, G.E. Schulz, The structure of a mycobacterial outer-membrane channel., *Science*. 303 (2004) 1189–92. doi:10.1126/science.1094114.
- [126] A.S. Perera, H. Wang, T.B. Shrestha, D.L. Troyer, S.H. Bossmann, Nanoscopic surfactant behavior of the porin MspA in aqueous media., *Beilstein J. Nanotechnol.* 4 (2013) 278–84. doi:10.3762/bjnano.4.30.
- [127] J. Stephan, C. Mailaender, G. Etienne, M. Daffé, M. Niederweis, Multidrug resistance of a porin deletion mutant of *Mycobacterium smegmatis*., *Antimicrob. Agents Chemother.* 48 (2004) 4163–4170. doi:10.1128/AAC.48.11.4163-4170.2004.
- [128] M. Niederweis, Mycobacterial porins - New channel proteins in unique outer membranes, *Mol. Microbiol.* 49 (2003) 1167–1177. doi:10.1046/j.1365-2958.2003.03662.x.
- [129] O. Danilchanka, M. Pavlenok, M. Niederweis, Role of porins for uptake of antibiotics by *Mycobacterium smegmatis*., *Antimicrob. Agents Chemother.* 52 (2008) 3127–3134. doi:10.1128/AAC.00239-08.
- [130] R. Benz, Permeation of hydrophilic solutes through mitochondrial outer membranes: review on mitochondrial porins, *Biochim. Biophys. Acta - Rev. Biomembr.* 1197 (1994) 167–196. doi:10.1016/0304-4157(94)90004-3.
- [131] O. Ludwig, R. Benz, J.E. Schultz, Porin of *Paramecium* mitochondria isolation, characterization and ion selectivity of the closed state., *Biochim. Biophys. Acta.* 978 (1989) 319–327. doi:10.1016/0005-2736(89)90131-4.
- [132] S.J. Schein, M. Colombini, A. Finkelstein, Reconstitution in planar lipid bilayers of a voltage-dependent anion-selective channel obtained from *paramecium* mitochondria., *J. Membr. Biol.* 30 (1976) 99–120.
- [133] S. Peng, E. Blachly-Dyson, M. Colombini, M. Forte, Determination of the number of polypeptide subunits in a functional VDAC channel from *Saccharomyces cerevisiae*, *J. Bioenerg. Biomembr.* 24 (1992) 27–31. doi:10.1007/BF00769527.
- [134] E. Blachly-Dyson, A. Baldini, M. Litt, E.R. McCabe, M. Forte, Human genes encoding the voltage-dependent anion channel (VDAC) of the outer mitochondrial membrane: mapping and identification of two new isoforms., *Genomics.* 20 (1994) 62–7. doi:10.1006/geno.1994.1127.
- [135] R. Pfaller, H. Freitag, M.A. Harmey, R. Benz, W. Neupert, A water-soluble form of porin from the mitochondrial outer membrane of *Neurospora crassa*. Properties and relationship to the biosynthetic precursor form., *J. Biol. Chem.* 260 (1985) 8188–8193.
- [136] S. Hiller, J. Abramson, C. Mannella, G. Wagner, K. Zeth, The 3D structures of VDAC represent a native conformation., *Trends Biochem. Sci.* 35 (2010) 514–21. doi:10.1016/j.tibs.2010.03.005.

- [137] N. Pfanner, M. Meijer, Mitochondrial biogenesis: The Tom and Tim machine, *Curr. Biol.* 7 (1997) R100–R103. doi:10.1016/S0960-9822(06)00048-0.
- [138] M. Romero-Ruiz, K.R. Mahendran, R. Eckert, M. Winterhalter, S. Nussberger, Interactions of mitochondrial presequence peptides with the mitochondrial outer membrane preprotein translocase TOM., *Biophys. J.* 99 (2010) 774–81. doi:10.1016/j.bpj.2010.05.010.
- [139] K.R. Mahendran, M. Romero-Ruiz, A. Schlösinger, M. Winterhalter, S. Nussberger, Protein translocation through Tom40: kinetics of peptide release., *Biophys. J.* 102 (2012) 39–47. doi:10.1016/j.bpj.2011.11.4003.
- [140] H. Weingart, M. Petrescu, M. Winterhalter, Biophysical characterization of in- and efflux in Gram-negative bacteria., *Curr. Drug Targets.* 9 (2008) 789–96.
- [141] P. Plésiat, H. Nikaido, Outer membranes of gram-negative bacteria are permeable to steroid probes., *Mol. Microbiol.* 6 (1992) 1323–33.
- [142] R.E. Hancock, P.G. Wong, Compounds which increase the permeability of the *Pseudomonas aeruginosa* outer membrane., *Antimicrob. Agents Chemother.* 26 (1984) 48–52.
- [143] H. Nikaido, E.Y. Rosenberg, J. Foulds, Porin channels in *Escherichia coli*: studies with beta-lactams in intact cells., *J. Bacteriol.* 153 (1983) 232–40.
- [144] H. Nikaido, Outer membrane barrier as a mechanism of antimicrobial resistance., *Antimicrob. Agents Chemother.* 33 (1989) 1831–1836. doi:10.1128/AAC.33.11.1831.
- [145] K.J. Harder, H. Nikaido, M. Matsushashi, Mutants of *Escherichia coli* that are resistant to certain beta-lactam compounds lack the ompF porin., *Antimicrob. Agents Chemother.* 20 (1981) 549–52.
- [146] R.N. Charrel, J.M. Pagès, P. De Micco, M. Mallea, Prevalence of outer membrane porin alteration in beta-lactam-antibiotic-resistant *Enterobacter aerogenes*., *Antimicrob. Agents Chemother.* 40 (1996) 2854–8.
- [147] A. Thiolas, C. Bornet, A. Davin-Régli, J.M. Pagès, C. Bollet, Resistance to imipenem, cefepime, and ceftazidime associated with mutation in Omp36 osmoporin of *Enterobacter aerogenes*, *Biochem. Biophys. Res. Commun.* 317 (2004) 851–856. doi:10.1016/j.bbrc.2004.03.130.
- [148] J. Vila, S. Martí, J. Sánchez-Céspedes, Porins, efflux pumps and multidrug resistance in *Acinetobacter baumannii*., *J. Antimicrob. Chemother.* 59 (2007) 1210–5. doi:10.1093/jac/dkl509.
- [149] J. Trias, H. Nikaido, Outer membrane protein D2 catalyzes facilitated diffusion of carbapenems and penems through the outer membrane of *Pseudomonas aeruginosa*., *Antimicrob. Agents Chemother.* 34 (1990) 52–7.

- [150] J. Trias, J. Dufresne, R.C. Levesque, H. Nikaido, Decreased outer membrane permeability in imipenem-resistant mutants of *Pseudomonas aeruginosa*., *Antimicrob. Agents Chemother.* 33 (1989) 1202–6.
- [151] J. Stephan, C. Mailaender, G. Etienne, M. Daffé, M. Niederweis, Multidrug resistance of a porin deletion mutant of *Mycobacterium smegmatis*., *Antimicrob. Agents Chemother.* 48 (2004) 4163–70. doi:10.1128/AAC.48.11.4163-4170.2004.
- [152] C. Danelon, E.M. Nestorovich, M. Winterhalter, M. Ceccarelli, S.M. Bezrukov, Interaction of zwitterionic penicillins with the OmpF channel facilitates their translocation., *Biophys. J.* 90 (2006) 1617–1627. doi:10.1529/biophysj.105.075192.
- [153] B.H. Normark, S. Normark, Evolution and spread of antibiotic resistance., *J. Intern. Med.* 252 (2002) 91–106.
- [154] J.A. DiMasi, R.W. Hansen, H.G. Grabowski, L. Lasagna, Cost of innovation in the pharmaceutical industry., *J. Health Econ.* 10 (1991) 107–42.
- [155] D.M. Shlaes, R.C. Moellering, The United States Food and Drug Administration and the end of antibiotics., *Clin. Infect. Dis.* 34 (2002) 420–2. doi:10.1086/338976.

Chapter 2

Molecular transport across the porin

from Gram-positive bacteria:

Nocardia farcinica

The porin from the Gram-positive *Nocardia farcinica* channel was first identified and characterized in 1998 by Franziska G. Rieß *et al.* The porin was later described by Klackta *et al.* to be hetero-oligomeric channel consisting of two subunits (*NfpA/NfpB*) and highly similar to that of the homo-octameric MspA channel from *Mycobacteria smegmatis*. We used these studies as a base to obtain detailed structural and functional feature of the porin. For this study, the *NfpA/NfpB* plasmids were obtained from Prof. Roland Benz and was later expressed and purified in *E. coli* BL21 (DE3) Omp8.

The first part of this chapter consists of a published manuscript in ACS Nano. This publication highlights the single channel characterization of the *NfpA/NfpB* *N. farcinica* porin, where the channel conductance, voltage asymmetry and threshold voltage for gating was measured. Homology modelling of the porin with respect to MspA porin was performed to obtain the structural features of the porin. The asymmetric opening of the porins similar to MspA was determined using single channel electrophysiology measurements by asymmetric addition of positive charged peptides to the two sides of the channel. Similarly, the kinetics of peptide interaction with the porin was studied in detail by distinguishing binding events from translocation events.

The second part of the chapter consists of a manuscript which is yet to be submitted. This chapter highlights the biological significance of the pore. The presences of porins in the outer-membrane of the cell envelop is to transport essential hydrophilic nutrients such as amino acids and sugars into the cell. We performed liposome swelling assay by reconstituting *Nocardia farcinica* porin into liposomes and studying the rate of solute (sugars and amino acids) transport. Similar to general diffusion porins OmpF and OmpC of *E. coli*, we see that the rate of permeation is higher of smaller sugars and amino acids compared to larger sugar molecules. Previous studies in Gram-negative bacteria have highlighted porins as the major pathway of permeation of hydrophilic antibiotics. However, little or no studies have been performed on antibiotic interaction through the porins from Gram-positive bacteria. Here, we characterize the interaction of different antibiotics with the *N. farcinica* porin using single channel ion-current analysis. Mutational studies on *N. farcinica* porin was also performed to highlight the importance of charge residues inside the channel. The changes in the kinetics rates of antibiotic interaction with the wild-type and mutant porin was studied and analyzed.

Chapter 2.1

Reprinted with permission from American Chemical Society

Singh, P. R., Bárcena-Uribarri, I., Modi, N., Kleinekathöfer, U., Benz, R., Winterhalter, M., & Mahendran, K. R. (2012). Pulling peptides across nanochannels: resolving peptide binding and translocation through the hetero-oligomeric channel from Nocardia farcinica. ACS Nano, 6(12), 10699–707. doi:10.1021/nn303900y

Copyright © 2012, American Chemical Society

Individual Contribution:

Protein expression and purification, Single channel measurements and analysis, Ion selectivity, Composition of manuscript

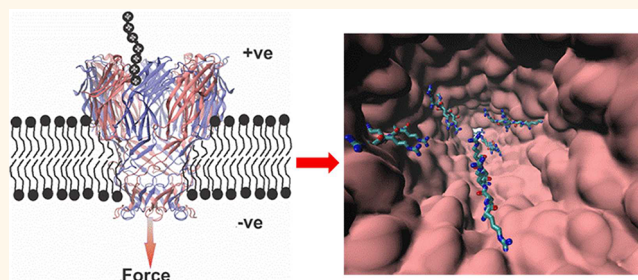
Pulling Peptides across Nanochannels: Resolving Peptide Binding and Translocation through the Hetero-oligomeric Channel from *Nocardia farcinica*

Pratik Raj Singh, Iván Bárcena-Uribarri, Niraj Modi, Ulrich Kleinekathöfer, Roland Benz, Mathias Winterhalter,* and Kozhinjampara R Mahendran*

Jacobs University Bremen, Campus Ring 1, D-28759 Bremen, Germany

ABSTRACT We investigated translocation of cationic peptides through nanochannels derived from the Gram-positive bacterium *Nocardia farcinica* at the single-molecule level. The two subunits NfpA and NfpB form a hetero-oligomeric cation selective channel. On the basis of amino acid comparison we performed homology modeling and obtained a channel structurally related to MspA of *Mycobacterium smegmatis*. The quantitative single-molecule measurements provide an insight into transport processes of solutes through nanochannels. High-resolution ion conductance measurements

in the presence of peptides of different charge and length revealed the kinetics of peptide binding. The observed asymmetry in peptide binding kinetics indicated a unidirectional channel insertion in the lipid bilayer. In the case of cationic peptides, the external voltage acts as a driving force that promotes the interaction of the peptide with the channel surface. At low voltage, the peptide just binds to the channel, whereas at higher voltage, the force is strong enough to pull the peptide across the channel. This allows distinguishing quantitatively between peptide binding and translocation through the channel.



KEYWORDS: *Nocardia* · cationic peptides · applied voltage · binding kinetics · affinity

Bacterial cells continuously need to exchange small molecules, nutrients, and proteins with the exterior environment, simultaneously keeping toxic substances out. Selective transport of molecules through the cell wall is a fundamental process in bacterial life. Many of these processes involve channels made by aggregation of peptides, membrane proteins, or receptors.^{1–6} For example, the cell walls of Gram-positive bacteria contain a thick peptidoglycan layer, which allows the permeation of hydrophilic substances up to a molecular mass of 100 kDa.⁷ From this follows that unlike Gram-negative bacteria, Gram-positive bacteria do not require pore-forming proteins in their cell wall to transport hydrophilic molecules.^{5,7} However, among this group of bacteria, a subgroup

belonging to the order actinomycetales contains an even thicker cell wall with a large amount of lipid covalently linked *via* arabinogalactan to the peptidoglycan layer, termed mycolic acid.⁷ This thick lipid layer is called the mycolic acid layer because of the presence of long-chain mycolic acids. It represents a second permeability barrier besides the cytoplasmic membrane. In recent years, water-filled pores have been identified in the mycolic acid layer of certain bacteria that allow the permeation of hydrophilic molecules into the space between the inner membrane and the mycolic acid layer. A well-studied channel belonging to this class of membrane channels includes MspA, a major porin of *Mycobacterium smegmatis*, mediating the exchange of hydrophilic solutes across the outer membrane.^{7–9}

* Address correspondence to
k.mahendran@jacobs-university.de,
m.winterhalter@jacobs-university.de.

Received for review August 25, 2012
and accepted November 2, 2012.

Published online November 02, 2012
10.1021/nn303900y

© 2012 American Chemical Society

This porin has an octameric goblet-like conformation. The constriction zone of the octameric MspA channel consists of 16 aspartate residues (D90/D91) creating a high density of negative charges, which likely explains the high cation selectivity of this porin.⁸ Similar to *M. smegmatis*, the cell wall of the Gram-positive bacterium *Nocardia farcinica* contains also a cation-selective channel composed of two subunits, *N. farcinica* porin A (NfpA) and *N. farcinica* porin B (NfpB), that form together a channel in artificial lipid bilayers.^{10–12} The *N. farcinica* channel (NfpA–NfpB) is a hetero-oligomer and structurally related to MspA of *M. smegmatis* based on amino acid comparison. The amino acid sequence alignment suggests an overall amino acid sequence identity of 11% between NfpA, NfpB, and MspA, whereas the identity between NfpA and NfpB is about 52%.^{10–12}

The complexity of biological systems makes it important to study specific functions of membrane proteins *in vitro*. Techniques such as electrophysiology, computer simulations, and X-ray crystallography are used to investigate the translocation pathways of antibiotics, nutrients, genetic material (DNA), polyelectrolytes, and peptides across protein channels.^{13–19} The purification from the native membrane and reconstitution of the purified protein into an artificial biomimetic membrane is the primary method by which the characterization of membrane proteins can be studied isolated from other components.²⁰ To obtain initial information on the function of membrane channels, the method of choice is to record the ion currents across the channel.^{13,14,17} The underlying measuring principle is the huge difference in ion conductance between the insulating lipid membrane and ion conducting channel, allowing readily a first characterization of single channels with respect to pore size or ion selectivity.^{2,16,17,22} Porins reconstituted into liposomes and planar lipid bilayers were recently used for measurements of substrate translocation.^{20–22} As the energy barriers for influx of several substrates are asymmetric with channel orientation, it becomes interesting to investigate the orientation of reconstituted porins relative to their directionality *in vivo*.^{22,23}

The interaction of polypeptides with transmembrane protein pores is of fundamental importance in biology.²⁴ Today most studies on the mechanism of protein and peptide translocation across lipid membranes used the ion channels alpha-hemolysin and aerolysin reconstituted into planar lipid bilayers as model translocation systems.^{25–31} Here in this work, we express and purify outer membrane porin subunits from *N. farcinica*, NfpA and NfpB, that form hetero-oligomeric channels when reconstituted into planar lipid bilayers. The single-channel properties such as ion conductance, selectivity, and channel gating were investigated. We analyzed also the interaction pathways of the peptides by reconstituting single porins

into artificial planar lipid bilayers and measuring the binding of peptides by time-resolved ion current blockages. Homology modeling of the *N. farcinica* channel with respect to MspA indicated that the channel is highly asymmetric in shape, and we probed the orientation of the channel in the lipid bilayers by adding peptides asymmetrically to either the cis or the trans side. Furthermore, we have shown that the entry and exit dynamics of charged peptides of different lengths with respect to the pore can be substantially altered by applying an external electric field. Therefore this effect can change the balance between the forces driving polymers into the pore and the forces driving them out.

RESULTS

Homology Modeling. The structural model of the *N. farcinica* channel was built based upon the Modeler suite of programs.^{8,12} Initially, several iterations of the PSI-BLAST protein sequence search program in the PDB database were performed to allow detection of remote homologues of the *N. farcinica* channel. Only the templates with nonredundant structures were kept and further used for building the homology model. These templates included the MspA protein from *M. smegmatis*. The three-dimensional structure of MspA is known (PDB code: 1UUN) and therefore was used as a template to model the *N. farcinica* channel (NfpA–NfpB) structure.⁸ From the modeled structure, it can be concluded that the *N. farcinica* channel forms a highly asymmetrically shaped channel similar to MspA, and in its heterooligomeric architecture, two subunits, NfpA and NfpB, are most likely to be arranged in an alternating fashion (Figure 1). In addition, the channel is cation selective with a cluster of negatively charged amino acids distributed through the channel lining and an electrostatic potential surface indicating a highly negative potential inside the lumen of the channel (Figure 1). Moreover, the periplasmic side (stem) of the channel consists of negatively charged residues clustered like a ring, yielding a high charge density, whereas, in the extracellular side (cap), negatively charged residues are scattered rather randomly along the channel surface.

Structural Asymmetry Causes Asymmetric Transport Properties. To test the structural prediction, single *N. farcinica* channels (NfpA and NfpB) were reconstituted into planar lipid bilayers. The single channel conductance was measured to be 3.0 ± 0.2 nS at 1 M KCl (Figure 2). The channel showed a slight asymmetry of conductance with respect to the polarity of the applied transmembrane potential, supporting the view of an asymmetrical channel reconstituted in lipid bilayers. In addition, the channels showed asymmetric closure with respect to the polarity of the applied voltage. At positive voltages, we observed that the threshold potential for channel closure was around 30 mV, whereas at negative voltage the threshold potential

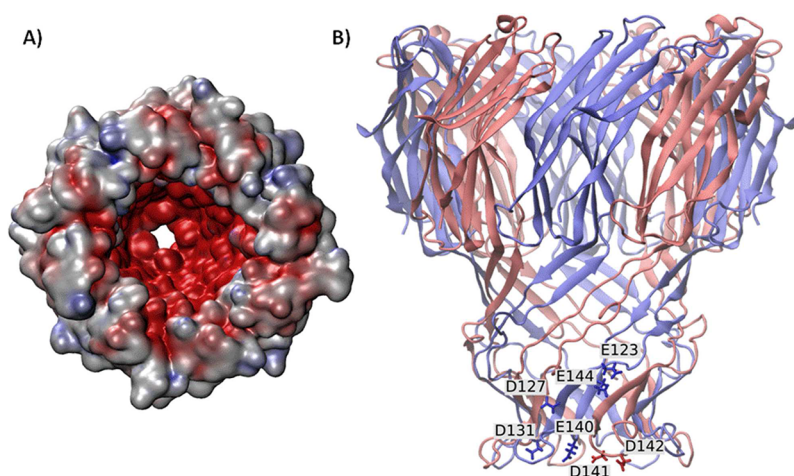


Figure 1. The modeled structure of the *N. farcinica* porin A (NfpA) and *N. farcinica* porin B (NfpB) subunits based on multiple templates of MspA from *M. smegmatis*. Negatively charged amino acid residues are clustered in the channel, resulting in high charge density. (A) Electrostatic potential surface of the modeled structure showing highly negative potential (red color surface) inside the lumen of the channel. (B) Four NfpA and four NfpB subunits are shown in red- and blue-colored secondary structures, respectively, where they are arranged in an alternating fashion. Negatively charged amino acid residues shown as sticks are clustered in the channel stem region, resulting in a high charge density.

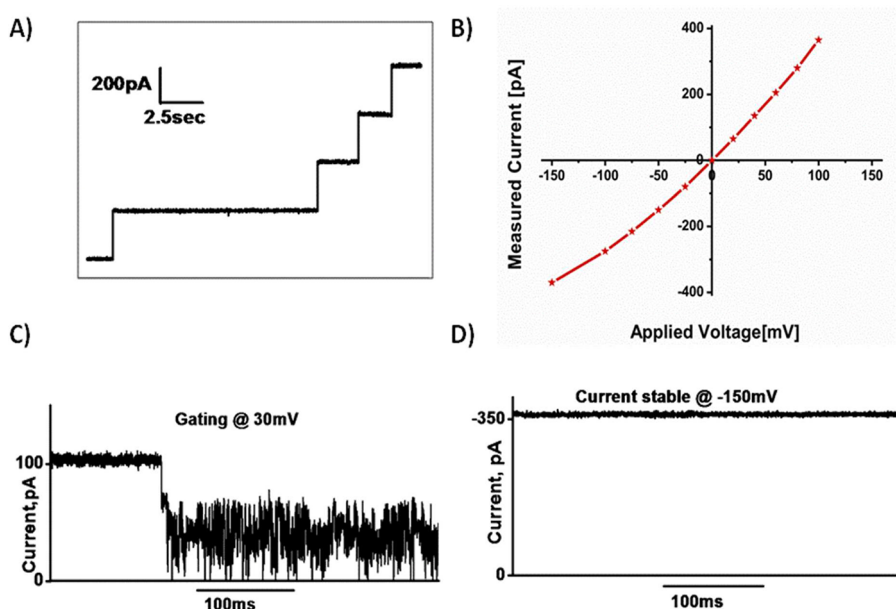


Figure 2. (A) Stepwise insertion of four *N. farcinica* channels reconstituted into planar lipid bilayers at -100 mV. (B) I – V curve of single-channel *N. farcinica* channel. Ionic currents through single *N. farcinica* channel at (C) $+30$ and (D) -150 mV. At 30 mV, the channel fluctuates between open and closed conductance state with random gating, whereas at -150 mV the channel exists in one open state. Experimental conditions are 1 M KCl, 10 mM HEPES, pH 7.4 .

for channel closure was above 200 mV (Figure 2). The mechanism of this voltage-dependent closure of the channel is so far unclear. Moreover, ion selectivity measurements indicated that the channel is cation selective.¹²

Our model (Figure 1) is used for the interpretation of possible binding sites and their effect on the ion current. To elucidate the effect of the asymmetric structure on the transport properties, we characterized the translocation of differently sized polyarginines (tri, penta, and hepta) using ion current fluctuation

analysis. Addition of triarginine to the cis side of the channel hardly induced any ion current blockages, showing negligible interaction of the peptide with the channel surface (Figure 3A). Titrating the channel with penta-arginine caused short, unresolved ion current flickering (Figure 3B). As expected, ion current flickering increased with increasing peptide concentration. Addition of the hepta-arginine causes fluctuations in a concentration- and voltage-dependent manner. However compared to penta-arginine, the number of events is higher (Figure 3C). Under negative potentials

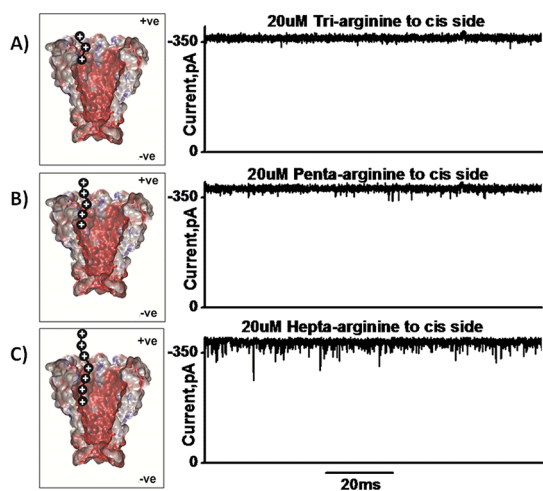


Figure 3. Typical ion current recordings through a single *N. farcinica* channel in the presence of 20 μM (A) triarginine, (B) penta-arginine, and (C) hepta-arginine added to the cis side of the lipid membrane with applied voltage of -150 mV. Experimental conditions are 1 M KCl, 10 mM HEPES, pH 7.4. Corresponding schematic representation showing peptide translocation through the channel driven by applied voltage.

the addition of peptides on the cis side of the chamber increased the number of events, whereas positive voltages had no effect (*i.e.*, created no blockage events). We hypothesize that when peptide enters the channel through the extracellular side, there is enough space for the ions to pass through, which means cis side addition of the peptide does not produce pronounced blocking.

Reversing the external voltage and the side of peptide addition revealed the asymmetry of the channel. Addition of peptides to the trans side induced pronounced blocking of the channel, indicating strong interaction with the channel surface but with reversed voltage dependence: positive voltages induced ion current blockages, whereas at negative voltages no ion current blockages were produced. As mentioned above, the frequency of channel closure (gating) in the absence of the peptide drastically increased at positive voltages. To distinguish between spontaneous and peptide-induced gating of the channel, we selected the time interval that showed only little intrinsic gating. Triarginine (1 μM) added to the trans side of the membrane produced short but visible ion current blockage events (Figure 4A). In contrast, penta-arginine and hepta-arginine strongly interacted with the channel, resulting in ion current blockages in different steps with reduction in the ion conductance (Figure 4B and C). The corresponding amplitude histogram showing the different conductance states is shown in supplementary Figure 1. This indicated that longer peptides have multiple binding sites in the channel. It is important to note that a concentration in the low nanomolar range of these peptides added to the trans side is strong enough to block the channel

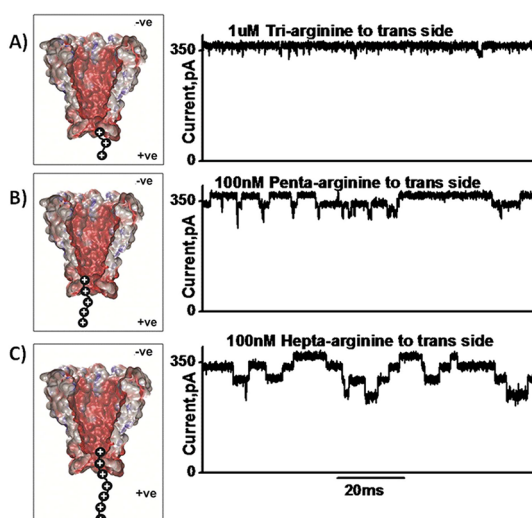


Figure 4. Typical ion current recordings through a single *N. farcinica* channel in the presence of (A) 1 μM triarginine, (B) 100 nM penta-arginine, and (C) 100 nM hepta-arginine added to the trans side of the lipid membrane with applied voltage of $+100$ mV. Experimental conditions are 1 M KCl, 10 mM HEPES, pH 7.4. Corresponding schematic representation showing peptide translocation through the channel driven by applied voltage.

as compared to addition of peptide to the cis side. The strength of the channel–peptide interaction is in the order hepta-arginine > penta-arginine > triarginine. The channel blockades caused by the peptides penta-arginine and hepta-arginine are greater in amplitude and duration than those for a short peptide, triarginine. We hypothesize that in the case of trans side addition of the peptide, the negative charges clustered in rings on the periplasmic entry strongly interact with the peptide and there is only limited space for the ions to pass through. As a result, we observed strong blocking of the channel by the peptide. From the asymmetrical addition of the peptide, we concluded that the channel is oriented in the bilayers with the extracellular part at the cis side and the periplasmic part inserted into lipid bilayers that can easily be accessed from the trans side.

Previously it has been shown that noise analysis of the single-channel level revealed asymmetries in channel transport.^{14,22} Such asymmetries are often hidden in membrane preparations with multiple insertions, in which the channel orientation appeared to be equally distributed. Previous analysis of the ion current fluctuations under asymmetric conditions revealed that the kinetics of sugar entry depends on the side of addition for maltoporin reconstituted into artificial lipid bilayers.²² Moreover, chemical modifications of the sugar allowed only the entry of the sugar on one side but no permeation. This enabled us to distinguish translocation from entry and bouncing back to the same side. It has been shown that maltoporin catalyzes the transport more efficiently from the outside to the inside than under reversed asymmetric conditions.^{14,22,23,34}

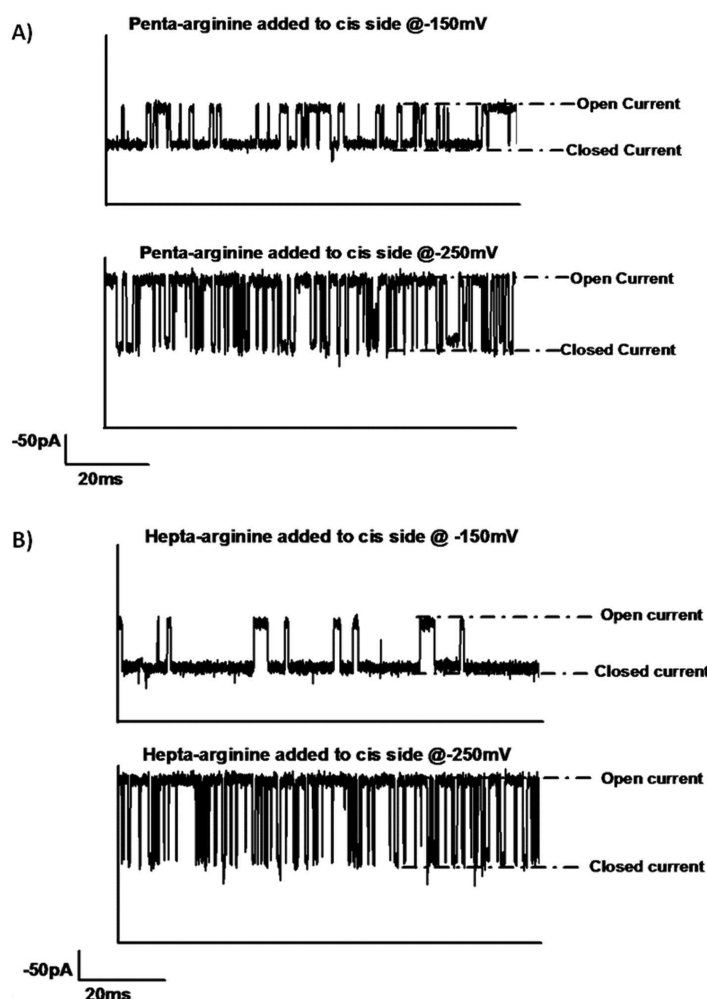


Figure 5. Typical ion current recordings through a single *N. farcinica* channel in the presence of (A) penta-arginine added to the cis side at -150 and -250 mV and (B) hepta-arginine added to the cis side at -150 and -250 mV. The closed current represents the time spent by the peptide in the channel or the residence time of the peptide. Experimental conditions are 150 mM KCl, 10 mM HEPES, pH 7.4.

Here we extended our study toward interaction of peptides with the hetero-oligomeric channel from *N. farcinica*. As shown in Figure 1, the channel consists of an extracellular part of large diameter, whereas the periplasmic side consists of a rather narrow opening. The addition of cationic peptides of different charge and length produced an asymmetry in the peptide binding kinetics that can be used to distinguish the orientation of the channel reconstituted into lipid bilayers.

Resolving Binding and Translocation. To elucidate the electrostatic contributions of peptide interaction with the channel surface, we reduced the salt concentration from 1 M to 150 mM KCl and investigated the peptide binding kinetics by single-channel analysis. Addition of penta-arginine and hepta-arginine to the cis side of the channel produced well-defined ion current blockage events. The channel fluctuated between the fully open conductance state and the closed conductance state (Figure 5). The frequency and duration of the ion current fluctuations depended strongly on the applied

voltage and peptide concentration. The number of peptide blocking events and the average residence time of the peptide blockage increased at low salt concentration, which indicated charge effects on the peptide–channel interaction. The peptide binding kinetics was derived from the two factors τ_c (blockage time) and τ_o (open time or time between successful blockage) fitted with an exponential fit of the open and closed time histogram. We found that the reciprocal of τ_o (the mean interevent interval) is linearly dependent on the polypeptide concentration, whereas τ_c (the mean dwell time) is independent of the polypeptide concentration. The applied voltage serves as the main driving force to pull the cationic peptides from the aqueous bath to the channel surface. We plotted τ_c and τ_o as a function of the applied voltage from -100 mV to -250 mV for the cis side addition of the peptide (Figure 6). The plot of average residence time as a function of the applied voltage allows distinguishing peptide binding from the translocation. The τ_c is higher for hepta-arginine as compared to penta-arginine (supplementary

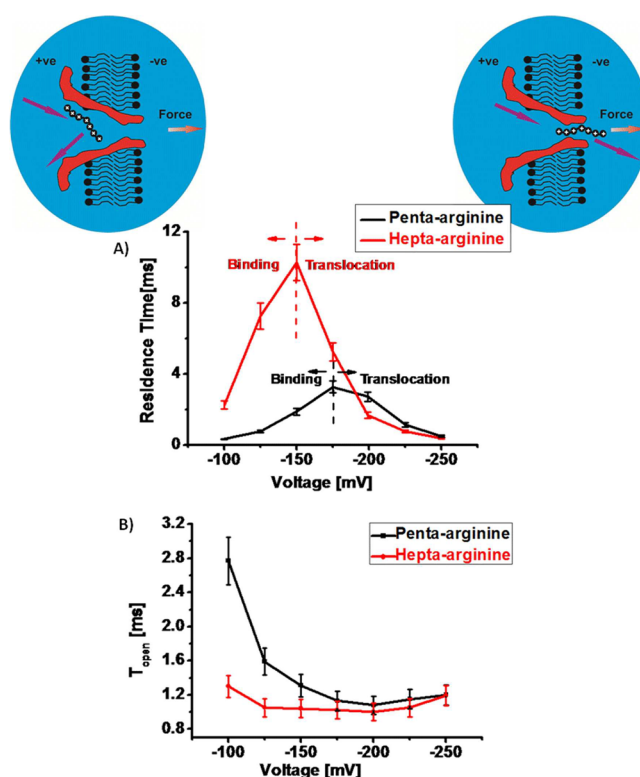


Figure 6. (A) The residence time and (B) the open channel time as a function of the applied voltage (-100 to -250 mV) for penta-arginine and hepta-arginine. Experimental conditions are 150 mM KCl, 10 mM HEPES, pH 7.4. Peptide is added to the cis side of the channel.

TABLE 1. Rate Constants of Peptide Association (k_{on}) and Dissociation (k_{off}) and Equilibrium Binding Constant K of the Interaction between Peptide and *Nocardia farcinica* Channel

penta-arginine				hepta-arginine			
voltage [mV]	k_{on} [$M^{-1} s^{-1}$] $\times 10^9$	k_{off} [s^{-1}] $\times 10^3$	K [M^{-1}] $\times 10^7$	voltage [mV]	k_{on} [$M^{-1} s^{-1}$] $\times 10^9$	k_{off} [s^{-1}] $\times 10^3$	K [M^{-1}] $\times 10^7$
-100	2.5 ± 0.2	2.4 ± 0.24	0.11 ± 0.01	-100	7.7 ± 0.8	0.4 ± 0.04	1.74 ± 0.02
-150	5.8 ± 0.5	0.6 ± 0.05	1.06 ± 0.1	-150	9.6 ± 0.9	0.09 ± 0.01	9.88 ± 0.04
-250	7.6 ± 0.7	1.9 ± 0.20	0.39 ± 0.04	-250	8.4 ± 0.8	2.7 ± 0.3	0.31 ± 0.02

Figure 2). In case of hepta-arginine τ_c increased with increasing voltage from -100 mV to -150 mV, which indicated that hepta-arginine just binds to the channel without effective translocation. Surprisingly, when the voltage was increased above -150 mV, we observed a decrease in the average residence time with increasing voltage, suggesting successful translocation of the peptide through the channel. The threshold potential for pulling hepta-arginine through the channel was calculated to be ~ -150 mV, where force is strong enough to drag the peptide from the binding site of the channel. In the case of penta-arginine, we observed a similar behavior of increase in the residence time at lower voltages and a decrease in residence time at higher voltage. However, the threshold potential for effective translocation to pull the peptide out of the channel was calculated to be ~ -175 mV. The τ_o decreased with increasing concentration of peptide and increasing applied voltage. Addition of the peptide to the trans side completely closed the channel

due to strong binding at low salt concentration caused by charge effects. Subsequently τ_o and τ_c could not be obtained. The results suggested a simple bimolecular interaction between the polypeptide and the pore. The rate constants of association k_{on} can be derived from the slopes of plots of $1/\tau_o$ vs [pept], where [pept] is the peptide concentration in the aqueous phase. The rate constants of dissociation (k_{off}) were determined by averaging the $1/\tau_c$ values recorded over the whole concentration range. The equilibrium association constant was then calculated by using $K = k_{on}/k_{off}$, which gives the affinity of the peptide to the channel. Peptide binding kinetics for penta-arginine and hepta-arginine are summarized in Table 1.

Most approaches investigate the modulation of the ion current through channels in the presence of permeating solutes caused by slight size differences.^{13,17,33} However, the translocation of macromolecules through nanopores is not only determined by the size but to a large extent also influenced by electrostatic,

hydrodynamic, hydrophobic, and van der Waals interactions with the nanopore walls.^{13–19} The quantification of transported uncharged molecules across a few nanometer long channels remains experimentally a challenge. Ensemble measurements on liposomes (liposome swelling) have only a limited time resolution.²⁰ The above-described method of noise analysis of the ion current has a number of unique advantages, among others, the use of very little material with single-molecule resolution, the potential for parallelization, and the relatively good time resolution. However, with respect to the translocation of uncharged molecules, a direct conclusion from binding on transport is not possible.³² In contrast for charged compounds, the applied transmembrane voltage is the driving force to pull the molecule out of the channel.

In particular pulling DNA through nanopores for next-generation sequencing remains a very prominent research area.^{6,19,36} Despite the rapid development of single-molecule techniques, the underlying mechanisms and forces in this molecular transport are poorly characterized and not fully understood. Previously it has been shown that solid-state nanopores and biological nanopores have been used to study the coupling between protein translocation and folding.^{7,24,28–31,33} This allows for detection and analysis in real-time protein translocation events. For example, alpha hemolysin was used to study the partitioning of synthetic cationic alanine-based peptides.^{25–27} The kinetics of association and dissociation rate constants obtained from a single alpha hemolysin channel in the presence

of micromolar concentrations of peptide are strongly dependent on the transmembrane voltage and peptide length.³¹

CONCLUSION

Here in this work, we introduced a new type of channel, a novel hetero-oligomeric nanochannel derived from *N. farcinica*. In the present contribution, we showed an experimental strategy to illuminate various kinetic contributions to polypeptide translocation through the *N. farcinica* channel reconstituted into lipid bilayers. We have been able to measure time-resolved single-molecule events of peptide entry into the pore and obtain detailed kinetic information. Moreover, it has been discussed that *N. farcinica* channels reconstituted into planar lipid bilayers have asymmetric properties in both ion conductance and peptide binding. This asymmetry in the peptide binding reveals that channel insertion is unidirectional. The applied transmembrane voltage acts as a possible driving force for diffusion of cationic macromolecules through the channel. We hypothesize that the binding is enhanced at low voltages and that with increasing applied voltage the peptide is pulled out of the channel, resulting in successful translocation. The kinetic data obtained from our single-channel measurements can be used to distinguish the peptide binding events from the translocation events. In conclusion this work demonstrates that a biological nanopore can represent a versatile single-molecule tool for exploring protein interactions.

METHOD

Purification of Two Subunits of Porins from *Nocardia farcinica*. The purification of the two subunits NfpA and NfpB expressed in *E. coli* BL21 (DE3) Omp8 was performed as described previously.^{12,37} In brief, the genes flanked with 10 histidine residues were cloned into the expression plasmid pARAJ52 containing an arabinose-induced promoter sequence.³⁸ This plasmid had been prepared, and the porin-deficient *E. coli* Omp8 cells containing the plasmid were grown in an LB-ampicillin media at 37 °C until it reached the OD₆₀₀ of 0.5–0.9. The cells were then induced with 0.02% of arabinose for overexpression and were grown at 16 °C for 16 h. The cell broth was centrifuged at 5000g for 10 min at 4 °C, and the pellet was resuspended in 10 mM Tris pH 8. The resuspended pellet was later broken down by French press, and the cell debris was obtained by centrifugation at 5000g for 10 min at 4 °C. The supernatant was ultracentrifuged at 48000g for 1 h at 4 °C to obtain a supernatant containing the cytosolic proteins and the pellet containing membrane proteins. Our proteins of interest were found to be present in both the supernatant and pellet fractions. The protein present in the supernatant fraction was obtained as inclusion bodies that were not large enough to pellet down during ultracentrifugation. The temperature of 16 °C used for cell growth after induction with arabinose facilitated the smaller aggregation of proteins as inclusion bodies. Nevertheless, the His-Tag protein purification from the supernatant fraction had to be performed under denaturing conditions using urea buffer. The purification under denaturing conditions was performed by suspending 1 mL of the supernatant in 4 mL of 8 M urea/10 mM Tris/200 μL

Ni-Sepharose High Performance/20 mM imidazole pH 8 buffer for 6 h at room temperature. The beads were then extensively washed with 8 M urea/10 mM Tris/100 mM imidazole pH 8 to remove impurities. Later the NfpA/NfpB proteins were eluted with the solution containing 8 M urea/10 mM Tris/500 mM imidazole pH 8. The expression and purification of proteins were monitored by SDS page and Western blot in every step. The two subunits, purified separately, were refolded together to form a hetero-oligomeric channel by ammonium sulfate precipitation. The two purified subunits were mixed together in a 1:1 ratio and precipitated using saturated ammonium sulfate solution. The solution was incubated overnight and was centrifuged at 18000g for 30 min to remove the supernatant. The precipitated protein pellet was refolded to native state by incubating for 12 h in 10 mM Tris-HCl with 1% Triton X-100 and 150 mM NaCl.¹²

Solvent-Free Lipid Bilayer Technique. Reconstitution experiments and noise analysis have been performed as described in detail previously.^{32,35} The phospholipid bilayer was formed with DPhPC (1,2-diphytanoyl-*sn*-glycero-3-phosphocholine) by employing the classic Montal and Muller technique.³⁵ A Teflon cell with an approximately 50 μm diameter aperture in the 25 μm thick Teflon partition was placed between the two chambers of the cuvette. The aperture was small enough to form a stable bilayer with the possibility of protein insertion. As the electrolyte, 1 M KCl, 10 mM HEPES, pH 7.4 was used and added to both sides of the chamber unless otherwise indicated. Standard silver–silver chloride electrodes from WPI (World Precision Instruments) were placed in each chamber to measure the ion current. For single-channel measurement, small amounts of porin were added to the cis-side of the chamber

(side connected to the ground electrode). Spontaneous channel insertion was usually obtained while stirring under applied voltage. In order to prevent insertion of more than one porin, the cis side of the chamber was carefully diluted with the same buffer to remove the remaining channels. Conductance measurements were performed using an Axopatch 200B amplifier (Axon Instruments) in the voltage clamp mode. Signals were filtered by an on board low pass Bessel filter at 10 kHz and recorded onto a computer hard drive with a sampling frequency of 50 kHz. Amplitude, probability, and noise analyses were performed using Origin (Microcal Software Inc.) and Clampfit (Axon Instruments) software. Single channel analysis was used to determine the peptide binding kinetics. To obtain good statistics for the results, the experiments were repeated five times with different *N. farcinica* channels. We determined the association and dissociation rate constants and the partitioning data from single-channel recordings of the *N. farcinica* channel. In a single-channel measurement the usual measured quantities as illustrated in Figure 6 are the duration of closed levels residence time (τ_c) and open channel time (τ_o), or for short blockages the average residence time (τ_c) and the number of blockage events per second.

Conflict of Interest: The authors declare no competing financial interest.

Acknowledgment. The authors are grateful for financial support through the Deutsche Forschungsgemeinschaft (DFG WI 2278/18-1) and from Jacobs University Bremen.

Supporting Information Available: Amplitude histogram showing fluctuation of the channel between different conductance steps in the presence of penta-arginine and hepta-arginine; dwell time histogram for closed time and open time in the presence of penta-arginine and hepta-arginine; concentration dependence of peptide interaction with the channel; hepta-arginine added to trans side of the chamber at low salt concentration. This information is available free of charge via the Internet at <http://pubs.acs.org>.

REFERENCES AND NOTES

- Benz, R.; Janko, K.; Boos, W.; Lauger, P. Formation of Large, Ion-Permeable Membrane Channels by the Matrix Protein (porin) of *Escherichia coli*. *Biochim. Biophys. Acta* **1978**, *511*, 305–319.
- Mueller, P.; Rudin, D. O. Induced Excitability in Reconstituted Cell Membrane Structure. *J. Theor. Biol.* **1963**, *4*, 268–280.
- Benz, R.; Schmid, A.; Hancock, R. E. Ion Selectivity of Gram-Negative Bacterial Porins. *J. Bacteriol.* **1985**, *162*, 722–727.
- Luckey, M.; Nikaido, H. Diffusion of Solutes Through Channels Produced by Phage Lambda Receptor Protein of *Escherichia coli*: Inhibition by Higher Oligosaccharides of Maltose Series. *Biochem. Biophys. Res. Commun.* **1980**, *93*, 166–171.
- Nikaido, H. Porins and Specific Channels of Bacterial Outer Membranes. *Mol. Microbiol.* **1992**, *6*, 435–442.
- Hall, A. R.; Scott, A.; Rotem, D.; Mehta, K. K.; Bayley, H.; Dekker, C. Hybrid Pore Formation by Directed Insertion of Alpha-Hemolysin into Solid-State Nanopores. *Nat. Nanotechnol.* **2011**, *5*, 874–877.
- Brennan, P. J.; Nikaido, H. The Envelope of Mycobacteria. *Annu. Rev. Biochem.* **1995**, *64*, 29–63.
- Faller, M.; Niederweis, M.; Schulz, G. E. The structure of a Mycobacterial Outer-Membrane Channel. *Science* **2004**, *303*, 1189–1192.
- Stahl, C.; Kubetzko, S.; Kaps, I.; Seeber, S.; Engelhardt, H.; Niederweis, M. MspA Provides the Main Hydrophilic Pathway through the Cell Wall of *Mycobacterium smegmatis*. *Mol. Microbiol.* **2001**, *40*, 451–464.
- Riess, F. G.; Lichtinger, T.; Yassin, A. F.; Schaal, K. P.; Benz, R. The Cell Wall Porin of The Gram-Positive Bacterium *Nocardia asteroides* forms Cation-Selective Channels that Exhibit Asymmetric Voltage Dependence. *Arch. Microbiol.* **1999**, *171*, 173–182.
- Riess, F. G.; Lichtinger, T.; Cseh, R.; Yassin, A. F.; Schaal, K. P.; Benz, R. The Cell Wall Porin of *Nocardia farcinica*: Biochemical Identification of The Channel-Forming Protein and Biophysical Characterization of The Channel Properties. *Mol. Microbiol.* **1998**, *29*, 139–150.
- Klackta, C.; Knorzer, P.; Riess, F.; Benz, R. Hetero-Oligomeric Cell Wall Channels (porins) of *Nocardia farcinica*. *Biochim. Biophys. Acta, Biomembr.* **2011**, *1808*, 1601–1610.
- Bezrukov, S. M.; Vodyanoy, I.; Parsegian, V. A. Counting Polymers Moving Through a Single Ion Channel. *Nature* **1994**, *370*, 279–281.
- Nekolla, S.; Andersen, C.; Benz, R. Noise Analysis of Ion Current Through The Open and The Sugar-Induced Closed State of the LamB Channel of *Escherichia coli* Outer Membrane: Evaluation of the Sugar Binding Kinetics to the Channel Interior. *Biophys. J.* **1994**, *66*, 1388–1397.
- Aksimentiev, A.; Schulten, K. Imaging Alpha-Hemolysin with Molecular Dynamics: Ionic Conductance, Osmotic Permeability, and the Electrostatic Potential Map. *Biophys. J.* **2005**, *88*, 3745–3761.
- Merzlyak, P. G.; Yuldasheva, L. N.; Rodrigues, C. G.; Carneiro, C. M.; Krasilnikov, O. V.; Bezrukov, S. M. Polymeric Nonelectrolytes to Probe Pore Geometry: Application to the Alpha-Toxin Transmembrane Channel. *Biophys. J.* **1999**, *77*, 3023–3033.
- Bezrukov, S. M. Ion Channels as Molecular Coulter Counters to Probe Metabolite Transport. *J. Membr. Biol.* **2000**, *174*, 1–13.
- Wong, C. T.; Muthukumar, M. Polymer Translocation through Alpha-Hemolysin Pore with Tunable Polymer-Pore Electrostatic Interactions. *J. Chem. Phys.* **2010**, *133*, 045101.
- Muthukumar, M. Mechanism of DNA Transport through Pores. *Annu. Rev. Biophys. Biomol. Struct.* **2007**, *36*, 435–450.
- Nikaido, H.; Rosenberg, E. Y. Porin Channels in *Escherichia coli*: Studies with Liposomes Reconstituted from Purified Proteins. *J. Bacteriol.* **1983**, *153*, 241–252.
- Eren, E.; Vijayaraghavan, J.; Liu, J.; Cheneke, B. R.; Touw, D. S.; Lepore, B. W.; Indic, M.; Movileanu, L.; Van den Berg, B. Substrate Specificity within a Family of Outer Membrane Carboxylate Channels. *PLoS Biol.* **2012**, *10*, e1001242.
- Danelon, C.; Brando, T.; Winterhalter, M. Probing the Orientation of Reconstituted Maltoporin Channels at the Single-Protein Level. *J. Biol. Chem.* **2003**, *278*, 35542–35551.
- Kullman, L.; Gurnev, P. A.; Winterhalter, M.; Bezrukov, S. M. Functional Subconformations in Protein Folding: Evidence from Single-Channel Experiments. *Phys. Rev. Lett.* **2006**, *96*, 038101.
- Dobson, C. M. Protein Folding and Misfolding. *Nature* **2003**, *426*, 884–890.
- Mohammad, M. M.; Movileanu, L. Excursion of a Single Polypeptide into a Protein Pore: Simple Physics, but Complicated Biology. *Eur. Biophys. J.* **2008**, *37*, 913–925.
- Movileanu, L.; Schmittschmitt, J. P.; Scholtz, J. M.; Bayley, H. Interactions of Peptides with a Protein Pore. *Biophys. J.* **2005**, *89*, 1030–1045.
- Wolfe, A. J.; Mohammad, M. M.; Cheley, S.; Bayley, H.; Movileanu, L. Catalyzing The Translocation of Polypeptides through Attractive Interactions. *J. Am. Chem. Soc.* **2007**, *129*, 14034–14041.
- Oukhaled, G.; Mathe, J.; Biane, A. L.; Bacari, L.; Betton, J. M.; Lairez, D.; Pelta, J.; Auvray, L. Unfolding of Proteins and Long Transient Conformations Detected by Single Nanopore Recording. *Phys. Rev. Lett.* **2007**, *98*, 158101–158104.
- Pastoriza-Gallego, M.; Rabah, L.; Gibrat, G.; Thiebot, B.; Van der Goot, F. G.; Auvray, L.; Betton, J. M.; Pelta, J. Dynamics of Unfolded Protein Transport through an Aerolysin Pore. *J. Am. Chem. Soc.* **2010**, *133*, 2923–2931.
- Bikwemu, R.; Wolfe, A. J.; Xing, X.; Movileanu, L. Facilitated Translocation of Polypeptides through a Single Nanopore. *J. Phys.: Condens. Matter* **2010**, *22*, 454117.
- Meng, H.; Detillieux, D.; Baran, C.; Krasniqi, B.; Christensen, C.; Madampage, C.; Stefureac, R. I.; Lee, J. S. Nanopore Analysis of Tethered Peptides. *J. Pept. Sci.* **2010**, *16*, 701–708.

32. Mahendran, K.; Hajjar, E.; Mach, T.; Lovelle, M.; Sousa, I.; Kumar, A.; Spiga, E.; Weingart, H.; Gameiro, P.; Winterhalter, M.; *et al.* Molecular Basis of Enrofloxacin Translocation through a Bacterial Porin –When Binding does not Imply Translocation. *J. Phys. Chem. B* **2010**, *114*, 5170–5179.
33. Cressiot, B.; Oukhaled, A.; Patriarche, G.; Pastoriza-Gallego, M.; Betton, J. M.; Auvray, L.; Muthukumar, M.; Bacri, L.; Pelta, J. Protein Transport through a Narrow Solid-State Nanopore at High Voltage: Experiments and Theory. *ACS Nano* **2012**, *6*, 6236–6243.
34. Berezhkovskii, A. M.; Bezrukov, S. M. Optimizing Transport of Metabolites through Large Channels: Molecular Sieves with and without Binding. *Biophys. J.* **2005**, *88*, L17–L19.
35. Montal, M.; Müller, P. Formation of Bimolecular Membranes from Lipid Monolayers and a Study of their Electrical Properties. *Proc. Natl. Acad. Sci. U. S. A.* **1972**, *69*, 3561–3566.
36. Wallace, E. V.; Stoddart, D.; Heron, A. J.; Mikhailova, E.; Maglia, G.; Donohoe, T. J.; Bayley, H. Identification of Epigenetic DNA Modifications with a Protein Nanopore. *Chem. Commun. (Cambridge, U.K.)* **2010**, *46*, 8195–8197.
37. Prilipov, A.; Phale, P. S.; Van Gelder, P.; Rosenbusch, J.; Koebnik, R. Coupling Site-Directed Mutagenesis with High-Level Expression: Large Scale Production of Mutant Porins from *E. coli*. *FEMS Microbiol. Lett.* **1998**, *163*, 65–72.
38. Polleichtner, G.; Andersen, C. The Channel-Tunnel HI1462 of *Haemophilus influenzae* reveals Differences to *Escherichia coli* TolC. *Microbiology* **2006**, *152*, 1639–1647.

Supplementary information

Pulling Peptides across Nano-Channels: Resolving Peptide Binding and Translocation through The Hetero-Oligomeric Channel from *Nocardia farcinica*

Pratik Raj Singh, Iván Bárcena-Uribarri, Niraj Modi, Ulrich Kleinekathöfer, Roland Benz, Mathias Winterhalter* and Kozhinjampara R Mahendran*

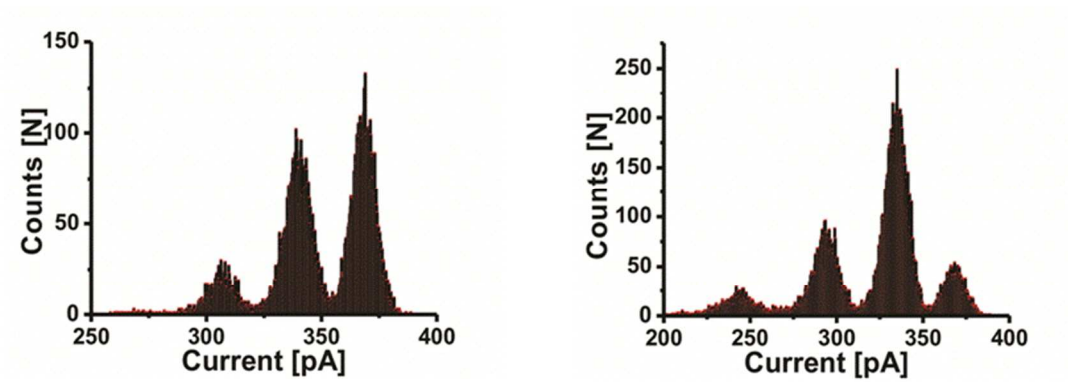
Jacobs University Bremen, Campus Ring 1, D-28759 Bremen, Germany

Correspondence*: k.mahendran@jacobs-university.de

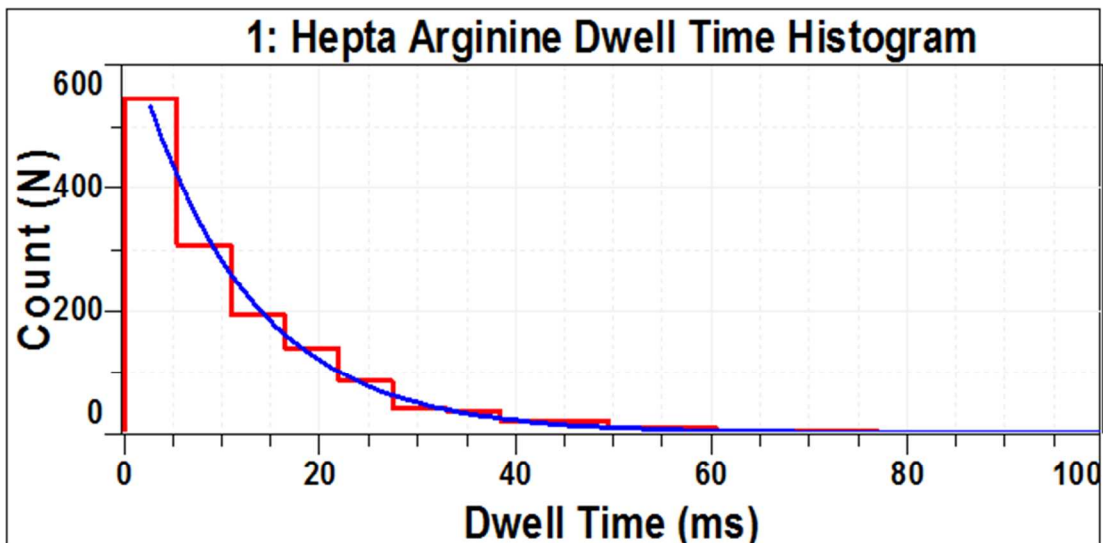
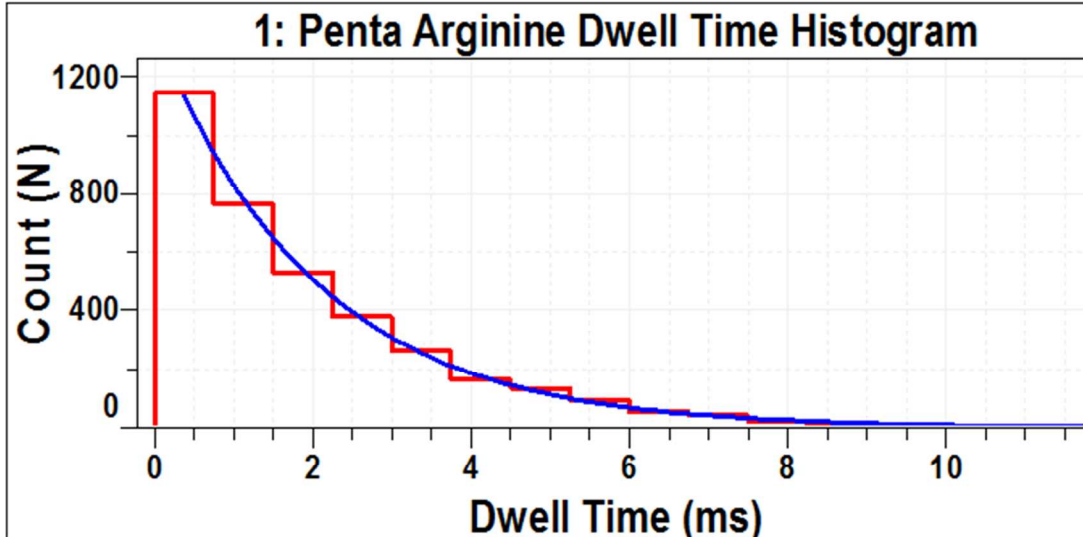
m.winterhalter@jacobs-university.de

Supplementary Figure

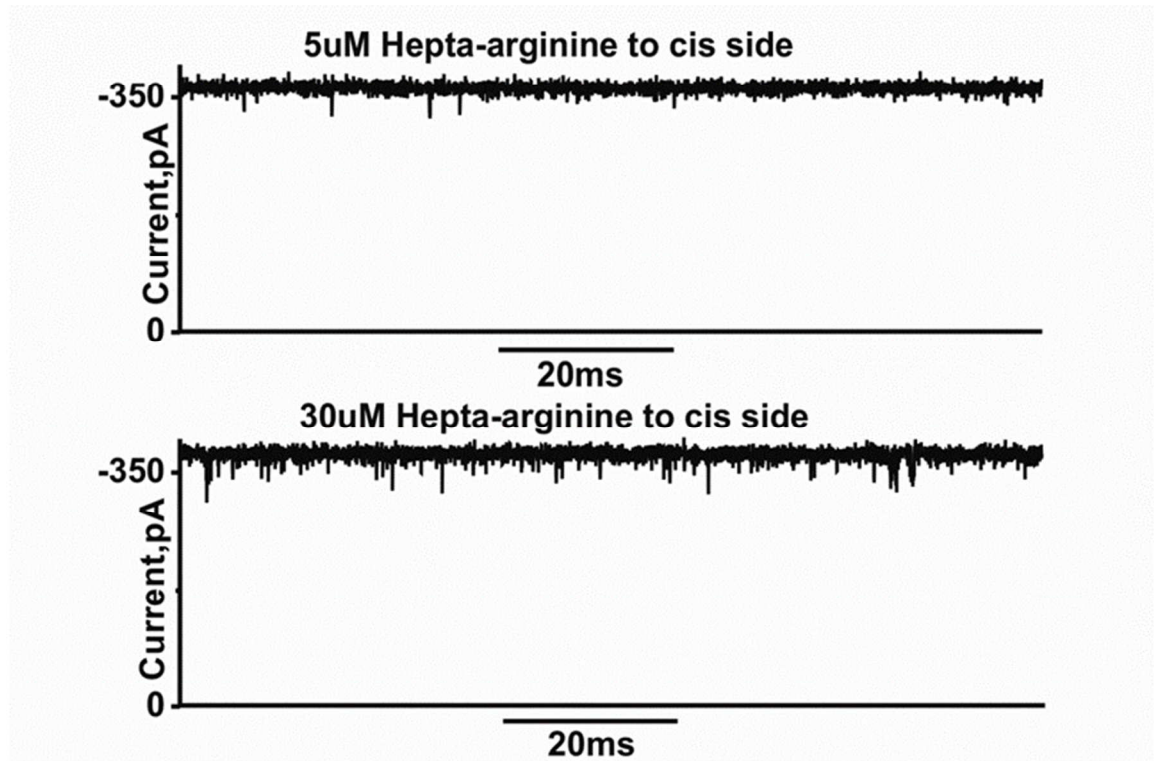
- 1) Current amplitude histogram showing fluctuation of the channel between different conductance steps in the presence of penta-arginine and hepta-arginine. Experimental conditions are 1 M KCl, 10 mM HEPES, pH 7.4.



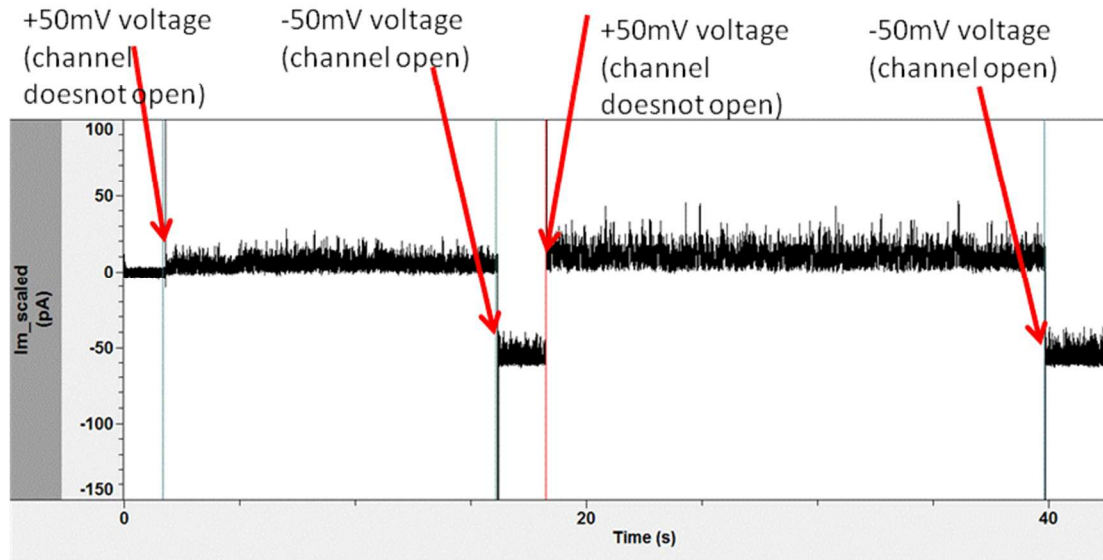
- 2) Dwell time histogram for closed time and open time in the presence of the penta-arginine and hepta-arginine. Experimental conditions are 150 mM KCl, 10 mM HEPES, pH 7.4. Peptide is added to the cis side of the channel.



- 3) Concentration dependence of peptide interaction with the channel. Increase in concentration of hepta-arginine added to the cis side shows increase in ion current fluctuation. Experimental conditions are 1 M KCl, 10 mM HEPES, pH 7.4.



- 4) Hepta-arginine added to trans side of the chamber at low salt concentration. The interaction effect is so high that the channel does not open at positive voltages, due to the blockage of ion passage by the interaction peptide. Experimental conditions are 150 mM KCl, 100nM Hepta-arginine, 10 mM HEPES, pH 7.4.



Chapter 2.2

Manuscript submitted to BBA Biomembranes

Individual Contribution:

**Protein expression and purification, Single channel measurements and analysis,
Composition of manuscript**

Transport across the outer membrane porin of mycolic acid containing actinomycetales: *Nocardia farcinica*

Pratik Raj Singh¹, Harsha Bajaj¹, Roland Benz¹, Mathias Winterhalter¹, and Kozhinjampara R Mahendran^{1, 2,*}

¹ School of Engineering and Science, Jacobs University Bremen, Campus Ring 1, D-28759 Bremen, Germany

² Present address: Department of Chemistry, University of Oxford, Oxford OX1 3TA, United Kingdom

Correspondence*: p.singh@jacobs-university.de (Tel: 00494212003588)
mahendran.kozhinjampararadhakrishnan@chem.ox.ac.uk

Abstract

The role of the outer-membrane channel from a mycolic acid containing Gram-positive bacteria *Nocardia farcinica*, which forms a hydrophilic pathway across the cell wall, was characterized. Single channel electrophysiology measurements and liposome swelling assays revealed the permeation of hydrophilic solutes including sugars, amino acids and antibiotics. The cation selective *Nocardia farcinica* channel exhibited strong interaction with the positively charged antibiotics; amikacin and kanamycin, and surprisingly also with the negatively charged ertapenem. Voltage dependent kinetics of amikacin and kanamycin were studied to distinguish binding from translocation. Moreover, the importance of charged residues inside the channel was investigated using mutational studies that revealed rate limiting interactions during the permeation.

Keywords: *Nocardia farcinica*, antibiotic resistance, Mycolata, porins, single channel electrophysiology

1. Introduction

With the increasing awareness of antibiotic resistance against bacteria, recent findings have revealed a strong correlation of resistance with permeability changes of the cell wall [1–3]. The outer membrane of Gram-negative bacteria contributes to the intrinsic resistance by decreasing the flow of antimicrobial agents into the cell [4–6]. In contrast, Gram-positive bacteria lacking an outer membrane in their cell wall are in general, more sensitive to antibiotics [7]. A further group of Gram-positive bacteria belonging to the actinomycetales taxon, also called mycolata, have a high intrinsic resistance to a wide range of antibiotics due to the presence of an additional mycolic acid layer [7–10]. The mycolic acid layer is mainly composed of long chain mycolic acids and free lipids. It resembles the function of an outer membrane of Gram-negative bacteria [11–13].

Surprisingly, the cell envelope of mycolata also contains water-filled protein channels called porins, which facilitate the diffusion of hydrophilic molecules into the cell [14]. Porins spanning the outer membrane have been identified in the cell wall of some members of the mycolata, such as *Mycobacterium chelonae* [14,15], *Corynebacterium glutamicum* [16], *Mycobacterium smegmatis* [17] and *Nocardia farcinica* [18]. For example MspA, a porin from *M. smegmatis*, forms pores which allows the uptake of various sugars and hydrophilic antibiotics [19,20]. In recent years the importance of the role of porins in the uptake of antibiotics has been recognized in Gram-negative bacteria [21]. Additionally, Gram-positive mycolata group of bacterium comprise microorganisms, such as *Mycobacterium tuberculosis* (TBC), *Mycobacterium leprae* (leprae), *N. farcinica* (nocardiosis) and *Corynebacterium diphtheriae* (diphtheria) that exhibit a pronounced and broad natural resistance to various antimicrobial drugs and contribute towards various dangerous infections worldwide [22,23]. Hence, there is a strong interest in understanding the rate limiting steps of antibiotic transport through the channels. In this study, we focus on understanding the pathway of various hydrophilic antibiotics as well as solutes through the outer-membrane porin from the Gram-positive mycolata, *Nocardia farcinica*.

The outer membrane porin from *N. farcinica* was first identified in 1998 [18], which was later resolved as a hetero-oligomeric channel composed of two different subunits; *NfpA* and *NfpB* [24]. The crystal structure of the protein is unknown but the sequence analysis suggests that it has a high homology to the MspA channel [24]. Previously, we have studied the translocation of polypeptides through the *N. farcinica* channel reconstituted into lipid bilayers [25]. In the present study, we focused on the functionality of the *N. farcinica* channel using planar lipid

bilayer electrophysiology and liposome swelling assay. Liposome swelling assay was employed to study translocation of various uncharged/zwitterionic hydrophilic nutrient molecules such as sugars and amino acids. Using single channel electrophysiology, we studied ion current fluctuations of the channel in presence of clinically relevant antibiotic molecules; positively charged amikacin and kanamycin, and negatively charged ertapenem [18]. Additionally, we selectively neutralized the negatively charged amino acid residues at the pore lumen to elucidate the effect of charge in antibiotic-solute interaction within the channel.

2. Materials and Methods

2.1 Bacterial strains and growth conditions

Escherichia coli cells containing the pARAJ2 vector with *NfpA* and *NfpB* genes were used in each experiment. For plasmid purification *E. coli* DH5Alpha cells were grown in LB medium at 37°C with ampicillin antibiotic used for selection. *E. coli* BL21 (DE3) Omp8 was utilized for expression experiments. 100 µg/mL ampicillin, 40 µg/mL kanamycin were used for selection.

2.2 Site directed mutagenesis of genes *NfpA* and *NfpB*

Cultures of *E. coli* DH5Alpha grown at 37°C, containing the pARAJ2 plasmids harboring wild-type (WT) genes, are used for extraction of the plasmid. *In vitro* site-directed mutagenesis was employed to obtain the desired mutations. The mutations were generated using two approaches; quick change site directed mutagenesis and the mega primer method using PCR. The primers used to introduce substitution-mutations were listed in **Supplementary Table 1**. The PCR conditions used for quick change mutagenesis were: initial denaturing at 95°C for 1 min, 30 cycles at 95 °C for 30 sec, 55 °C for 1 min, 68 °C for 7 min and final extension at 68 °C for 10 min. Forward primer *NfpA* and reverse primer *NfpA* D141N D142N led to complete copy of pARAJ2 plasmid containing desired mutations. The mega primer required two steps of PCR, first step led to mega primers with typical lengths of 250-300 bp and in the second step these mega primers were used as primers for second PCR. The conditions used were: first step 95°C for 1 min, 30 cycles at 95°C for 30 sec, 55°C for 1 min, 68°C for 45 sec and final extension at 68°C for 5 min. The second step consisted of 95°C for 10 min, 30 cycles at 95°C for 1min, 72°C for 7 min and final extension at 72°C for 30

min. *DpnI* digestion was carried out on the PCR product and then run on 1% agarose gel.

2.3 Protein expression and purification

The purification of the two subunits *NfpA* and *NfpB* expressed in *E. coli* BL21 (DE3) Omp8 was performed as described previously with slight modifications [24,25]. Briefly, pARAJ52_*nfpA* (mutant)/*nfpB* (mutant) transformed in the porin-deficient *E. coli* BL21(DE3)Omp8 cells were grown in an LB media at 37°C to an OD₆₀₀ of 0.5-0.9. The cells were then induced with 0.02% of arabinose for over-expression of proteins and were grown at 16°C for 16 h. The cells are collected by centrifugation at 5000 x g for 20 min at 4°C, and the resulting pellet was re-suspended in 10 mM Tris pH 8. The re-suspended pellet was broken down by French press, and the cell debris was separated by centrifugation at 5,000 x g for 10 min at 4°C. The supernatant was ultra-centrifuged at 48,000 x g for 1 h at 4°C to separate the cytosolic proteins present in supernatant and the pellet containing membrane proteins. The protein of interest was further purified from the supernatant fraction to avoid contamination from membrane proteins of *E. coli* present in the pellet fraction. His-tagged protein purification from the supernatant fraction was then performed using Ni-NTA beads under denaturing conditions. The protein of interest was eluted using a gradient of imidazole concentration. The two subunits, purified separately, were refolded together to form a hetero-oligomeric channel by ammonium sulfate precipitation. The two purified subunits are mixed together in a 1:1 ratio and precipitated using saturated ammonium sulfate solution. The solution was incubated overnight at 4°C and centrifuged at 18,000 x g for 30 min. The precipitated protein pellet was refolded to native state by incubating at 4°C in 150 mM NaCl, 25 mM Tris-HCl and 1% Genapol.

2.4 Liposome swelling assays

N. farcinica porin was reconstituted into liposomes as described by Nikaido and Rosenberg [26]. *E. coli* total lipid extract was used to form liposomes; 15% Dextran (MW 40,000) was used to entrap the liposomes, and their final size was checked using a Nano-ZS ZEN3600 zetasizer (Malvern Instruments, Malvern, United Kingdom). Control liposomes were prepared in the same manner but without the addition of porin. The concentrations of test solute were adjusted so that diluents were apparently isotonic with control liposomes. Stachyose was also tested with

proteoliposomes to confirm the isotonicity of the multilamellar liposomes. Liposome or proteoliposome solution (30 μL) was diluted into 630 μL of an isotonic test/solute solution made in 10 mM Tris-HCl pH 7.5 buffer in a 1 mL cuvette and mixed manually. The change in absorbance at 500 nm was monitored using a Cary-Varian UV-vis spectrophotometer in the kinetic measurement mode. The swelling rates were taken as averages from at least five different sets of experiments, calculated as described previously [27].

2.5 Solvent free lipid bilayer technique

Reconstitution experiments and noise analysis have been performed as described in detail previously. The Montal and Muller technique was used to form phospholipid bilayer using DPhPC (Avanti polar lipids) [28]. A Teflon cell comprising an aperture of approximately 30-60 μm diameter was placed between the two chambers of the cuvette. The aperture was pre-painted with 1% hexadecane in hexane for stable bilayer formation. 1 M KCl (or 150 mM KCl), 10 mM HEPES, pH 7.4 was used as the electrolyte solution and added to both sides of the chamber. Ion current was detected using standard silver-silver chloride electrodes from WPI (World Precision Instruments) that were placed in each side of the cuvette. Single channel measurements were performed by adding the protein to the *cis*-side of the chamber (side connected to the ground electrode). Spontaneous channel insertion was typically obtained while stirring under applied voltage. After successful single channel reconstitution, the *cis*-side of the chamber was carefully perfused to remove any remaining porins to prevent further channel insertions. Conductance measurements were performed using an Axopatch 200B amplifier (Molecular Devices) in the voltage clamp mode. Signals were filtered by an on board low pass Bessel filter at 10 kHz and with a sampling frequency set to 50 kHz. Amplitude, probability, and noise analyses were performed using Origin pro 8 (OriginLab) and Clampfit softwares (Molecular devices). Single channel analysis was used to determine the antibiotics binding kinetics. In a single-channel measurement the typical measured quantities were the duration of closed blocked levels residence time (τ_c) and the frequency of blockage events (ν). The association rate constants k_{on} were derived using the number of blockage events, $k_{on} = \nu / [c]$, where c is the concentration of antibiotic. The dissociation rate constants (k_{off}) were determined by averaging the $1/\tau_c$ values recorded over the entire concentration range [29]. Similarly, the selectivity measurements were performed using two different salt solutions in the two chambers of the cuvette. The reverse potential required to

obtain zero-current was calculated and the ratio of the permeabilities of cation / anion was calculated using the Goldman-Hodgkin-Katz equation [30,31].

3. Results and Discussion

3.1 Mutational studies on *N. farcinica* cell wall channel

Based on the homology modeling of the porin with the known structure of MspA, we selected various negatively charged amino acids; located strategically at the periplasmic side of the channel in the two different subunits, *NfpA* and *NfpB*, and mutated them to neutral amino acids with a similar length of the side chain. **Table 1** shows the selected mutations in both subunits and the corresponding channel conductance of the mutant channels in 1 M KCl solution. In particular, we performed at maximum two mutations (D141N and D142N) in *NfpA* and 4 ones (E123Q, E144Q, D127N, E140Q) in *NfpB*, resulting in a total number of at maximum 24 mutations in the pore-forming oligomer. **Figure 1** shows the expected positions of the mutations. Some other mutations led to proteins that had no channel-forming activity. This is presumably the result of the loss of channel function caused by the mutation of residues that were crucial for protein folding and assembly of the oligomers (**Table 1**). To elucidate the effect of charge residues inside the pore on the interaction with antibiotics, we choose the mutant oligomer with the highest number of negatively charged residues mutated to neutral ones and compared the effect of antibiotics on channel conductance with those on wild-type (WT) porin.

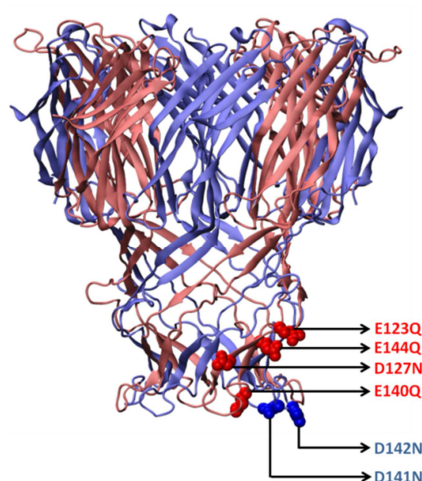


*Figure 1: Homology modeling of hetero-oligomeric *N. farcinica* channel based on the template MspA porin from *M. smegmatis* [25]. Selected mutations are shown for one *NfpA* monomer (blue) and one *NfpB* monomer (red) resulting in total of 24 mutations in the channel-forming oligomer. Note that the bottom side of the oligomer is exposed to the inner side of the mycolic acid layer and the top to the external medium. Reconstitution into lipid bilayer membranes occurs exclusively with the periplasmic side of the oligomer exposed to the trans-side of the bilayer.*

Based on homology modeling we created the surface potential of the porin and compared both the WT and the mutant channel as shown in **Supplementary Figure 1**. The mutations rendered its periplasmic side rather neutral compared to the WT channel. To study the interaction of the mutant channel with cationic peptide we performed single-channel measurements to determine the approximate locations of these mutations. As shown in **Supplementary Figure 1A**, we observed that hepta-arginine showed a very strong interaction with the WT channel resulting in frequent blockages of ionic current in multiple steps when added to the periplasmic side (*trans*) of the channel [25]. However, when the same experiment was performed with the mutant porins (**Supplementary Figure 1B**), we observed reduced interactions of hepta-arginine with the channel. This reduction was due to the absence of negatively charged amino acids in the periplasmic entry of the pore, suggesting that the mutations were located at the correct positions.

Table 1: Mutations performed in both the NfpA and NfpB subunits of N. farcinica porin. Table shows the conductance at 1 M KCl, 20 mM HEPES pH 7.5 once the mutants have been refolded.

Mutations in <i>NfpA</i>	Mutations in <i>NfpB</i>	Average Conductance (nS) n = 10
Wild-type (WT)	E123Q, E144Q, D127N, E140Q	3.1 ± 0.2
D141N , D142N	E123Q, D127N	2.8 ± 0.3
D141N , D142N	E123Q, E144Q, D127N, E140Q	2.7 ± 0.3 (selected for further studies)
D141N , D142N	E123Q, E144Q, D127R, E140Q	2.2 ± 0.1
E101K, D141N, D142N, D181R	E123Q, E144Q, D127N, E140Q	No channel-forming activity observed

3.2 Ion selectivity measurements

Ion selectivity measurements of both the WT and mutant pore were performed using different concentration of monovalent KCl salt solutions on both sides of DphPC membranes. As expected, the channel was highly cation selective due to the large number of negatively charged residues inside the channel as shown in **Table 2**. As shown previously, the cation selectivity of the channel is not caused due to a particular binding site inside the channel but by the presence of point negative charges inside the lumen of the channel [18,32]. This changes the cation selectivity of the channel using different concentrations of the electrolyte solution on both sides of the membrane. At high salt concentration (1 M KCl/150 mM KCl), caused by electrostatic effects, the cation selectivity of the channel ($pK^+/pCl^- = 3.8$) was lower

compared to the selectivity (7.8) at lower salt concentration on both sides of the membranes (500 mM KCl/ 75 mM KCl). Similarly, the ion selectivity of the mutant pore was lower compared to WT pore in both salt concentrations, making it slightly less cation selective because many negatively charged groups became neutral by mutation.

Table 2: Ion selectivity of WT and mutant *N. farcinica* channels using different KCl concentration gradients on both sides of the DphPC membranes.

<i>N. farcinica</i>	Concentration Gradient [cis/trans]	Reverse Potential on the more dilute side [mV]	Pc/Pa (n=3)
Wild-type (WT)	1 M KCl/150 mM KCl	23 ± 1	3.8 ± 0.2
	500 mM KCl/ 75 mM KCl	33 ± 1	7.8 ± 0.3
Mutant <i>NfpA</i> (D141N, D142N) <i>NfpB</i> (E123Q, E144Q, D127N, E140Q)	1 M KCl/150 mM KCl	21 ± 1	3.2 ± 0.2
	500 mM KCl/ 75 mM KCl	27 ± 1	4.8 ± 0.2

3.3 Functional assays with liposomes

The channel functionality of *NfpA/NfpB* WT and mutant oligomers was further confirmed by reconstituting them in liposomes and measuring their permeability for small hydrophilic molecules such as sugars and amino acids. The rate of diffusion of sugars and amino acids was calculated by measuring the change in optical density of proteoliposomes in the presence of an isotonic concentration of sugars/amino acids [26]. Permeation rates were obtained within the same batch allowing us to normalize the diffusion rates with respect to arabinose [26]. We found that the exclusion limit of the channel was slightly higher than that observed in the case of Gram-negative porins, as shown in **Figure 2** by the considerably higher diffusion rate of large molecules, such as raffinose [26]. This suggested a larger exclusion limit of the channel which may be due to the larger pore size of the channel. Importantly, these results were coherent with previous results for porin from *M. chelonae* which has similar properties as the *N. farcinica* channel [14]. The highest diffusion rates were obtained for the two amino acids glycine and L-serine; they were approximately 80% higher than that observed for arabinose. The diffusion rates of other sugars including maltose, sucrose and glucose were approximately 20% lower than arabinose. Liposome swelling assays performed on *N. farcinica* channel indicated passive diffusion of different sugars and amino acids through the channel with the rate of permeation proportional to the size of the substrate. The diffusion rate was found to decrease with the increase of molecular mass of solutes as

reported previously [14, 26]. There was no significant difference in diffusion rates of sugar and amino acids between the WT and mutant protein. This was expected since all the sugars or amino acids tested were neutral or zwitterionic. Furthermore, we also performed single channel electrophysiology experiment on sugar transport through the *N. farcinica* channel. However, it seemed that the sugar molecules did probably not bind inside the channel. They diffused through the channel which means that our instrumental set-up could not resolve any interaction between sugars and channel in terms of ion current fluctuations.

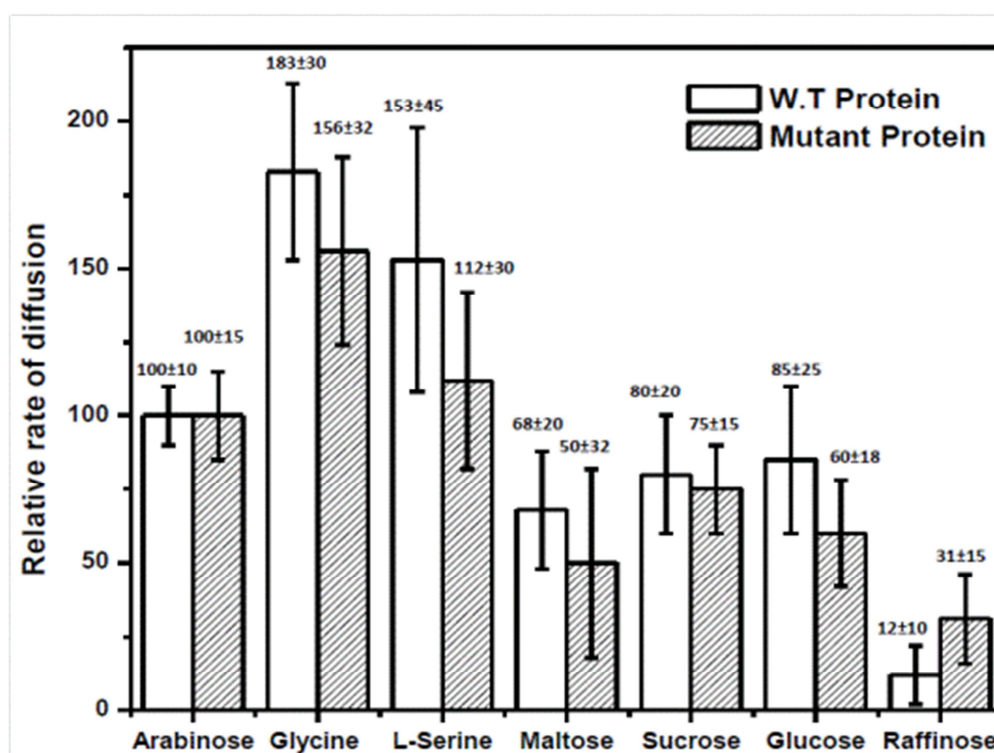


Figure 2: Liposome swelling assay performed for both WT and mutant *N. farcinica* porins reveal the qualitative diffusion rate of different sugars and amino acids based on their sizes. Note that the difference of the relative rate of diffusion between the WT channel and its mutant was within the SD of the experimental error.

3.4 Interaction between antibiotics and the *N.farcinica* channel

One of the main focuses in this study was to investigate the interaction of clinically relevant antibiotics with the *N. farcinica* channel. Identifying the antibiotic affinity site and its position inside the channel helps to understand the rate limiting interaction and sheds light on the pathway of the antibiotic through the channel [33–35]. Based on the selectivity of the *N. farcinica* channel and the presence of negatively charged residues in the channel’s mouth, it has been postulated that positively charged antibiotic may utilize this channel as the pathway for permeation [18]. Using this assumption, we selected two positively charged aminoglycosides for our study, kanamycin and amikacin.

The *N. farcinica* channel has a strong asymmetry of the channel gating such that it is highly stable at negative voltages but gates significantly at positive voltages as low as +30 mV (protein addition to the *cis*/ground side) [25]. Thus the majority of the experiments were performed at negative voltages at the *trans*-side. In the absence of antibiotics, no fluctuation in the ion current was detected here and in a previous study [18, 25]. This changed completely when amikacin and kanamycin were added in μM concentration to the *cis*-side of the membranes. Ion current fluctuations observed for both amikacin and kanamycin at 150 mM KCl solution are shown in **Figure 3A and 4A**, respectively. Addition of antibiotics to the *cis* (ground) side of the channel induced ion current blocks, suggesting possible antibiotic-porin interaction. In contrast to this, we did not observe at applied positive voltages any interactions, which might be caused by the positive voltage repelling the positively charged antibiotic molecules from the channel. As a control we reversed the experiment with respect to voltage. Addition of the antibiotics to the *trans* side under negative voltages, caused also no ion current fluctuations.

The most prominent interactions were observed at *cis* addition and applied negative voltages with a lowered salt solution from 1 M KCl to 150 mM KCl. This suggested that the interaction between the antibiotic and porin had a strong charge-charge interaction component. Similarly, previous experiments that have been performed on peptides and DNA molecules have also reported this enhanced interaction, upon lowering of the salt concentration [36,37].

Amikacin is an aminoglycoside with a net positive charge of 4 at pH 7.4 [38]. Increasing the concentration of amikacin showed increased interaction with both the WT and mutant channels. However, addition of amikacin to the mutant pore with <24 negative amino acid residues showed significantly less interaction than the WT channel, as depicted by the ion current trace in **Figure 3D**. The current amplitude histogram shown in **Figure 3B and 3E** provides the decreased current counts of the closed state (blocked state) in the mutant pore compared to those of WT. The scatter plot of amplitude (y-axis) and dwell time (x-axis), **Figure 3C and 3F**, represents the antibiotic-channel interactions. The residence (dwell) time of antibiotic interaction with the porin ranged from 100 μs - 800 μs with an average residence time of 200 μs for the WT channel. In the case of the mutant channel, the average residence time decreased to something like 100 μs close to the time resolution limit of our instrumentation.

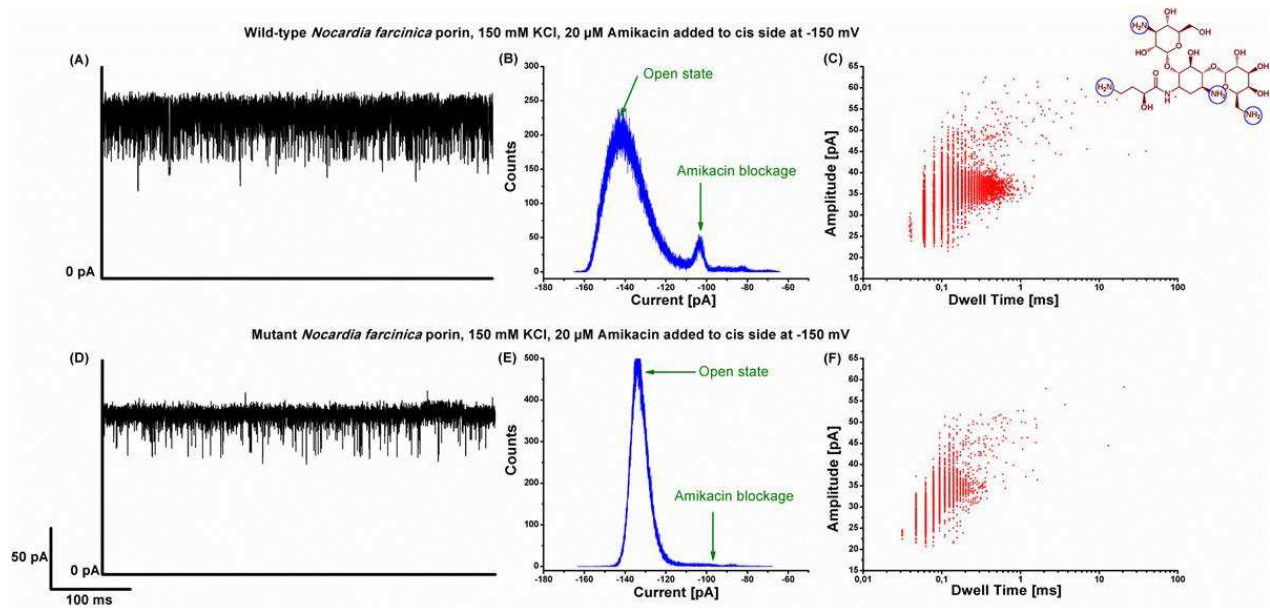


Figure 3: Interaction of amikacin (chemical structure top right) with WT and mutant *N. farcinica* channel. (A) 20 μM amikacin was added to the cis side of the WT channel at an applied voltage of -150 mV. (B) Event histogram of amikacin with the WT channel. (C) Amplitude-dwell time scatter plot of amikacin events with the WT channel. (D) 20 μM amikacin was added to the cis side of the mutant channel at an applied voltage of -150 mV. (E) Event histogram of amikacin with the mutant channel. (F) Amplitude-dwell time scatter plot of amikacin events with the mutant channel. Experimental conditions were 150 mM KCl, 10 mM HEPES, pH 7.4.

Similarly, kanamycin is also an aminoglycoside with a net positive charge of 4 and as expected, kanamycin also showed interaction with the pore. Nevertheless, the interaction of kanamycin was significantly different to that observed for amikacin (**Figure 3A and 4A**). Kanamycin exhibited lower frequency of events compared to amikacin. In addition, the interaction of kanamycin with the pore was not uniform as depicted in the plots in **Figure 4B and 4E**. From **Figure 4C**, we observed that the dwell times of the kanamycin interaction ranged from 100 μs to 80 ms. This suggested that kanamycin may have more than one binding site within the channel surface. Likewise to amikacin, the number of events and the residence time of kanamycin interaction decreased in the mutant pore as shown in **Figure 4D and 4F**.

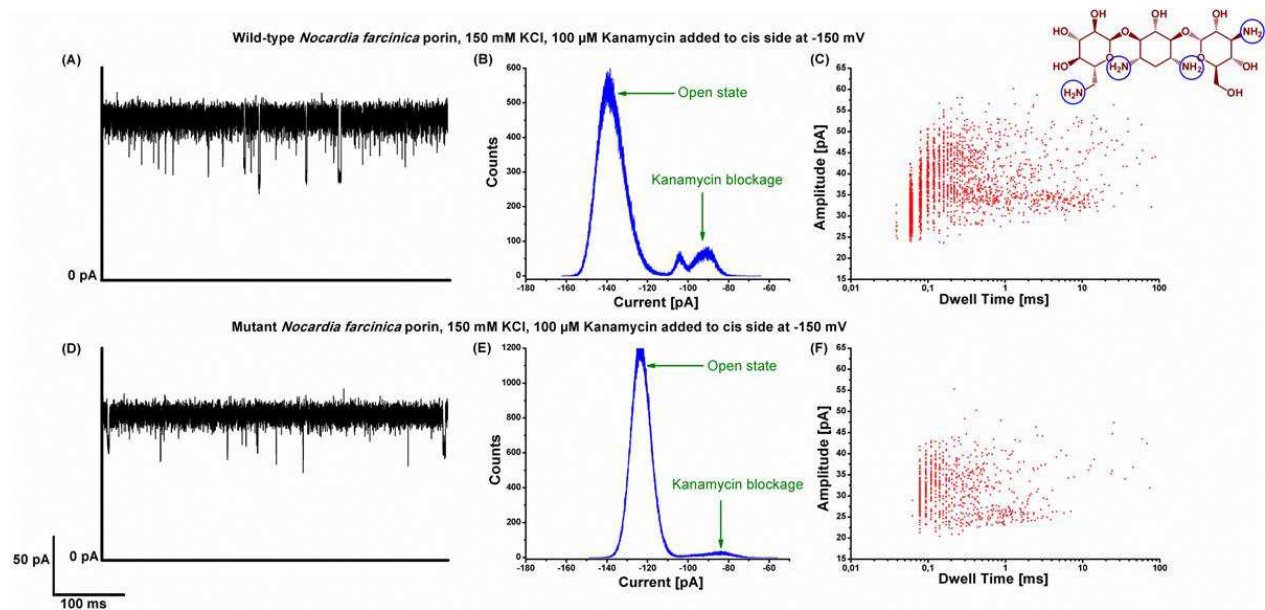


Figure 4: Interaction of kanamycin (chemical structure top right) with WT and mutant *N. farcinica* channel. (A) 100 μM kanamycin was added to the cis side of the WT channel at an applied voltage of -150 mV. (B) Event histogram of kanamycin with the WT channel. (C) Amplitude-dwell time scatter plot of kanamycin events with the WT channel. (D) 100 μM kanamycin was added to the cis side of the mutant channel at an applied voltage of -150 mV. (E) Event histogram of kanamycin with the mutant channel. (F) Amplitude-dwell time scatter plot of kanamycin events with the mutant channel. Experimental conditions were 150 mM KCl, 10 mM HEPES, pH 7.4.

Previous reports on antibiotic translocations through porins of Gram-negative bacteria highlight that charged residues within a pore influence the interaction between the antibiotics and pore and hence the rate of translocation [39–44]. Mutation of amino acid D113N of *E. coli* OmpF loop 3 shows an increased rate of permeation of ampicillin [41]. Similarly, a single mutation in the loop 3 region (glycine to aspartate) of *Enterobacter aerogenes* Omp36 porin exhibits a reduced pore conductance and decreased cephalosporin permeation [45]. To elucidate the importance of charge and the presence of affinity site inside the porin, we performed an antibiotic titration experiments with *N. farcinica* mutant pore, where 24 amino-acids were neutralized. In such an experiment, (**Supplementary Table 2**) we observed that both the on rate as well as the residence time of amikacin and kanamycin was reduced for the mutated pore, emphasizing the importance of affinity sites inside the channel.

In our experiment, both the positively charged antibiotics belong to the antibiotic class of aminoglycoside. Amikacin and kanamycin both possess 4 positive charges at pH 7.4 and the structures of the antibiotics share a similar scaffold. However, we observed a very sharp difference in the binding kinetics of these two antibiotics with the pore. Amikacin had a significantly higher on rate as compared to kanamycin (**Supplementary Table 2**). *In vivo* Minimum Inhibitory Concentration (MIC) assay of different antibiotics performed with *N. farcinica* showed amikacin to be an effective drug compared to kanamycin [46,47]. Could the

higher on-rate of amikacin compared to kanamycin be the reason for such difference in effectiveness? However, the presented results of channel blocking cannot be converted directly into translocation, since binding does not always imply translocation. For uncharged solutes, liposome swelling assays can be performed to distinguish if the molecule is indeed permeating through the channel, which is not feasible with charged molecules. For charged molecules, as in our case; we performed a voltage dependent analysis of kinetic off-rate to distinguish binding from translocation as previously reported to distinguish binding from translocation for short peptides [25,48].

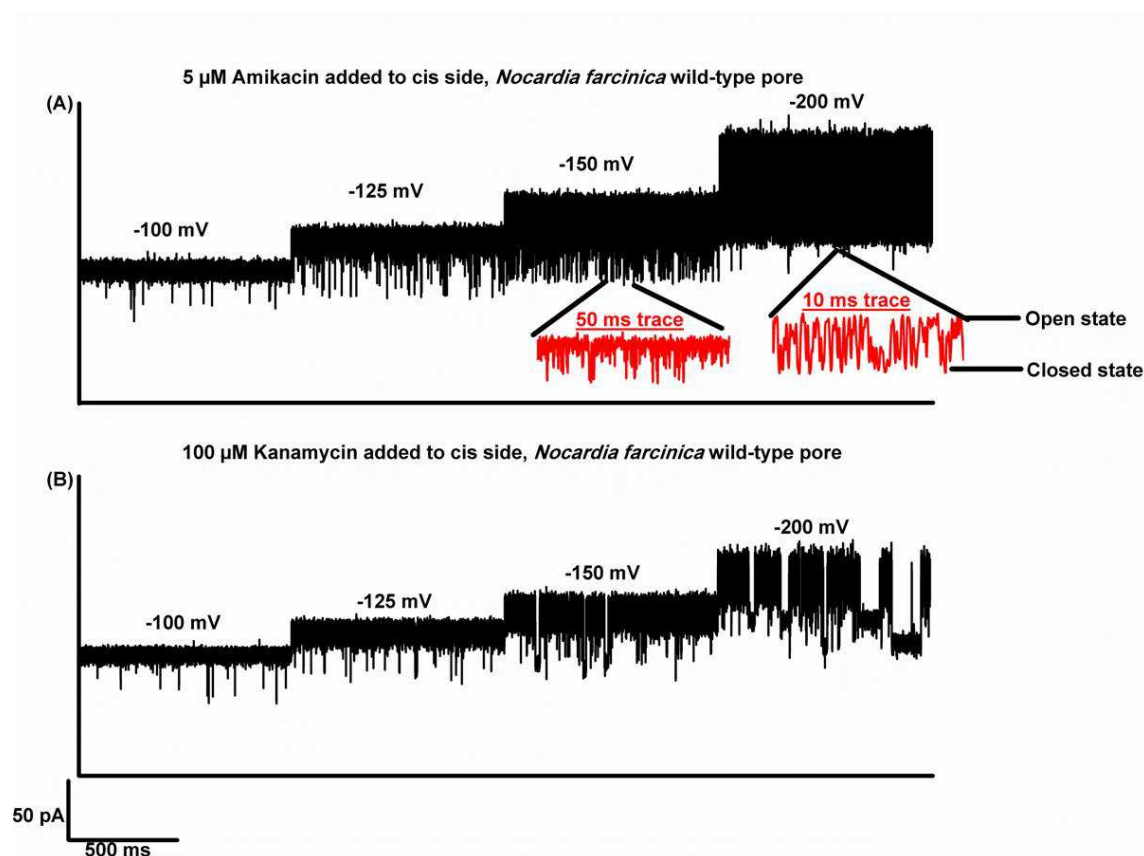


Figure 5: Distinguishing binding from translocation: Voltage scan of ion current fluctuation of antibiotics through the *N. farcinica* channel. (A) Increasing the application of external voltage with addition of amikacin to the cis side of the channel. At higher voltages, the residence time of the channel decreased to the limit of the instrument and could not be resolved. (B) Increasing the application of external voltage with addition of kanamycin to the cis side of the channel. With increasing voltage, the binding of kanamycin with the channel increases. Experimental conditions were 150 mM KCl, 10 mM HEPES, pH 7.4.

Increasing voltages tended to increase the residence time of the kanamycin, whereas the residence time of amikacin decreased as shown in the **Figure 5**. As mentioned earlier, the average residence time of amikacin was 200 μs at -150mV. An increase of the external voltage up to -200 mV resulted in an overall decrease of the channel conductance instead of observing single ion fluctuation events. This may be due to significantly fast permeation events. However, in the case of kanamycin, increasing the voltage increased the residence time of the

antibiotic. At high voltages (> 200 mV), we observed an apparent strong binding which suggested that the molecule is held inside the pore in such a way that the pore remained in its closed state (figure not shown). The above mentioned observation suggested that amikacin is permeating through the channel; whereas kanamycin is not able to penetrate the channel, supporting the susceptibility of *N. farcinica* for amikacin over kanamycin. The impermeability of kanamycin through the homologous MspA porin using MIC assays has also been reported earlier, which correlated with our results [20,49].

Apart from the positively charged antibiotics, we also investigated various chemically and structurally/clinically relevant antibiotics such as; fluoroquinolones, penicillins, carbapenems and sulfonamides [46,47,50]. Most of these antibiotics are either zwitterionic or negatively charged and thus no interaction was observed with the highly negatively charged amino acids inside the pore lumen of the *N. farcinica* porin. Surprisingly, addition of the carbapenem antibiotic ertapenem showed ion current fluctuation with the single *N. farcinica* channel (**Figure 6A**). Ertapenem, which is a negatively charged antibiotic, is prone to repulsive forces from the negatively charged interior of the channel. This implies the interaction observed with the antibiotic and the pore could be due to non-ionic interactions. To confirm the role of electrostatic interaction between antibiotic and pore, we performed our experiments in both 1 M and 150 mM KCl solution and found that the interaction was similar (*i.e.* residence time of ertapenem inside the pore was ~ 200 μ s) in both cases, supporting the assumption of non-ionic interaction (**Supplementary Figure 2**). By looking at the structure of ertapenem, we noted that it consists of multiple aromatic rings; which, as we hypothesize, may interact with the hydrophobic amino acids inside the pore lumen.

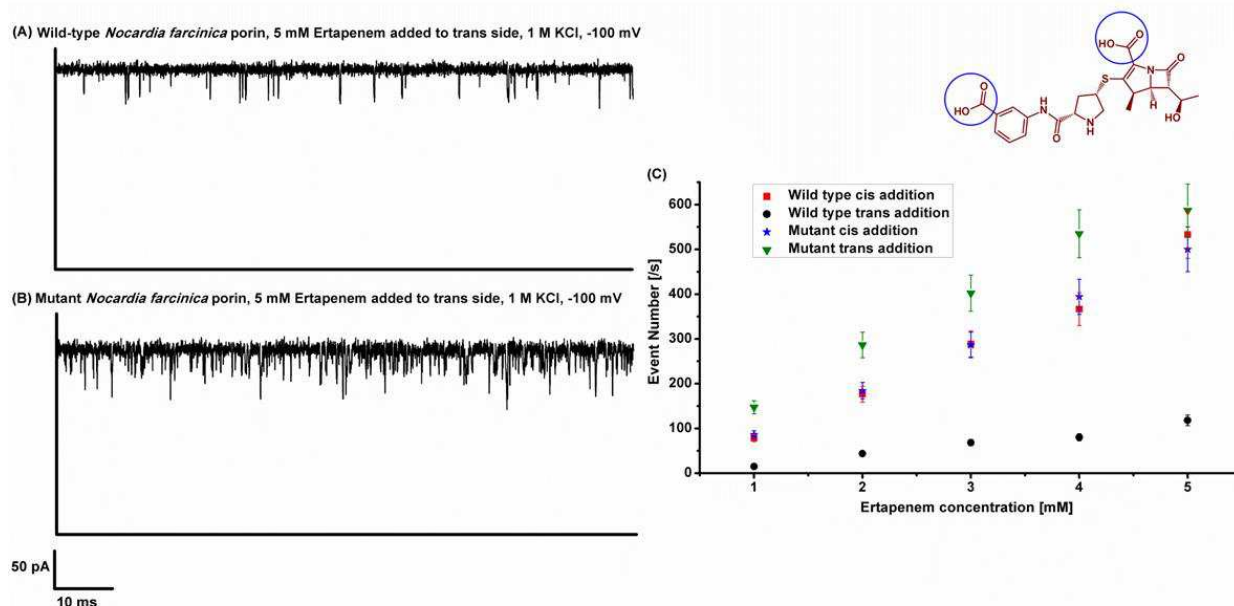


Figure 6: Interaction of ertapenem (chemical structure top right) with WT and mutant *N. farcinica* channel. Ion current trace obtained when ertapenem was added to the trans side of the channel at an applied voltage of -100 mV for (A) WT porin and (B) mutant porin. (C) Number of event plotted against concentration of ertapenem added to both WT and mutant porin in both extracellular (cis) and periplasmic (trans) side of the channel. Experimental conditions were 1 M KCl, 10 mM HEPES, pH 7.4.

Ion current blockages were observed for both the WT and mutant porins in presence of ertapenem and an increased number of events were observed with increased ertapenem concentration as shown in **Figure 6C**. The event frequency of ertapenem was similar in both WT and mutant when the antibiotic was added to the *cis* (extracellular) side, however a significant difference was observed for the event frequency when the antibiotic was added to the *trans* (periplasmic) side as shown in **Figure 6A and 6B**. The mutant pore exhibited a higher number of ertapenem interactions in comparison to WT pore. During the entry of ertapenem into the channel from the periplasmic side, it faces strong repulsive forces from the surrounding negatively charged amino acids. In contrast, when the negatively charged residues in the periplasmic space were neutralized, the lower repulsive forces in this case seemed to enhance the on-rate of ertapenem with the channel. Previous reports on MspA porin from *M. smegmatis* that has point negative charges in the mouth of the channel reported a 10- fold lower permeability of mono-anionic beta-lactams compared to zwitterionic cephaloridine [51]. The presence of negatively charged residue in the mouth of the channel affected the permeation of negatively charged molecule, which correlates well with our observations.

4. Conclusion

Mycolata have evolved a complex cell wall, comprising peptidoglycan - arabinogalactan polymer covalently bound to mycolic acids of considerable size (up to 90 carbon atoms), a variety of extractable lipids, and pore-forming proteins [11,52,53]. Since the role of the outer-membrane is indispensable in the mycobacterial resistance to antibiotics, it is tempting to reconstitute the porins in a mycolic acid containing bilayer to retain its physiological environment. Reconstitution of MspA from *M. smegmatis* in mycolic acid membrane has been studied before, [54] however, our effort to form and reconstitute the *N. farcinica* porin in the mycolic acid containing membrane was unsuccessful. Nonetheless, we were able to successfully reconstitute the protein in phospholipid bilayers and liposomes to perform single channel measurements and liposome swelling assays.

Current investigation represents one of the first detailed studies on solute and antibiotic permeation through porin from bacterium belonging to mycolata. We have confirmed the channel functionality of *N. farcinica* porin using liposome swelling assays and permeation of nutrient molecules including different sized sugars and amino acids. In addition to different solutes, the interaction of clinically relevant antibiotics such as amikacin, kanamycin and ertapenem was also studied at the single molecule level. Well defined ion current fluctuations were observed in the presence of these antibiotics that interact with the pore. We were also able to distinguish between translocation and binding for amikacin and kanamycin using voltage dependent analysis. Our results indicated that kanamycin was unable to translocate while amikacin was able to translocate through the channel. This observation correlated very well with the *in vivo* MIC assays performed, which specified amikacin to be more potent against *N. farcinica* than kanamycin [46]. Furthermore, we elucidated the effect of various charged amino acids present inside the channel on the permeation of charged antibiotics and uncharged/zwitterionic molecules.

Acknowledgement

We would like to thank Dr. Niraj Modi for discussions and modeling of the *N. farcinica* channel.

5. References

- [1] H. Nikaido, Prevention of drug access to bacterial targets: permeability barriers and active efflux., *Science*. 264 (1994) 382–388. doi:10.1126/science.8153625.
- [2] H. Nikaido, Molecular basis of bacterial outer membrane permeability revisited., *Microbiol. Mol. Biol. Rev.* 67 (2003) 593–656.
- [3] A.H. Delcour, Outer Membrane Permeability and Antibiotic Resistance, *Biochim Biophys Acta*. 1794 (2009) 808–816. doi:10.1016/j.bbapap.2008.11.005.
- [4] J.-M. Pagès, C.E. James, M. Winterhalter, The porin and the permeating antibiotic: a selective diffusion barrier in Gram-negative bacteria., *Nat. Rev. Microbiol.* 6 (2008) 893–903. doi:10.1038/nrmicro1994.
- [5] K. Poole, Outer membranes and efflux: the path to multidrug resistance in Gram-negative bacteria., *Curr. Pharm. Biotechnol.* 3 (2002) 77–98.
- [6] H. Nikaido, Outer membrane barrier as a mechanism of antimicrobial resistance., *Antimicrob. Agents Chemother.* 33 (1989) 1831–1836. doi:10.1128/AAC.33.11.1831.
- [7] T.J. Silhavy, D. Kahne, S. Walker, The bacterial cell envelope., *Cold Spring Harb. Perspect. Biol.* 2 (2010) a000414. doi:10.1101/cshperspect.a000414.
- [8] V. Jarlier, H. Nikaido, Mycobacterial cell wall: structure and role in natural resistance to antibiotics., *FEMS Microbiol. Lett.* 123 (1994) 11–18.
- [9] V. Jarlier, L. Gutmann, H. Nikaido, Interplay of cell wall barrier and beta-lactamase activity determines high resistance to beta-lactam antibiotics in *Mycobacterium chelonae*., *Antimicrob. Agents Chemother.* 35 (1991) 1937–1939. doi:10.1128/AAC.35.9.1937.
- [10] D.E. Minnikin, S.M. Minnikin, M. Goodfellow, J.L. Stanford, The mycolic acids of *Mycobacterium chelonae*., *J. Gen. Microbiol.* 128 (1982) 817–822. doi:10.1099/00221287-131-9-2237.
- [11] D.E. Minnikin, Chemical principles in the organization of lipid components in the mycobacterial cell envelope, *Res. Microbiol.* 142 (1991) 423–427. doi:http://dx.doi.org/10.1016/0923-2508(91)90114-P.
- [12] P.J. Brennan, H. Nikaido, The envelope of mycobacteria., *Annu. Rev. Biochem.* 64 (1995) 29–63. doi:10.1146/annurev.biochem.64.1.29.
- [13] D.E. Minnikin, S.M. Minnikin, J.H. Parlett, M. Goodfellow, M. Magnusson, Mycolic acid patterns of some species of *Mycobacterium*, *Arch. Microbiol.* 139 (1984) 225–231. doi:10.1007/BF00402005.
- [14] J. Trias, V. Jarlier, R. Benz, Porins in the cell wall of mycobacteria., *Science*. 258 (1992) 1479–1481. doi:10.1126/science.1279810.

- [15] M. Niederweis, Mycobacterial porins - New channel proteins in unique outer membranes, *Mol. Microbiol.* 49 (2003) 1167–1177. doi:10.1046/j.1365-2958.2003.03662.x.
- [16] T. Lichtinger, A. Burkovski, M. Niederweis, R. Krámer, R. Benz, Biochemical and biophysical characterization of the cell wall porin of *Corynebacterium glutamicum*: The channel is formed by a low molecular mass polypeptide, *Biochemistry.* 37 (1998) 15024–15032. doi:10.1021/bi980961e.
- [17] J. Trias, R. Benz, Permeability of the cell wall of *Mycobacterium smegmatis*, *Mol. Microbiol.* 14 (1994) 283–290. doi:10.1111/j.1365-2958.1994.tb01289.x.
- [18] F.G. Riess, T. Lichtinger, R. Cseh, A.F. Yassin, K.P. Schaal, R. Benz, The cell wall porin of *Nocardia farcinica*: Biochemical identification of the channel-forming protein and biophysical characterization of the channel properties, *Mol. Microbiol.* 29 (1998) 139–150. doi:10.1046/j.1365-2958.1998.00914.x.
- [19] V. Jarlier, H. Nikaido, Mycobacterial cell wall: Structure and role in natural resistance to antibiotics, *FEMS Microbiol. Lett.* 123 (1994) 11–18. doi:10.1111/j.1574-6968.1994.tb07194.x.
- [20] O. Danilchanka, M. Pavlenok, M. Niederweis, Role of porins for uptake of antibiotics by *Mycobacterium smegmatis*., *Antimicrob. Agents Chemother.* 52 (2008) 3127–3134. doi:10.1128/AAC.00239-08.
- [21] R. Benz, *Bacterial Cell Wall*, Elsevier, 1994. doi:10.1016/S0167-7306(08)60422-6.
- [22] World Health Organization, *Global Tuberculosis Control 2011*, 2011. doi:ISBN 978 92 9061 522 4.
- [23] B.R. Bloom, Vaccines for the Third World, *Nature.* 342 (1989) 115–120.
- [24] C. Kläckta, P. Knörzer, F. Riess, R. Benz, Hetero-oligomeric cell wall channels (porins) of *Nocardia farcinica*, *Biochim. Biophys. Acta - Biomembr.* 1808 (2011) 1601–1610. doi:10.1016/j.bbamem.2010.11.011.
- [25] P.R. Singh, I. Bárcena-Uribarri, N. Modi, U. Kleinekathöfer, R. Benz, M. Winterhalter, et al., Pulling peptides across nanochannels: resolving peptide binding and translocation through the hetero-oligomeric channel from *Nocardia farcinica*., *ACS Nano.* 6 (2012) 10699–707. doi:10.1021/nn303900y.
- [26] H. Nikaido, E.Y. Rosenberg, Porin channels in *Escherichia coli*: studies with liposomes reconstituted from purified proteins., *J. Bacteriol.* 153 (1983) 241–252.
- [27] F. Yoshimura, H. Nikaido, Diffusion of beta-lactam antibiotics through the porin channels of *Escherichia coli* K-12., *Antimicrob. Agents Chemother.* 27 (1985) 84–92.
- [28] M. Montal, P. Mueller, Formation of bimolecular membranes from lipid monolayers and a study of their electrical properties., *Proc. Natl. Acad. Sci. U. S. A.* 69 (1972) 3561–3566. doi:10.1073/pnas.69.12.3561.

- [29] E.M. Nestorovich, C. Danelon, M. Winterhalter, S.M. Bezrukov, Designed to penetrate: time-resolved interaction of single antibiotic molecules with bacterial pores., *Proc. Natl. Acad. Sci. U. S. A.* 99 (2002) 9789–94. doi:10.1073/pnas.152206799.
- [30] A.L. Hodgkin, B. Katz, The effect of sodium ions on the electrical activity of the giant axon of the squid, *J. Physiol.* 108 (1949) 37–77.
- [31] C. Danelon, A. Suenaga, M. Winterhalter, I. Yamato, Molecular origin of the cation selectivity in OmpF porin: Single channel conductances vs. free energy calculation, *Biophys. Chem.* 104 (2003) 591–603. doi:10.1016/S0301-4622(03)00062-0.
- [32] J. Trias, R. Benz, Characterization of the channel formed by the mycobacterial porin in lipid bilayer membranes. Demonstration of voltage gating and of negative point charges at the channel mouth., *J. Biol. Chem.* 268 (1993) 6234–6240.
- [33] K.R. Mahendran, M. Kreir, H. Weingart, N. Fertig, M. Winterhalter, Permeation of antibiotics through *Escherichia coli* OmpF and OmpC porins: screening for influx on a single-molecule level., *J. Biomol. Screen. Off. J. Soc. Biomol. Screen.* 15 (2010) 302–307. doi:10.1177/1087057109357791.
- [34] B.K. Ziervogel, B. Roux, The binding of antibiotics in OmpF porin, *Structure.* 21 (2013) 76–87. doi:10.1016/j.str.2012.10.014.
- [35] P.R. Singh, M. Ceccarelli, M. Lovelle, M. Winterhalter, K.R. Mahendran, Antibiotic permeation across the OmpF channel: modulation of the affinity site in the presence of magnesium., *J. Phys. Chem. B.* 116 (2012) 4433–8. doi:10.1021/jp2123136.
- [36] D. Fologea, J. Uplinger, B. Thomas, D.S. McNabb, J. Li, Slowing DNA translocation in a solid-state nanopore, *Nano Lett.* 5 (2005) 1734–1737. doi:10.1021/nl051063o.
- [37] K.R. Mahendran, M. Romero-Ruiz, A. Schlösinger, M. Winterhalter, S. Nussberger, Protein translocation through Tom40: Kinetics of peptide release, *Biophys. J.* 102 (2012) 39–47. doi:10.1016/j.bpj.2011.11.4003.
- [38] R.S. Kane, P.T. Glink, R.G. Chapman, J.C. McDonald, P.K. Jensen, H. Gao, et al., Basicity of the amino groups of the aminoglycoside amikacin using capillary electrophoresis and coupled CE-MS-MS techniques, *Anal. Chem.* 73 (2001) 4028–4036. doi:10.1021/ac010173m.
- [39] C. Danelon, E.M. Nestorovich, M. Winterhalter, M. Ceccarelli, S.M. Bezrukov, Interaction of zwitterionic penicillins with the OmpF channel facilitates their translocation., *Biophys. J.* 90 (2006) 1617–1627. doi:10.1529/biophysj.105.075192.
- [40] K.R. Mahendran, E. Hajjar, T. MacH, M. Lovelle, A. Kumar, I. Sousa, et al., Molecular basis of enrofloxacin translocation through OmpF, an outer membrane channel of *Escherichia coli* - When binding does not imply translocation, *J. Phys. Chem. B.* 114 (2010) 5170–5179. doi:10.1021/jp911485k.
- [41] E. Hajjar, K.R. Mahendran, A. Kumar, A. Bessonov, M. Petrescu, H. Weingart, et al., Bridging timescales and length scales: from macroscopic flux to the molecular

- mechanism of antibiotic diffusion through porins., *Biophys. J.* 98 (2010) 569–75.
doi:10.1016/j.bpj.2009.10.045.
- [42] S. Vidal, J. Bredin, J.M. Pagès, J. Barbe, β -lactam screening by specific residues of the OmpF eyelet, *J. Med. Chem.* 48 (2005) 1395–1400. doi:10.1021/jm049652e.
- [43] S.A. Benson, J.L. Occi, B.A. Sampson, Mutations that alter the pore function of the OmpF porin of *Escherichia coli* K12., *J. Mol. Biol.* 203 (1988) 961–970.
doi:10.1016/0022-2836(88)90121-0.
- [44] R. Misra, S.A. Benson, Isolation and characterization of OmpC porin mutants with altered pore properties., *J. Bacteriol.* 170 (1988) 528–533.
- [45] A. Thiolas, C. Bornet, A. Davin-Régli, J.M. Pagès, C. Bollet, Resistance to imipenem, cefepime, and ceftiofime associated with mutation in Omp36 osmoporin of *Enterobacter aerogenes*, *Biochem. Biophys. Res. Commun.* 317 (2004) 851–856.
doi:10.1016/j.bbrc.2004.03.130.
- [46] J. Ishikawa, A. Yamashita, Y. Mikami, Y. Hoshino, H. Kurita, K. Hotta, et al., The complete genomic sequence of *Nocardia farcinica* IFM 10152., *Proc. Natl. Acad. Sci. U. S. A.* 101 (2004) 14925–14930. doi:10.1073/pnas.0406410101.
- [47] E. Cercenado, M. Marín, M. Sánchez-Martínez, O. Cuevas, J. Martínez-Alarcón, E. Bouza, In vitro activities of tigecycline and eight other antimicrobials against different *Nocardia* species identified by molecular methods., *Antimicrob. Agents Chemother.* 51 (2007) 1102–1104. doi:10.1128/AAC.01102-06.
- [48] L. Movileanu, J.P. Schmittschmitt, J.M. Scholtz, H. Bayley, Interactions of peptides with a protein pore., *Biophys. J.* 89 (2005) 1030–1045.
doi:10.1529/biophysj.104.057406.
- [49] J. Stephan, C. Mailaender, G. Etienne, M. Daffé, M. Niederweis, Multidrug resistance of a porin deletion mutant of *Mycobacterium smegmatis*., *Antimicrob. Agents Chemother.* 48 (2004) 4163–4170. doi:10.1128/AAC.48.11.4163-4170.2004.
- [50] O.H. Torres, P. Domingo, R. Pericas, P. Boiron, J.A. Montiel, G. Vázquez, Infection caused by *Nocardia farcinica*: case report and review., 2000.
doi:10.1007/s100960050460.
- [51] V. Jarlier, H. Nikaido, Permeability barrier to hydrophilic solutes in *Mycobacterium chelonae*., *J. Bacteriol.* 172 (1990) 1418–1423.
- [52] H. Gebhardt, X. Meniche, M. Tropis, R. Krämer, M. Daffé, S. Morbach, The key role of the mycolic acid content in the functionality of the cell wall permeability barrier in *Corynebacterineae*., *Microbiology.* 153 (2007) 1424–1434.
doi:10.1099/mic.0.2006/003541-0.
- [53] C.E. Barry, R.E. Lee, K. Mdluli, A.E. Sampson, B.G. Schroeder, R.A. Slayden, et al., Mycolic acids: Structure, biosynthesis and physiological functions, *Prog. Lipid Res.* 37 (1998) 143–179. doi:10.1016/S0163-7827(98)00008-3.

- [54] K.W. Langford, B. Penkov, I.M. Derrington, J.H. Gundlach, Unsupported planar lipid membranes formed from mycolic acids of *Mycobacterium tuberculosis*., *J. Lipid Res.* 52 (2011) 272–277. doi:10.1194/jlr.M012013.

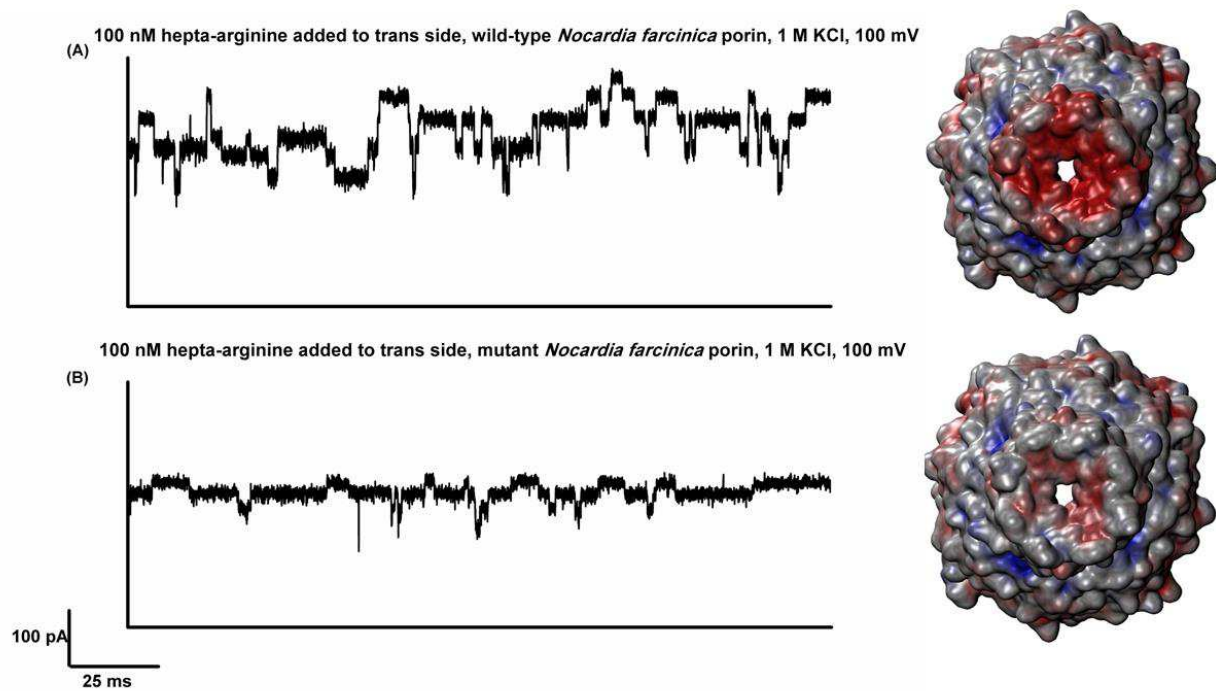
Supplementary Table 1: Primers used in this study to generate mutants, pARAJ52_ *nfpA/nfpB* was used as template. (The bases to be mutated are highlighted in red with small letters)

Primers	Sequence 5' → 3'
FP <i>nfpA</i> D141N D142N	GC CAG GTC AGC ATC GGT aACaAC GCC ATC TCG GCC GGCC
RP <i>nfpA</i> D141N D142N	G GCC GGC CGA GAT GGC GTtGTt ACC GAT GCT GAC CTG GC
FP <i>nfpB</i> E123Q D127N	G GGC GGC GTG cAA GGC TCG GCC aAt TGG AGC GGT GAC
FP <i>nfpB</i> E140Q and E144Q	GGC GTG GGC GCC cAG TCC GGC GGC cAG CTG ACG CTC GG
RP <i>nfpB</i>	A GCC GAG GCT GAA CGG CTG GCC CCA CAG GG
FP pARAJ52	GCA CGG CGT CAC ACT TTG C
RP pARAJ52	GAC CCG TTT AGA CCG CCC

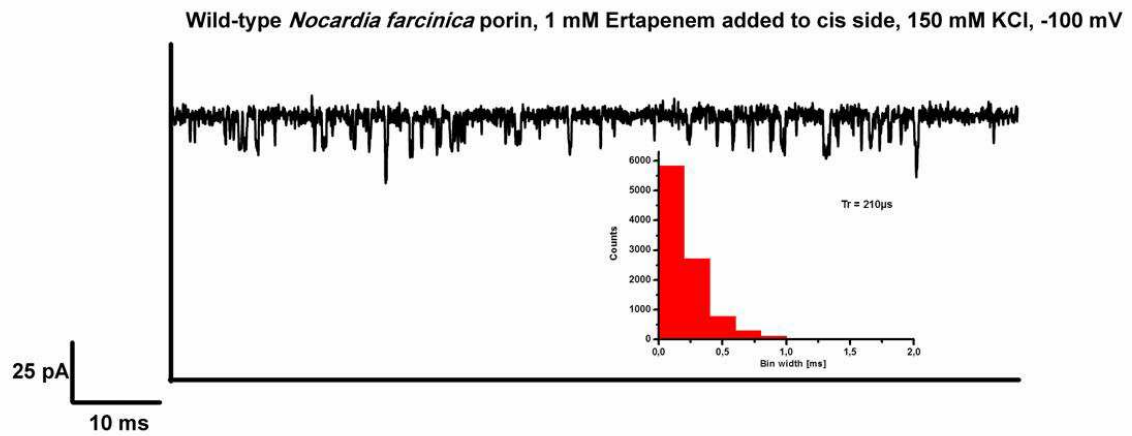
Supplementary Table 2: Amikacin and kanamycin binding kinetics were measured at 150 mM KCl, pH 7.4 at an application of -150 mV voltage. Ertapenem binding kinetics was measured at 1 M KCl, pH 7.4 at -100 mV.

	Wildtype porin			Mutant porin		
	K_{on}^{cis} [M ⁻¹ s ⁻¹ *10 ⁴]	K_{on}^{trans} [M ⁻¹ s ⁻¹ *10 ⁴]	K_{off} [s ⁻¹ *10 ³]	K_{on}^{cis} [M ⁻¹ s ⁻¹ *10 ⁴]	K_{on}^{trans} [M ⁻¹ s ⁻¹ *10 ⁴]	K_{off} [s ⁻¹ *10 ³]
Amikacin	2300 ± 200	NA	5 ± 1	750 ± 50	NA	10 ± 1
Kanamycin	27.5 ± 2	NA	NA	17 ± 2	NA	NA
Ertapenem	10.1 ± 1	2.4 ± 0.5	5.5 ± 1	10 ± 1	12 ± 1	5.5 ± 1

*NA= Not Applicable



Supplementary Figure 1: Functional activity of the hepta-arginine with the (A) WT and (B) mutant *N. farcinica* channel. The structures on the right panel show the electro-potential surface of both the channels visualized from the periplasmic (*trans*) side.



Supplementary Figure 2: Elucidating the electrostatic interaction of ertapenem with the *N. farcinica* cell wall channel. Ion current fluctuations were observed at 150 mM KCl, 10 mM MES, pH 7.4.

Chapter 3

Modulation of antibiotic permeation across OmpF channel in presence of Magnesium

Translocation of hydrophilic antibiotics through the outer-membrane of *E. coli* has been studied extensively. Interaction of different β -lactams, carbapenems and fluoroquinolones with the residues inside the OmpF and OmpC channels have shown the importance of affinity sites present inside the pore lumen. However, most of the experiments performed for such interactions have been done in a monovalent KCl salt solution. Physiological buffers constitutes of many different ions such as calcium, magnesium, iron, and phosphates, which can also interact with the amino acids residues inside the channel. In this chapter, we provide a simple experiment performed with an additional magnesium ion in the buffer solution and show the change in the interaction of antibiotics.

Chapter 3.1

Reprinted with permission from American Chemical Society

Singh, P. R., Ceccarelli, M., Lovelle, M., Winterhalter, M., & Mahendran, K. R. (2012). Antibiotic permeation across the OmpF channel: modulation of the affinity site in the presence of magnesium. The Journal of Physical Chemistry. B, 116(15), 4433–8. doi:10.1021/jp2123136

Copyright © 2012, American Chemical Society

Individual Contribution:

Single channel measurements and analysis, Contribution to composition of Manuscript

Antibiotic Permeation across the OmpF Channel: Modulation of the Affinity Site in the Presence of Magnesium

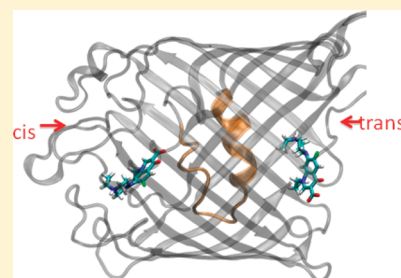
Pratik Raj Singh,[†] Matteo Ceccarelli,[‡] Marcos Lovelle,[†] Mathias Winterhalter,^{*,†} and Kozhinjampara R Mahendran^{*,†}

[†]Jacobs University Bremen, Campus Ring 1, D-28759 Bremen, Germany

[‡]Dipartimento di Fisica and Istituto Officina dei Materiali/CNR, UOS-SLACS, Università degli Studi di Cagliari, I-09042 Monserrato (CA), Italy

S Supporting Information

ABSTRACT: We characterize the rate-limiting interaction of the antibiotic enrofloxacin with OmpF, a channel from the outer cell wall of *Escherichia coli*. Reconstitution of a single OmpF trimer into planar lipid membranes allows measurement of the ion current through the channel. Penetration of antibiotics causes ion current blockages, and their frequency allows a conclusion on the kinetics of channel entry and exit. In contrast to other antibiotics, enrofloxacin is able to block the OmpF channel for several milliseconds, reflecting high affinities comparable to substrate-specific channels such as the maltodextrin-specific maltoporin. Surprisingly, the presence of a divalent ion such as Mg^{2+} leads to fast flickering with an increase in the rates of association and dissociation. All-atom computer modeling provides the most probable pathway able to identify the relevant rate-limiting interaction during antibiotic permeation. Mg^{2+} has a high affinity for the aspartic acid at the 113 position (D113) in the center of the OmpF intracellular binding site. Therefore, the presence of Mg^{2+} reverses the charge and enrofloxacin may cross the constriction region in its favorable orientation with the carboxylic group first.



INTRODUCTION

Gram-negative bacteria account for half of the life-threatening infections in clinics today, and in particular, increasing antibiotic resistance is an emerging problem. The first line of defense against antibiotics is the outer cell wall. Water-soluble antibiotics cross this barrier through membrane channels called porins. For example, β -lactams and quinolones have been commonly used for the treatment of bacterial infections.^{1–5} β -Lactams act on the peptidoglycan layer that is located between the outer and inner bacterial membranes, whereas quinolones target the DNA–topoisomerase complex in bacteria.^{1–5} To cross the outer membrane, the β -lactams and quinolones must pass through porins located in the outer membrane. In *Escherichia coli* two porins—OmpF and OmpC—are considered as a major pathway for antibiotic translocation.^{4,5} Both OmpF and OmpC channels are homotrimers, and in each monomer 16 β -strands span the outer membrane to form a barrel.^{6,7} Downregulation of these porins as well as point mutations can lead to reduced accumulation of quinolones (and other agents) within the cell.^{2–4} OmpF facilitates the diffusion of fluorinated quinolones such as norfloxacin and the cephalosporins such as cefoxitin into the periplasm, with marked reductions in accumulation of these agents in the OmpF-deficient bacterial strains.^{8,9} Therefore, quantifying the barrier for influx through porins might contribute to the complex question of multiple-drug resistance.

Recently we applied ion current fluctuation analysis on a single-channel level to gain insight into the interaction of

solutes with the channel interior.^{10–12} Permeation of molecules inside the channel causes fluctuations in the ion current, reflecting the particular interactions with the channel wall. The analysis of the ion current fluctuation allows permeation rates to be obtained as previously shown for sugars and antibiotics.^{10–12} As previously discussed, this approach has a number of limitations.¹³ First, ion current fluctuations can only be used as a signal for binding under the condition that the ion current occlusion during binding is strong enough to be recorded. However, binding does not imply translocation. Moreover, the time resolution is limited, and events faster than 0.1 ms will not be detected.¹³ In the case of charged molecules, the external field is an additional driving force; increasing the force should lead to faster translocation. In particular, for peptides, the residence time as a function of applied voltage can be used as a probe for true translocation.¹⁴ However, in the case of zwitterionic substances, a further method to evaluate translocation is needed.¹³ For example, molecular modeling provides details on the interaction of the molecules with the channel surface and reveals the preferred orientation of the antibiotic along its pathway.^{11,16}

Here, we investigate the interaction of the fluoroquinolone enrofloxacin with OmpF. In particular, we study the effect of applied transmembrane voltage and the presence of divalent ions,

Received: December 21, 2011

Revised: February 19, 2012

Published: February 27, 2012

in particular magnesium chloride, on antibiotic interaction. The hydrophobicity of enrofloxacin is very high, and its structure is shown in the inset in Figure 1. To allow a molecular

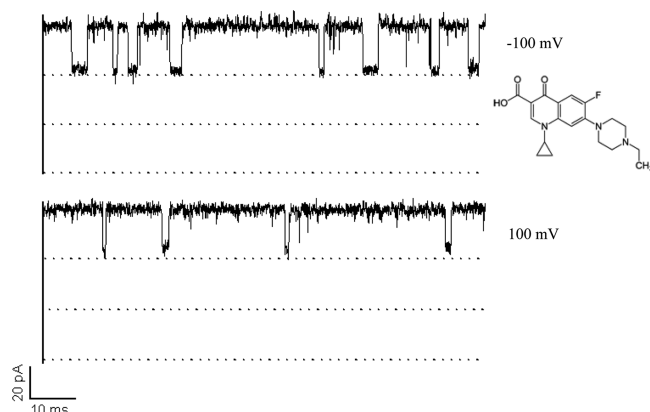


Figure 1. Ion current through a single OmpF trimeric channel in the presence of 1 mM enrofloxacin (cis side) at -100 and $+100$ mV. Ion current blockage events strongly depend on the polarity of the applied voltage. Reagents and conditions: 150 mM KCl, 5 mM MES, pH 6. The neutral structure of enrofloxacin is shown in the inset.

interpretation of the conductance measurements, we complement our study with all-atom molecular dynamics simulation. This allows identification of the antibiotic affinity sites in the channel and associated rate-limiting interactions.

■ EXPERIMENTAL SECTION

The following chemical reagents were used in this study: NaCl, KCl, $MgCl_2$, MES, *n*-pentane, and hexadecane (Sigma), enrofloxacin (Fluka), *n*-octylpoly(oxyethylene) (octyl-POE) (Bachem, Bubendorf, Switzerland), and 1,2-diphytanoyl-*sn*-glycero-3-phosphatidylcholine (DPhPC) (Avanti Polar Lipids, Alabaster, AL). Doubly distilled and deionized water was used to prepare all solutions.

Single-Channel Conductance Measurements. Virtually solvent-free planar lipid membranes were formed using diphytanoylphosphatidylcholine (DPhPC) (Avanti Polar Lipids, Alabaster, AL) according to the Montal–Mueller technique.¹⁵ The measurements were carried out with standard buffer containing 150 mM KCl and 5 mM MES, pH 6.0, that serves as an electrolyte. Complementary experiments contained in addition 5 mM $MgCl_2$. A Teflon cell with an approximately 50–100 μm diameter aperture in the 25 μm thick Teflon partition was used together with standard silver–silver chloride electrodes from WPI (World Precision Instruments). Small amounts of OmpF porin from a diluted stock solution of 1 mg/mL were added to the cis side of the chamber (side connected to the ground electrode). Spontaneous channel insertion was usually obtained with stirring under an applied voltage. Conductance measurements were performed using an Axopatch 200B amplifier (Axon Instruments) in the voltage clamp mode. Signals were filtered by an on-board low-pass Bessel filter at 10 kHz and recorded onto a computer hard drive with a sampling frequency of 50 kHz. Amplitude, probability, and noise analyses were performed using Origin (Microcal Software Inc.) and Clampfit (Axon Instruments) software. The enrofloxacin stock solution for conductance measurements was made at a final concentration of 2.0 mM in 150 mM KCl, 5 mM $MgCl_2$, and 5 mM MES (pH 6.0). Enrofloxacin was added

to the cis and trans sides of the chamber to investigate their permeation rates through the porin channels. Kinetic parameters of the enrofloxacin binding for the asymmetric and symmetric drug addition were calculated by single-channel analysis. The association rate constant k_{on} gives the permeation of the antibiotic molecule from the cis or trans side to the affinity site in the channel. The dissociation rate constant k_{off} gives the rate at which antibiotic molecules were released from the channel affinity site to the cis or trans aqueous phase. The equilibrium binding constant K (ratio of k_{on} to k_{off}) defines the affinity of the drug for the porin molecule.^{10–12}

Molecular Dynamics Simulations. The starting structure for the OmpF channel was prepared as shown previously.¹⁶ We used one monomer of the crystal structure (PDB code 2OMF) that was resolved at a resolution of 2.4 Å. We embedded the system in a hydrophobic environment of detergent molecules (lauryldimethylamine oxide, LDAO) and solvated the system with ~ 8000 water molecules; we used the Amber potential and TIP3P for water. The force field for the enrofloxacin antibiotic was derived following the Amber force field rules with charges obtained from the Gaussian program (6-31G** basis set) on the optimized geometry of the molecule. We performed MD simulations with the Orac²⁷ program: we simulated a periodic box in the NVT ensemble using the Nose thermostat (300 K), a 10 Å cutoff, and soft particle mesh Ewald (SPME) (fifth order, grid less than 1 Å in size) for electrostatic interactions and the multiple-time-step algorithm (time steps of 0.5, 1.0, 2.0, 4.0, and 12 fs).

Using the metadynamics algorithm, we employed MD simulations to reveal the translocation mechanism of enrofloxacin through the OmpF channel.¹⁶ The metadynamics algorithm allows the reconstruction of the free energy in the subspace of the collective variables by integrating the history-dependent terms. Molecular dynamics simulations of the enrofloxacin–OmpF complex started with the antibiotic added on the extracellular side at 10 Å from the constriction region, as discussed previously.¹⁶ We added a magnesium ion near the constriction region, substituting for a potassium ion there, and to maintain the box neutral, we eliminated an additional potassium ion. For the magnesium ion, we used the standard Amber parameters¹⁷ derived from free energy perturbation simulations ($R^* = 0.7926$ Å, $\epsilon = 0.8947$ kcal/mol). Recently new parameters were obtained by fitting the osmotic pressure,²⁶ and the main problem was representing ions as a uniformly charged sphere. We allowed the system to equilibrate from 100 to 300 K for 1.5 ns before starting the metadynamics simulations. As shown previously,¹⁶ we used two collective variables: (1) the angle θ , the orientation of the enrofloxacin long axis (almost parallel to the dipole moment) with respect to the z axis of OmpF, and (2) the distance Z , the projection along the z axis of the position of the center of mass of enrofloxacin with respect to the center of mass of OmpF. We added with a frequency of 4 ps a bias to force the system to sample more efficiently the subspace of the two collective variables, a repulsive Gaussian potential of 1.0 kJ/mol height and 5.0° and 0.4 Å width, respectively, for the two variables. The choice of these parameters allows an equilibration of the other degree of freedom and the reconstruction of the free energy with an error not exceeding 2 kcal/mol.¹⁶ We used a single metadynamics trajectory allowing enrofloxacin to go from the extracellular space to the periplasmic space to identify the free energy minima in the space of the two collective variables, the angle θ and distance Z . Additional standard MD

simulations were performed with enrofloxacin in the different minima to analyze its specific interactions.

RESULTS AND DISCUSSION

Ion Current Blockage To Reveal On and Off Rates. To quantify the kinetics of enrofloxacin interaction, we reconstituted a single OmpF trimer in artificial planar lipid membranes. Studying OmpF channels at different voltages reveals a slight asymmetry with respect to ion conductance. For example, if the porin is added to the cis side of the chamber, the single-channel conductance is slightly higher ($G = 1.0$ nS) at positive voltage compared to negative voltage ($G = 0.9$ nS). As we obtain a strong correlation of this asymmetry with the side of protein addition, we use this feature as a test for the direction of the channel insertion.^{12,16} Addition of enrofloxacin to the system caused transient blockage of the ionic current through a single trimeric OmpF channel in a voltage-dependent manner. Figure 1 shows that penetrating enrofloxacin interacts with the OmpF channel, resulting in channel blockages. At low drug concentration, enrofloxacin interacts with the OmpF channel, resulting in monomer blocking, and at increasing concentration, dimer and trimer blocking is visible.¹⁶

The number of blockage events and average residence time were calculated by ion current fluctuation analysis. Figure 2

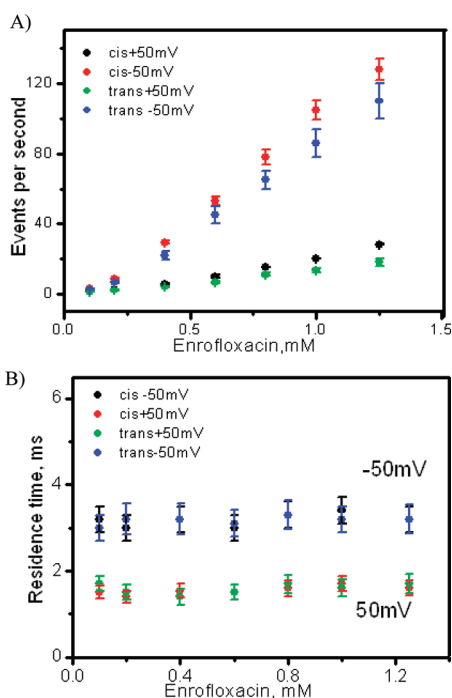


Figure 2. (a) The number of events is linear with the concentration of the enrofloxacin used and depends on the applied voltage. (B) The average residence time does not depend on the concentration of drug but the applied voltage.

summarizes the number of events and residence times of penetrating enrofloxacin under various concentrations and applied voltages. Surprisingly, Figure 2 shows high asymmetry in the residence time and blocking events with respect to the polarity of the applied transmembrane potential. At negative voltages, blockages are 10 times more frequent than at positive voltages irrespective of the concentration of the antibiotic used (Figure 2A). Single-channel analysis revealed an exceptionally long residence time for enrofloxacin in the OmpF channel.

The average residence time of enrofloxacin strongly depends on the applied voltage but not on the concentration of antibiotic used (Figure 2B). The average residence time was calculated to be 3.5 ± 0.5 ms at -100 mV and 1 ± 0.3 ms at $+100$ mV. Such a long residence time is a result of strong interaction between the penetrating antibiotic and the binding site in the porin and is approximately 1 order of magnitude higher than those for various β -lactams.^{10,11,18} Previously, it has been shown that wild-type OmpF has two symmetric binding sites for enrofloxacin located at each channel entry separated by a large energy barrier in the center and the ion current blockages are caused by enrofloxacin molecules occupying either one of these peripheral binding sites.¹⁶ However, this longer residence time of enrofloxacin does not imply an effective translocation.^{16,19} The affinity constant of enrofloxacin in the case of OmpF is comparable to the specific affinity of maltooligosaccharides to maltoporin.¹² The ability of enrofloxacin to specifically block the ion currents through the OmpF channel for a longer time can be used to identify this channel.

In a second series of measurements, we investigate the effect of magnesium ion on the interaction of enrofloxacin with OmpF. Surprisingly, addition of magnesium causes a dramatic change in the enrofloxacin binding kinetics. Figure 3 shows the

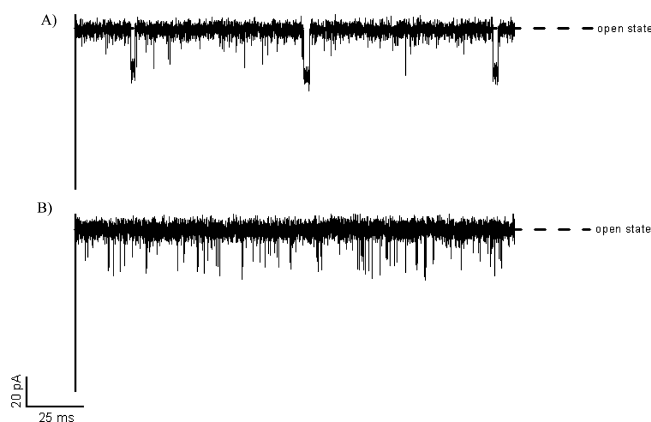


Figure 3. Enrofloxacin ($100 \mu\text{M}$) induced ionic current fluctuations through a single OmpF channel in the (A) absence and (B) presence of magnesium chloride. Reagents and conditions: 150 mM KCl, 5 mM MgCl_2 , 5 mM MES, pH 6, 100 mV.

ion current blockage events of enrofloxacin through a single trimeric OmpF channel in the presence and absence of magnesium chloride. In the presence of magnesium chloride, enrofloxacin (cis side addition) blocks the ion current through the OmpF channel with fast flickering events. The effect observed in the presence of MgCl_2 strongly depends on the polarity of the applied voltage and the side of drug addition. The number of enrofloxacin blocking events increased and the average residence time decreased at positive voltages but not at negative voltages. The effect of interaction is stronger if enrofloxacin is added to the trans side of the chamber. The strong blocking at trans side addition does not allow individual blocking events to be distinguished but causes rather a reduction in the ion conductance. To resolve individual blocking events, we lowered the concentration of enrofloxacin to $5 \mu\text{M}$. As shown in Supplementary Figure 1 (Supporting Information), we observed clear monomer blockage events. The average residence time of enrofloxacin in the OmpF was calculated to

be 1.2 ± 0.3 ms in the absence of magnesium ions and $100 \mu\text{s}$ in the presence of magnesium chloride at 100 mV (Figure 4).

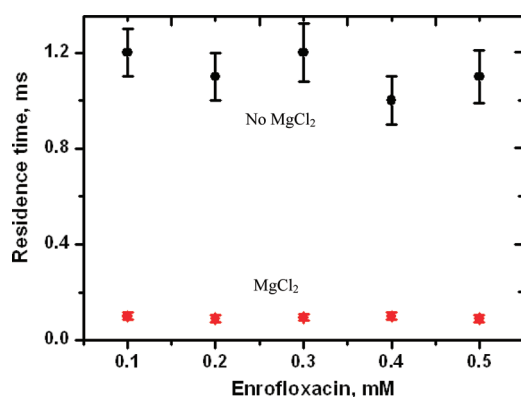


Figure 4. Average residence time of enrofloxacin through the OmpF channel in the absence and presence of magnesium chloride at different antibiotic concentrations. Reagents and conditions: 150 mM KCl , 5 mM MgCl_2 , 5 mM MES , $\text{pH } 6$, 100 mV .

Kinetic constants and on and off rates of enrofloxacin binding to the OmpF channel in the absence and presence of magnesium chloride are presented in Table 1.

Free Energy Profiles and Rate-Limiting Interactions.

The crystal structure of the OmpF channel in the presence of 1 M MgCl_2 shows that the Mg^{2+} cation was bound between residues D113 and E117.²⁰ Although the conditions used there are not specific to investigation of the binding of ions, previous theoretical and experimental investigations confirmed a specificity of this region to interact with divalent cations.^{21,25} In our simulation, the Mg^{2+} interacts directly with two oxygens of the protein and with four water molecules. We reconstructed the free energy surface using our reactive metadynamics path with enrofloxacin that moves from the extracellular to the periplasmic space (Figure 5A). We identified two minima, the first in the extracellular side, at position ($\theta = 160^\circ$, $Z = +7 \text{ \AA}$), and the second near the constriction region and shifted more toward the periplasmic space, at position ($\theta = 130^\circ$, $Z = -4 \text{ \AA}$). The latter is not present in the simulation without magnesium ion¹⁶ (Figure 5B), where we identified a minimum with a different orientation ($\theta = 50^\circ$, $Z = -4 \text{ \AA}$). From the reconstructed free energy surface, we evaluated the effective barrier to translocate from the extracellular to the periplasmic space at 10 kcal/mol , to be compared to 15 kcal/mol without magnesium (Figure 5 C,D). In Figure 6, we report a snapshot of enrofloxacin in the new central minimum. We calculated the area accessible to the solvent when enrofloxacin occupies this affinity site, and it has a value of 6.2 \AA^2 , while the minimum dimension of the pore is on average 26.3 \AA^2 ,

only 23% availability of the total space, which explains the current blockages observed experimentally. The enrofloxacin transverses the constriction region with the carboxylic group pointing down, and the same orientation is kept in the central affinity site with the hydrophobic group, which carries the positive charge, close to the L3 loop (Figure 6). It is important to note that in our simulation there is no external electric field biasing the orientation of enrofloxacin during translocation. Interestingly, in our simulation, the Mg^{2+} ion, positioned near the L3 loop, is able to screen completely the carboxylic group of residue D113, producing local charge inversion.²⁵

We show that, in the presence of magnesium chloride, enrofloxacin has completely different binding kinetics for the OmpF channel. The antibiotic blocks the channel with more frequent binding events and a shorter residence time of $100 \mu\text{s}$, which indicates that the rates for association (k_{on}) and dissociation (k_{off}) drastically increase in the presence of magnesium chloride. MD simulations show that enrofloxacin now can traverse the constriction region with the carboxylic group pointing down, while without magnesium this orientation is inhibited by the strong repulsion with the aspartic acid at the 113 position (D113). The position of the magnesium ion allows the complete screening of D113 and increases the probability of antibiotic reaching the central affinity site starting from the cis side. The antibiotic crosses the constriction region and further translocates through the channel. Interestingly, the enrofloxacin binding kinetics in the presence of magnesium strongly depends on the polarity of the applied voltage. The increase in k_{on} and k_{off} was observed only at positive voltages (Table 1). The positive voltages promote the orientation of enrofloxacin with the carboxylic group pointing down. This is also the position assumed by enrofloxacin at the central affinity site; see Figure 5A. However, at negative voltages, enrofloxacin orientation has the carboxylic group up and it is not favored to occupy the new central affinity site. In our study, we observed ion current blockage in channels when enrofloxacin was added asymmetrically to either the cis or trans side of the channel. When the antibiotic was added to the trans side (periplasmic side) of the chamber, the binding events were about twice as frequent as when the antibiotic was added to the cis side (extracellular side) in the presence of magnesium chloride (Table 1). This is also suggested by inspection of the free energy surface of Figure 5A: Because the central affinity site is more shifted toward the trans side, the addition of antibiotics here favors its occupation, resulting in faster kinetics. On the other hand, when the antibiotic is added on the cis side, it has to traverse the constriction region before it can occupy the central affinity site, with a barrier that we calculated to be 10 kcal/mol .

Table 1. Association (k_{on}) and Dissociation (k_{off}) Rate Constants and Equilibrium Constant (K) Obtained by Single-Channel Conductance Measurements on OmpF^a

	$k_{\text{on}}^{\text{cis}} (\text{M}^{-1} \text{s}^{-1}) \times 10^3$	$k_{\text{on}}^{\text{trans}} (\text{M}^{-1} \text{s}^{-1}) \times 10^3$	$k_{\text{off}}^{\text{total}} (\text{s}^{-1}) \times 10^3$	$K (\text{M}^{-1})$
+100 mV	4 ± 0.3	4 ± 0.3	0.7 ± 0.05	11 ± 1
+100 mV (MgCl_2)	2100 ± 200	26000 ± 2000	11 ± 1	2500 ± 200
-100 mV	12 ± 1	11 ± 1	0.29 ± 0.02	80 ± 7
-100 mV (MgCl_2)	11 ± 1	10 ± 1	0.30 ± 0.02	70 ± 6

^a $k_{\text{on}} = (\text{number of events s}^{-1}) / (\text{antibiotic concentration})$, $k_{\text{off}} = 1 / (\text{average residence time})$, and $K = k_{\text{on}} / k_{\text{off}}$. The enrofloxacin concentration was $100 \mu\text{M}$.

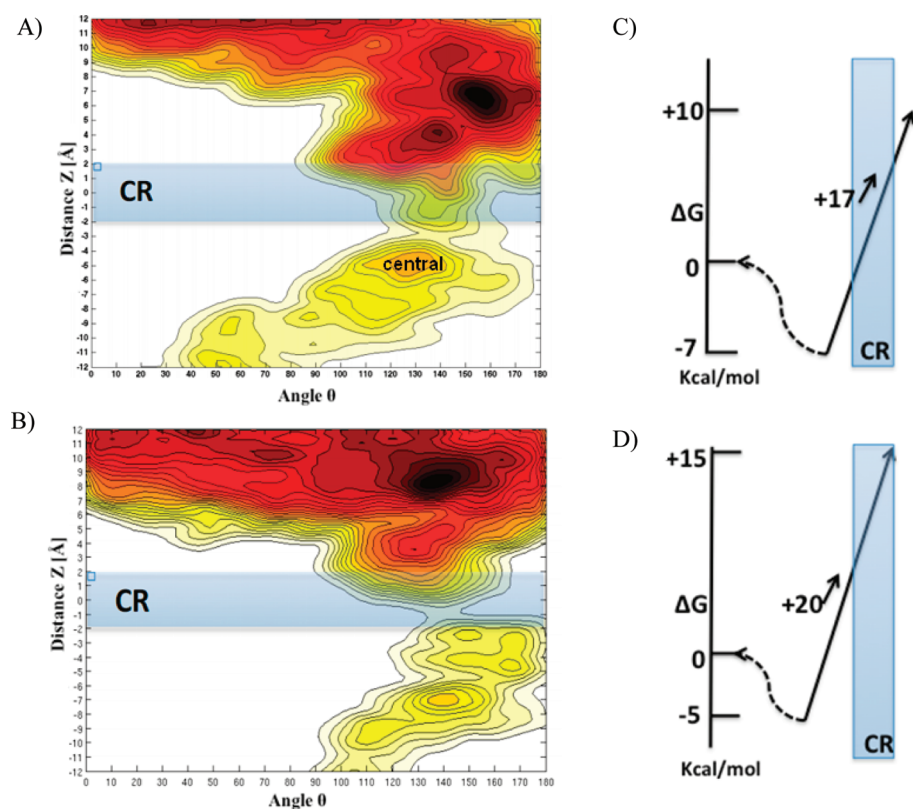


Figure 5. Reconstructed free energy surface from metadynamics for enrofloxacin traversing the OmpF channel in the presence of magnesium (A) and without magnesium (B). Panel B is reprinted from ref 16. Copyright 2010 American Chemical Society. The two collective variables are the angle θ along the x direction and the distance Z along the y direction. Each color corresponds to a 1 kcal/mol energy difference. In panels C and D we report the 1-D minimum free energy path for the two simulations as extracted from panels A and B, respectively.

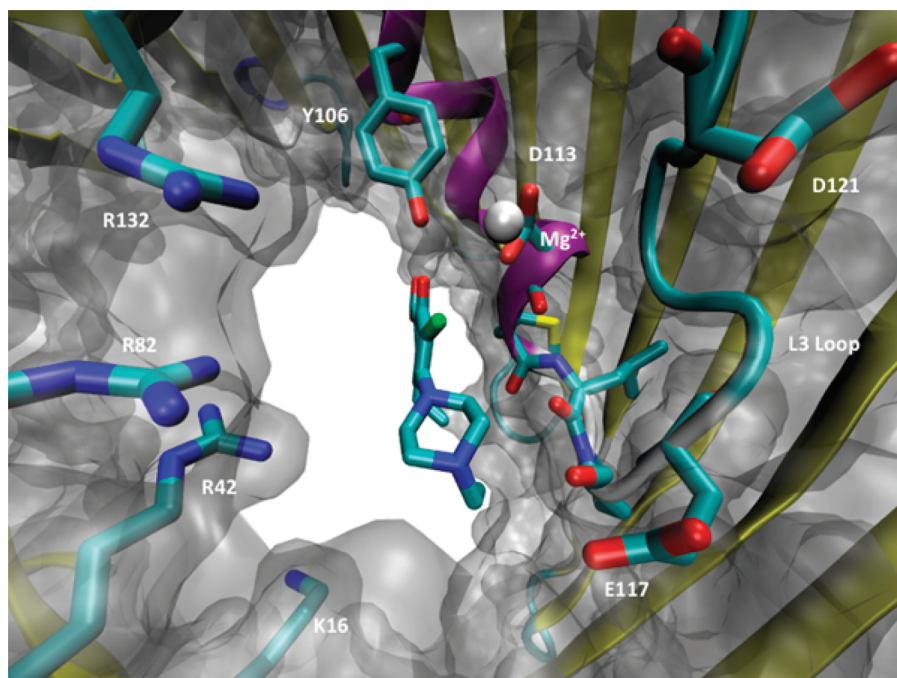


Figure 6. Molecular interaction of enrofloxacin with the OmpF channel in the preferential affinity site near the constriction region in the presence of magnesium (white sphere), showing specific interactions between enrofloxacin and the residues of the channel affinity site.

CONCLUSION

Ion current fluctuation analysis has often been used to characterize permeation of water-soluble antibiotics through a

membrane channel. Favorable interaction increases the concentration of the drug inside the channel and enhances the number of translocation events. Combining ion current

fluctuation analysis and atomistic computer simulations, we arrive at a picture demonstrating enrofloxacin translocation through the OmpF porin. Although most of the antibiotic shows a very low affinity for the OmpF channel, enrofloxacin is a striking exception. Pronounced blocking of OmpF channels with enrofloxacin was observed, and blocking does not imply translocation. However, the presence of magnesium chloride alters the affinity of the antibiotic for the channel wall. Binding of Mg^{2+} to residue D113 completely screens the charge, producing a local charge inversion that favors the antibiotic to cross the constriction region and further translocate with a faster kinetics. Our results reinforce the idea that OmpF works as an electrostatic filter against antibiotic translocation.^{23,24} This is in agreement with a recent analysis of all marketed drugs: among these, antibiotics have the strongest polar character.²² Translocation of antibiotics is dominated by electrostatics, and in the future trivalent ion La^{3+} could be tried to understand new physical insights into translocation.²⁵ Our analysis of the data provides a full quantitative description of relevant kinetic and electric parameters of enrofloxacin interaction with the channel surface in the presence of magnesium.

■ ASSOCIATED CONTENT

● Supporting Information

Structure of enrofloxacin and ionic currents through the single OmpF channel in the presence of 5 μM enrofloxacin added to the trans side at +100 mV. This material is available free of charge via the Internet at <http://pubs.acs.org>.

■ AUTHOR INFORMATION

Corresponding Author

*E-mail: k.mahendran@jacobs-university.de (K.R.M.); m.winterhalter@jacobs-university.de (M.W.).

Notes

The authors declare no competing financial interest.

■ ACKNOWLEDGMENTS

We are grateful for financial support from the Deutsche Forschungsgemeinschaft (Grant DFG WI 2278/18-1) and from Jacobs University Bremen. M.C. thanks the Cybersar consortium at the University of Cagliari for CPU time allocation. We acknowledge an anonymous reviewer for the suggestion to test La^{3+} .

■ REFERENCES

- (1) Nikaido, H. *Microbiol. Mol. Biol. Rev.* **2003**, *67*, 593–656.
- (2) Mazzariol, A.; Tokue, Y.; Kanegawa, T. M.; Cornaglia, G.; Nikaido, H. *Antimicrob. Agents Chemother.* **2000**, *44*, 3441–3443.
- (3) Webber, M.; Piddock, L. J. *Vet. Res.* **2001**, *32*, 275–284.
- (4) Yoshimura, F.; Nikaido, H. *Antimicrob. Agents Chemother.* **1985**, *27*, 84–92.
- (5) Pagès, J. M.; James, C. E.; Winterhalter, M. *Nat. Rev. Microbiol.* **2008**, *6*, 893–903.
- (6) Cowan, S. W.; Schirmer, T.; Rummel, G.; Steiert, M.; Ghosh, R.; Paupit, R. A.; Jansonius, J. N.; Rosenbusch, J. P. *Nature* **1992**, *358*, 727–733.
- (7) Basle, A.; Rummel, G.; Storici, P.; Rosenbusch, J. P.; Schirmer, T. *J. Mol. Biol.* **2006**, *362*, 933–942.
- (8) Lou, H.; Chen, M.; Black, S. S.; Bushell, S. R.; Ceccarelli, M.; Mach, T.; Beis, K.; Low, A. S.; Bamford, V. A.; Booth, I. R.; Bayley, H.; Naismith, J. H. *PLoS ONE* **2011**, *6*, e25825.
- (9) Bredin, J.; Saint, N.; Malléa, M.; De, E.; Molle, G.; Pagès, J. M.; Simonet, V. *Biochem. J.* **2002**, *363*, 521–528.
- (10) Nestorovich, E. M.; Danelon, C.; Winterhalter, M.; Bezrukov, S. M. *Proc. Natl. Acad. Sci. U.S.A.* **2002**, *99*, 9789–9794.
- (11) Danelon, C.; Nestorovich, E. M.; Winterhalter, M.; Ceccarelli, M.; Bezrukov, S. M. *Biophys. J.* **2006**, *90*, 1617–1627.
- (12) Kullman, L.; Winterhalter, M.; Bezrukov, S. M. *Biophys. J.* **2002**, *82*, 803–812.
- (13) Mahendran, K. R.; Chimere, C.; Mach, T.; Winterhalter, M. *Eur. Biophys. J.* **2009**, *38*, 1141–1145.
- (14) Movileanu, L.; Schmittschmitt, J. P.; Scholtz, J. M.; Bayley, H. *Biophys. J.* **2005**, *89*, 1030–1045.
- (15) Montal, M.; Mueller, P. *Proc. Natl. Acad. Sci. U.S.A.* **1972**, *69*, 3561–3566.
- (16) Mahendran, K. R.; Hajjar, E.; Mach, T.; Lovelle, M.; Kumar, A.; Sousa, I.; Spiga, E.; Weingart, H.; Gameiro, P.; Winterhalter, M.; Ceccarelli, M. *J. Phys. Chem. B* **2010**, *114*, 5170–5179.
- (17) Åqvist, J. *J. Phys. Chem.* **1990**, *94*, 8021–8024.
- (18) Mahendran, K. R.; Kreir, M.; Weingart, H.; Fertig, N.; Winterhalter, M. *J. Biomol. Screening* **2010**, *15*, 302–307.
- (19) Berezhkovskii, A. M.; Bezrukov, S. M. *Biophys. J.* **2005**, *88*, L17–L19.
- (20) Yamashita, E. M.; Zhalnina, V.; Zakharov, S. D.; Sharma, O.; Cramer, W. A. *EMBO J.* **2008**, *27*, 2171–2180.
- (21) García-Giménez, E.; López, M. L.; Aguilera, V. M.; Alcaraz, A. *Biochem. Biophys. Res. Commun.* **2011**, *404*, 330–334.
- (22) Payne, D. J.; Gwynn, M. N.; Holmes, D. J.; Pompliano, D. L. *Nat. Rev. Drug Discovery* **2007**, *6*, 29–40.
- (23) Delcour, A. H. *Front. Biosci.* **2003**, *8*, d1055–71.
- (24) Berezhkovskii, A. M.; Pustovoit, M. A.; Bezrukov, S. M. *J. Chem. Phys.* **2002**, *116*, 9952–9956.
- (25) Aguilera-Arzo, M.; Calero, C.; Faruqi, J. *Soft Matter* **2010**, *6*, 6079–6082.
- (26) Yoo, J.; Aksimentiev, A. *J. Phys. Chem. Lett.* **2012**, *3*, 45–50.
- (27) Procacci, P.; Darden, T. A.; Paci, E.; Marchi, M. *J. Comput. Chem.* **1997**, *18*, 1848–1862.

Supporting information

Antibiotic permeation across OmpF channel: Modulation of affinity site in the presence of magnesium

Pratik Raj Singh¹, Matteo Ceccarelli², Marcos Lovelle¹, Mathias Winterhalter*¹, Kozhinjampara R Mahendran*¹

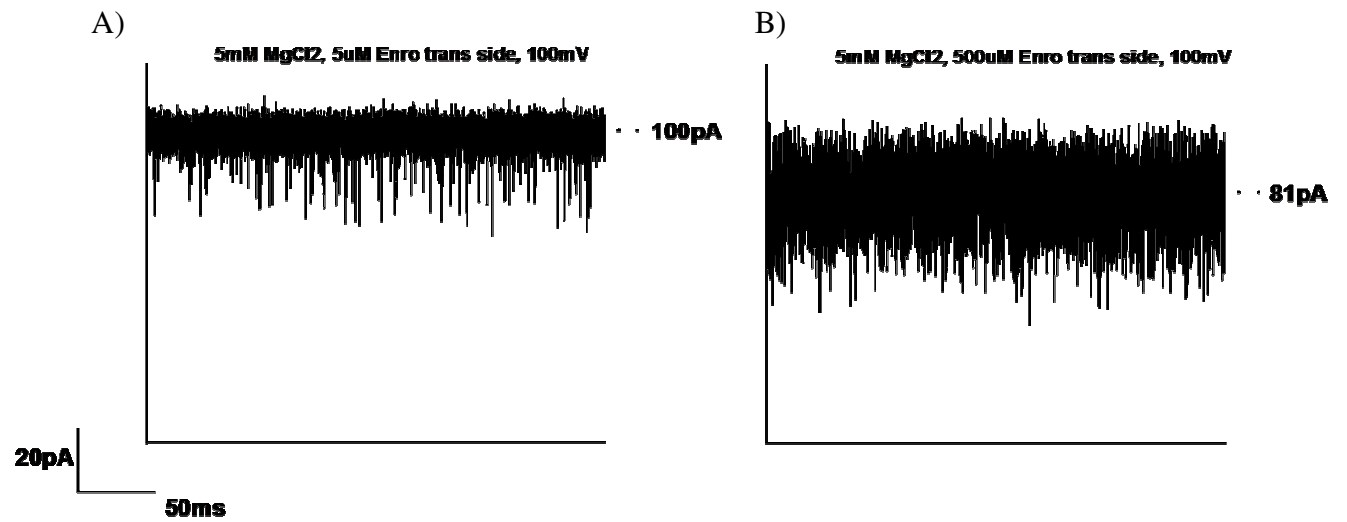
¹ Jacobs University Bremen, Campus Ring 1, D-28759 Bremen, Germany

² Dipartimento di Fisica and Istituto Officina dei Materiali/CNR, UOS-SLACS
Università degli Studi di Cagliari, I-09042 Monserrato (CA), Italy

Correspondence*: k.mahendran@jacobs-university.de
m.winterhalter@jacobs-university.de

Supplementary Figure 1

Ionic currents through single OmpF channel in presence of A) 5 μ M enrofloxacin and B) 500 μ M enrofloxacin added to trans side at +100mV. 150mM KCl, 5mM MgCl₂, 5mM MES, pH 6



Chapter 4

Slowing down antibiotic permeation **using Ionic Liquids**

There has been a constant improvement in the instrumentation technology for electrophysiology measurements. Better amplifiers, higher signal-to-noise ratio, multiple throughput possibility, miniaturization of devices etc. have significantly increased our capability of data collection and analysis. However, we are still limited with the temporal resolution of the instrument. The inefficiency of the instrument to detect fast permeation events in the time scale lower than 100 μ s has become problematic. Various approaches such as lowering the temperature of the system and reducing the kinetic energy of the molecules to slow down the permeation of solutes have been reported. In this chapter, we use bulky ionic-liquids as a substitute electrolyte solution to KCl in order to slow down antibiotic permeation events.

The first part of the chapter consists of a publication in *Journal of Physics: Condensed matter*. This publication depicts the use of 1-Butyl 3-methyl Imidazolium Chloride electrolyte solution to slow down the kinetics of ampicillin through the OmpF channel. The conductance of the OmpF channel in presence of ionic liquids was measured and the kinetics of ampicillin through the channel was analyzed. We observe that the residence time of ampicillin inside the OmpF channel increased from 300 μ s (in KCl solution) to 1ms, slowing down its permeation.

The second part of the chapter consists of a publication in *Journal of physical chemistry letters*. This publication illustrates the atomistic details of permeation of ionic liquid through the OmpF channel using applied field molecular dynamics simulation. The experimental bulk conductivity of ionic liquid at various temperatures was measured and compared to with the simulation bulk conductivity to obtain a suitable model. This was later used to compare with the experimental values of OmpF conductance at different temperature. We also extended the approach to mutant OmpF D113N pore.

The third part of the chapter is an unpublished supplement, where we study the changes in conductance of OmpF mutants in presence of ionic liquid. We also combine two known approaches, ionic liquids and temperature, to slow down the permeation of ampicillin. Combining them, we were successfully able to slow down the permeation of ampicillin by 20 times. We also plotted an Arrhenius plot to show the increase in the energy barrier of ampicillin translocation through the OmpF pore using Ionic liquid.

Chapter 4.1

Reprinted with permission from Journal of Physics: Condensed Matter

Mahendran, K. R., Singh, P. R., Arning, J., Stolte, S., Kleinekathöfer, U., & Winterhalter, M. (2010). Permeation through nanochannels: revealing fast kinetics. Journal of Physics. Condensed Matter : An Institute of Physics Journal, 22(45), 454131. doi:10.1088/0953-8984/22/45/454131

Individual Contribution:

Single channel measurements and analysis

Permeation through nanochannels: revealing fast kinetics

This content has been downloaded from IOPscience. Please scroll down to see the full text.

2010 J. Phys.: Condens. Matter 22 454131

(<http://iopscience.iop.org/0953-8984/22/45/454131>)

View [the table of contents for this issue](#), or go to the [journal homepage](#) for more

Download details:

IP Address: 212.201.44.247

This content was downloaded on 12/06/2014 at 15:04

Please note that [terms and conditions apply](#).

Permeation through nanochannels: revealing fast kinetics

Kozhinjampara R Mahendran¹, Pratik Raj Singh¹,
Jürgen Arning², Stefan Stolte²,
Ulrich Kleinekathöfer¹ and Mathias Winterhalter¹

¹ School of Engineering and Science, Jacobs University Bremen, Campus Ring 1, Bremen 28759, Germany

² Center for Environmental Research and Sustainable Technology (UFT), Universität Bremen, Leobenerstrasse, Bremen 28359, Germany

Received 3 June 2010, in final form 11 August 2010

Published 29 October 2010

Online at stacks.iop.org/JPhysCM/22/454131

Abstract

The permeation of water soluble molecules across cell membranes is controlled by channel-forming proteins and, in particular, the channel surface determines the selectivity. An adequate method to study the properties of these channels is electrophysiology and, in particular, analyzing the ion current fluctuation in the presence of permeating solutes. Ion current fluctuation analysis provides information on possible interactions of solutes with the channel surface. Due to the limited time resolution, fast permeation events are not visible using standard techniques. Here, we demonstrate that miniaturization of the lipid bilayer; varying the temperature or changing the solvent may enhance the resolution. Although electrophysiology is considered as a single molecule technique, it does not provide atomic resolution. Molecular details of solute permeation can be revealed by combining electrophysiology and all-atom computer modeling; these methods include ion conductance, selectivity, ion pair formation, and rate limiting interactions of the solute with the channel walls during permeation.

(Some figures in this article are in colour only in the electronic version)

1. Introduction

Cell walls are barriers separating the interior functional space from the outside, while at the same time these two volumes need to be connected in a selective manner. To control the passage across the separating membrane, nature has created a large number of membrane channels which act as selective gates for water soluble molecules. The most suited method to characterize such membrane channels is electrophysiology either via reconstitution of the channels into planar lipid membranes or through patching a small fraction of an intact cell membrane [1, 2]. The basic principle is to apply a transmembrane voltage to drive ions through the channel. The insulating property of a lipid membrane provides an extreme contrast to the ion conducting channel. For more than 40 years, such measurements have provided information of the possible channel size, selectivity or conformational changes [1–3]. For example, to a first approximation the pore sizes can be estimated by measuring the conductance and assuming the pore to be an homogeneous cylinder. However,

often the true pore size deviates substantially from a cylindrical model. To rule out apparent large or small pore sizes, different ions and concentrations need to be applied. Furthermore multimeric or wedge shaped pores can be discriminated using the conductance contrast between channel penetrating/non-penetrating polymers [4]. Likewise ion selectivity can be revealed under quasi-equilibrium conditions of a salt gradient [1, 2, 5]. Unfortunately, the complex geometry and charge distribution together with the underlying long range electrostatic interactions often makes a simplified description of the system problematic. To date, the most accurate dynamical modeling for systems of this kind can be obtained using all-atom molecular dynamics (MD) simulations [6–15].

Typical biological channels have pore radii of around one nanometer or less and a length of about 4–5 nm which corresponds to a volume of 10^{-23} l. This implies that already about one molecule inside the channel correspond to molar concentrations. Thus, the additional presence of charged or uncharged molecules which may penetrate or permeate through the channel will modify the conductance. Moreover, small

molecules have typically a self-diffusion coefficient of around $10^{-9} \text{ m}^2 \text{ s}^{-1}$ in aqueous solution; subsequently allowing molecules to freely diffuse through the channel in a few nanoseconds. The permeation of freely diffusing molecules is too fast to be resolved by current experimental techniques.

The confinement of the ion current in molecular dimensions allows for detecting minor changes in the channel size. Any substrate molecule within the channel will automatically interact with the channel surface and eventually cause fluctuations in the ion current. Some years ago Nekolla and coworker introduced the power density spectra of ion current fluctuations to reveal the rates and energy barrier for maltooligosaccharides' permeation through maltoporin [16]. In a seminal investigation, this principle has been applied to distinguish individual nucleotides of single stranded DNA [17]. Later it was shown that binding of maltodextrins to the maltoporin channel blocks the passage of ions through the channel at the single molecule level [18]. Moreover, exploiting the selectivity of such natural or bioengineered channels has promising applications for detecting molecules, characterizing molecular interaction, observing peptide folding, and a potential to be utilized as selective gates in self-assembled nanoscale engineered systems [19].

Our group recently focused on the entry pathway of antibiotics into bacteria [20–25]. Obviously a channel like OmpF is not optimized by the bacteria to allow uptake of antibiotics. Nevertheless some drug molecules turned out to be efficiently translocated as they show an affinity with the interior of the channel. In our initial studies, zwitterionic ampicillin and OmpF were investigated, which showed a similar type of ion current blockage as known from maltodextrins in maltoporin [21]. Comparing other antibiotics, e.g. penicillin G, revealed no additional noise despite their biological activity, indicating permeation through the OmpF channel. Originally this was interpreted as no interaction and subsequently no translocation. Now it is understood that the temporal resolution of the instrument limits the detection of fast translocation events [25]. Consequently, we have tried to improve the time resolution to catch the fast events.

A first approach to improve the time resolution of an electrophysiological measurement is to reduce the capacity of the system through reducing the size of the lipid membrane patch. To this end we replace the Teflon holes by glass chips with micro-meter sized holes purchased from Nanion Technologies (Munich, Germany) [26, 27]. Based on their commercial system, the so-called Port-a-Patch for cell patch-clamping, we have combined the low-noise measurement characteristics of bilayers formed in patch-pipettes with a novel and simple way of forming small area planar bilayers by giant liposome adsorption. The technique has been shown to allow very low-noise measurements on OmpF and OmpC channels [27] and requires very low sample volumes, for which two electrolyte drops of several microliters placed on the two sides of the glass aperture can be used. Employing this technique, we characterized the permeation of antibiotics through different channels and obtained the binding kinetics at a single molecule level [27].

A different approach is to modify the underlying physicochemical conditions of the transport processes:

slowing down the kinetics by, for example, lowering the temperature [13, 24, 25]. Moreover, a temperature scan allows us to perform a Van't Hoff plot yielding the internal enthalpic barrier which can be compared to MD modeling [23, 24].

In this work we follow another approach by modifying the interaction between the substrate molecules and the channel walls, i.e. by using ionic liquids as solvent [28]. A large and highly heterogeneous substance class of salts is termed 'ionic liquids' whose unifying physicochemical parameter is a melting point smaller than 100°C . In recent years ionic liquids have gained more and more importance in manifold technological applications—reviewed in detail, for example, in Li *et al* and Zhao [29, 30]—owing to the fact that ionic liquids offer nearly all possible molecular interaction potentials and chemical properties available. When dealing with ionic liquids two different situations need to be distinguished: (i) ionic liquids as a solvent and (ii) ionic liquids as solutes. While in the first case ionic liquids can be treated as liquid phase on their own with certain solvent parameters such as density, viscosity polarity, and dielectricity, in the latter case more or less separately dissolved cations and anions are present as solutes in a solvent. Additionally, since ionic liquids are generally composed of bulky and asymmetric organic cations combined with bulky anions showing a largely distributed negative charge (except chloride, bromide, and iodide), ionic liquids can be referred to as so-called weakly coordinating ions. Hence, compared to other ions their interactions with solvent molecules and biomolecules cannot be described exclusively by their sole electrostatic properties but also, for example, van der Waals interactions and hydrogen bond donor and acceptor potentials need to be considered. As a consequence, the chemical or biochemical environment the ionic liquid ions are facing and their available interaction potentials determine their interaction with other solutes and especially with biomolecules like proteins. In the present study, ionic liquids were employed to slow down the ampicillin translocation through OmpF channels. Instead of KCl, the ionic liquid butylmethylimidazolium chloride (BMIM-Cl) solution was used as an electrolyte that improved the resolution of the measurement as shown below [28].

2. Materials and methods

The following chemical reagents were used in this study: BMIM-Cl, KCl, MES, potassium phosphate, n-pentane, and hexadecane (Sigma Aldrich, Buchs, Switzerland); ampicillin sodium salt (Applichem, Darmstadt, Germany); 1, 2-diphytanoyl-sn-glycero-3-phosphatidylcholine (DPhPC) (Avanti Polar Lipids, Alabaster, AL). Doubly distilled and deionized water was used to prepare solutions. After preparation, all solutions were purified by filtration through a 0.4 mm filter.

A typical classical setup for the characterization of channel forming proteins is based on conductance measurements and is shown in figure 1. Solvent-free black lipid bilayers were formed according to the classical Montal–Mueller technique [31]. For the sake of stability we used 1,2-diphytanoyl-*sn*-glycero-3-phosphatidylcholine

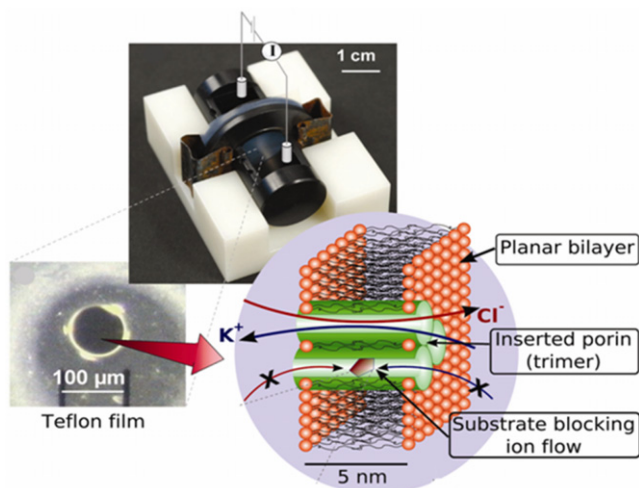


Figure 1. The top picture shows a classical planar lipid bilayer measurement setup. In between the two Delrin half cells a Teflon film with a hole (see middle left side) is sandwiched. Across the hole a planar bilayer is formed separating both aqueous solutions. A single porin spontaneously inserts, visible by a sudden jump in the ion current. The schema shows the flux of the ion and the interruption in the case of molecule blocking.

(DPhPC) [Avanti Polar Lipids, Alabaster, AL]. This lipid is in the fluid phase over the entire temperature range of measurement and thus is a good matrix for channel forming proteins. Purified OmpF from a stock of 1 mg ml^{-1} in 1% *n*-octylpolyoxyethylene (octyl-POE) (Alexis, Lausen, Switzerland) was diluted 10^2 – 10^5 times depending on the exact measurement conditions in a buffer also containing 1% octyl-POE. Membrane currents were measured through homemade or commercially available (World Precision Instruments, Sarasota, FL) Ag/AgCl electrodes. One electrode was used as ground and the other connected to the headstage of an Axopatch 200B amplifier (Axon Instruments, Foster City, CA), allowing the application of adjustable potentials (typically, 100 mV) across the membrane. The ion current was digitized by an Axon Digidata 1440A digitizer and controlled by the Clampex 10.0 software and analyzed by the Clampfit 10.0 software (all from Molecular Devices, Sunnyvale, CA). A typical recording is shown in figure 2 including the insertion

of a single OmpF trimer into the membrane visible by a jump in conductance. Titration with ampicillin causes channel blocking depending on the concentration, corresponding to binding and penetration of the antibiotic molecule through the channel. For formation of a miniaturized lipid bilayer containing the channels, giant unilamellar vesicles (GUVs) were prepared by the electroformation method and OmpF in 1% Octyl-POE was reconstituted into GUVs as described previously [26, 27]. For formation of a lipid bilayer containing single trimeric OmpF, 3 μl of the proteoliposome solution was pipetted onto the microstructured glass chip containing an aperture approximately 1 μm in diameter [26, 27]. Enrofloxacin measurements were done in 150 mM KCl, 10 mM MES pH 6 due to solubility problems.

3. Results and discussion

To study the effect of ionic liquids on translocation of antibiotics, a single trimeric OmpF channel was reconstituted into planar lipid membranes. First the channel properties were analyzed in the absence and presence of ampicillin in various KCl solutions. In agreement with previous measurements, OmpF trimers reconstituted into planar lipid bilayers showed a single trimeric channel conductance of 4 nS in 1 M KCl. Repeating this experiment in 1 M BMIM-Cl revealed a channel conductance of only $0.6 \pm 0.05 \text{ nS}$ (pH 6). Figure 2 shows the single step increase in conductance corresponding to the insertion of a single trimeric OmpF channel into a stable lipid bilayer. This dramatic decrease in the open channel ion conductance can be attributed to a decrease in bulk conductivities and to elucidate this we measured the latter and obtained 4.25 S m^{-1} for a 1 M BMIM-Cl solution compared to 10.5 S m^{-1} for 1 M KCl. Similar to our previous observation, we observed in both solutions voltage induced gating between 150–200 mV in 1 M salt. The closure occurred in three steps, confirming a trimeric organization of OmpF (data not shown). Moreover, in both cases the channel conductance was slightly asymmetric with respect to the applied voltage, suggesting an asymmetric conformation of the OmpF protein but it was not possible to identify the exact orientation by this type of measurement.

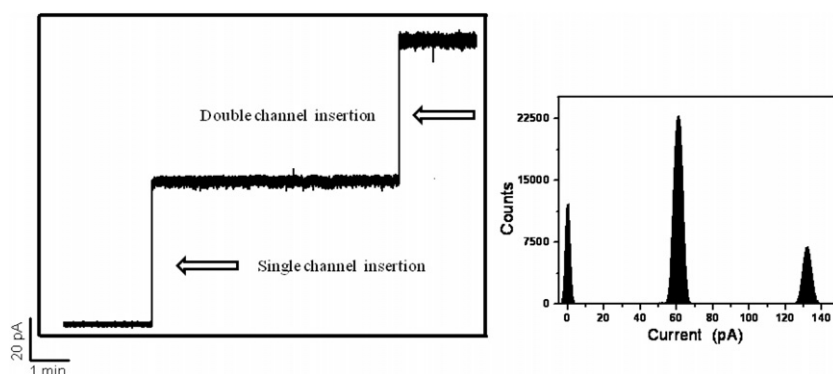


Figure 2. Typical recording of the OmpF insertions into a planar lipid bilayer. A: current recording with +100 mV applied voltage in 1 M BMIM-Cl, 20 mM MES, pH 6, room temperature, showing the sealed bilayer and the single step increase in conductance corresponding to the insertion of an OmpF channel (approximately 0.65 nS).

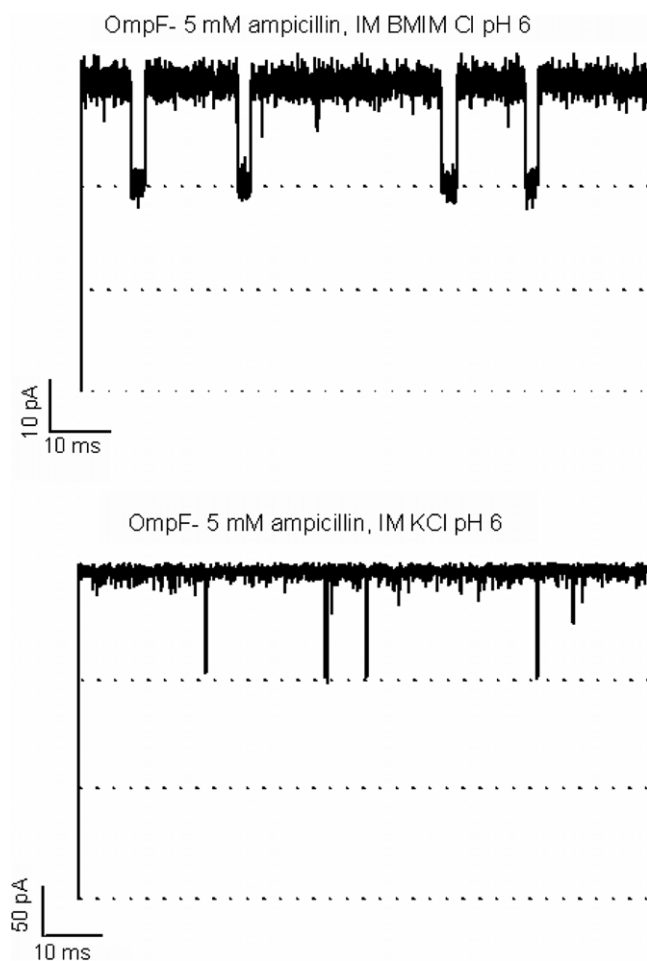


Figure 3. Addition of 5 mM ampicillin creates strong ion fluctuations in the channel conductance measured at +100 mV applied voltage in (A) 1 M BMIM-Cl and (B) 1 M KCl. Zooming in with a higher time resolution shows clearly isolated closures of single monomers. These closures correspond to the penetration of ampicillin molecules into the channel, hindering the ions passing through. Raising the concentration increases the number of blocking events.

In a second series of measurements, we investigated the effect of added antibiotics. Time-resolved ion current blockages through the channels were analyzed after adding antibiotic to the cis- or trans-side of the lipid membrane. Ampicillin produces a time-dependent interruption in the ionic current characteristics of reversible blocking of one monomer belonging to a single trimeric OmpF channel. Figure 3 shows a typical recording and shows longer residence time in 1 M BMIM-Cl compared to measurements performed in 1 M KCl. In figure 4 we show the average residence time of ampicillin in the channel for both solvents and this is within the experimental error constant. The average value was calculated to be 0.9 ± 0.1 ms in 1 M BMIM-Cl compared to 0.3 ± 0.05 ms in 1 M KCl. In contrast, the number of ampicillin blockage events remains the same in the case of 1 M KCl and 1 M BMIM-Cl. The number of blockage events strongly depends in both cases on the concentration of the antibiotics and increases linearly with the concentration. Noise analysis of ion currents through

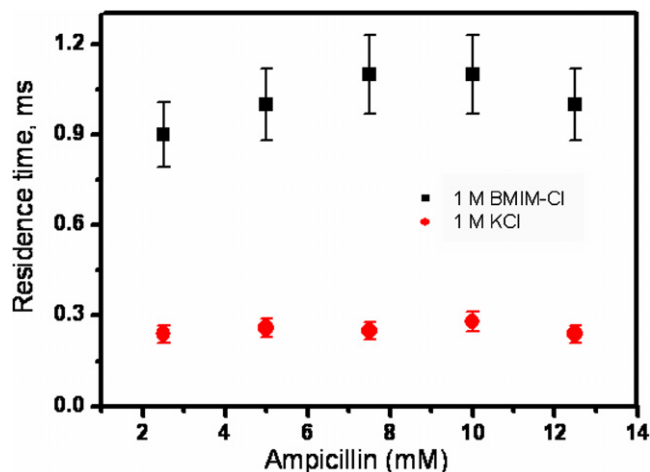


Figure 4. Dependence of residence time on the concentration of antibiotics. Note that the blocking is in the range of milliseconds in the case of BMIM-Cl whereas it is microseconds in the case of KCl.

the OmpF channel in the presence of ampicillin produced measurable excess noise. In figure 5 we show the power spectral density of the antibiotics-induced fluctuations in the ionic currents. The spectral analysis of the fluctuations in the ionic current induced by ampicillin shows a Lorentzian behavior [21]. This suggests that the translocation process can be described by a two-state Markovian model. The spectrum can be fitted to a Lorentzian $S(f) = S(0)/(1+(f/f_c)^2)$, where $S(0)$ denotes the low-frequency spectral density and f_c the corner frequency, yielding the relaxation time constant defined as $\tau = 1/2\pi f_c$. At $[c] \ll k_{off}/k_{on}$, the characteristic time is close to the average residence time of the drug $\tau = \tau_r = k_{off}^{-1}$, where $[c]$ is the drug concentration (figure 5). Other than in the case of KCl, our results clearly show that the BMIM-Cl electrolyte enhances the strength of antibiotic interactions with the channel surface. Previously it has been shown that increase in the viscosity of the solvent slowed down the kinetics of solute permeation [32, 37]. However, the viscosity of the BMIM-Cl and the KCl solution is not significantly different and therefore the increased residence time of ampicillin in the BMIM-Cl solution is not due to the increased viscosity of the medium [33].

Despite the possible new insight from the above described measurements, such measurements do not allow us to distinguish channel closure from substrate translocation. Although statistical analysis may distinguish shorter from longer permeation events an additional proof is required. This could be obtained by the liposome swelling assay, in which channels are directly incorporated into liposomes. Although this technique lacks the precision required for accurate quantitative results, it does provide qualitative information on the possibility of translocation [23].

With respect to miniaturization, we performed reconstitution of a single OmpF into a miniaturized bilayer. For example, figure 6 shows the effect of addition of enrofloxacin. The penetration of enrofloxacin caused fluctuations in the ion current indicates strong interactions of the antibiotics molecule with the interior of the channel walls. In figure 6

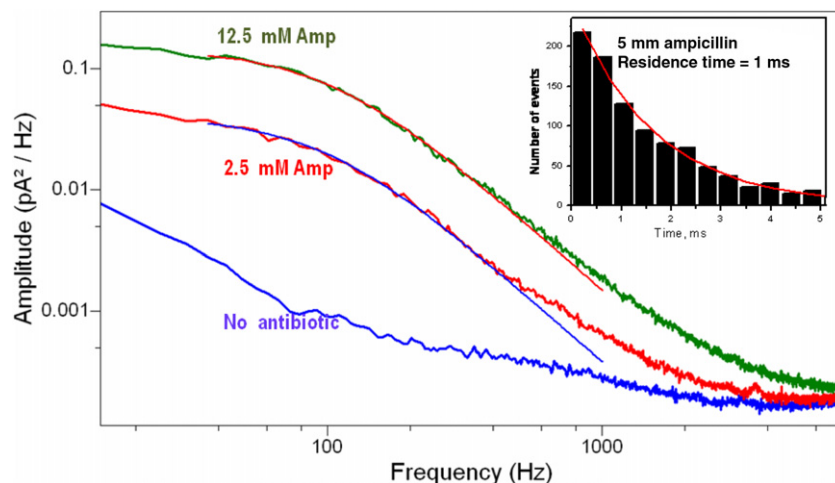


Figure 5. Power spectra density of ion currents through the OmpF channel in the presence of antibiotics revealing excess noise reflecting strong antibiotic–channel interactions. The inset shows a time histogram from which we calculated residence time. Solutions used were 1 M BMIM–Cl, 20 mM MES, pH 6.

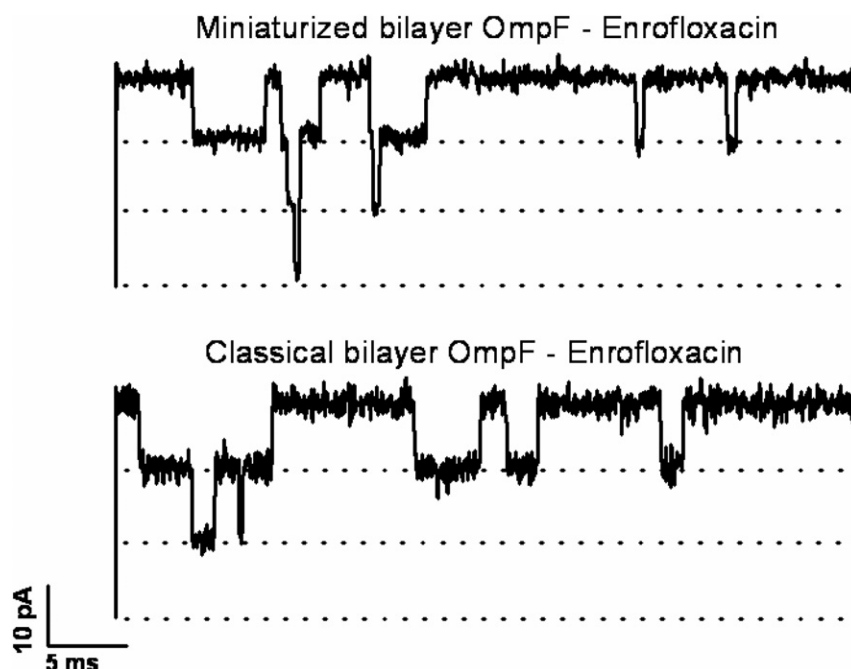


Figure 6. Typical recording of the ion current through OmpF in the presence of enrofloxacin measured in miniaturized free-standing bilayer setup. The lipid bilayer is formed by flushing GUVs through micro-meter glass chips and applying gentle suction. Classical lipid bilayers are formed by the technique developed by Montal and Mueller.

we show the measurement for two types of setup. The upper one was obtained with a miniaturized bilayer, as described in section 2. In general the miniaturization of electrophysiological setups implies the following advantages: fast and precise solute perfusion with low sample and buffer consumption, miniaturization of the system as a whole to decrease noise and electromagnetic interference problems, and the option of a simultaneous optical observation. The stability of the bilayers is significantly superior to the traditionally built bilayers especially concerning perturbations by electrical as well as mechanical forces. It has to be kept in mind that larger membrane areas create larger background noise,

which represents a serious problem to resolve short binding events. The described concept can readily be upgraded to fully automate the formation of the bilayer, so that a solvent-free ‘ μ BLM’ can be produced with minimal intervention by an operator.

Electrophysiology measures integral properties of the entire channel and does not provide molecular details. MD simulations made substantial progress to characterize dynamical properties of channels. From the theoretical point of view, the description of the above experiments can be split into two parts (see figure 7): the calculation of the ion conductance without substrate molecules in the pores and the

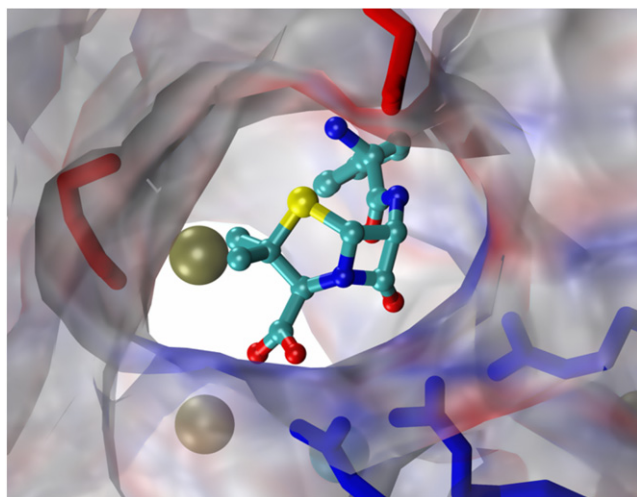


Figure 7. Molecular view of an ampicillin molecule in the constriction zone of OmpF in the presence of ions (depicted as spheres). The blue color indicates positive charges or charge distributions and the red color negative ones. The figure was created using the molecular graphics viewer VMD [34].

calculation of static free energy profiles for certain antibiotics within channels such as OmpF.

Concerning the ion conductance, several approximate techniques such as Poisson–Nernst–Planck equations [8] and Brownian dynamics simulations [9] have been applied in the past. Some of these simulations actually use the crystal structure of the membrane channel as a starting point but the dynamics is treated on an approximate level and the water is treated only implicitly. Important details of the transport cannot be captured under these circumstances such as hydration shells, ion pairing, movement of protein side chains, etc. On the other hand it is now possible to treat the ion transport through pores using all-atom MD simulations [10–15, 35]. This has become possible with recent advances in computing capacities allowing for large-scale applied-field MD simulations and a direct calculation of the ionic conductance. Simulations of this kind give access to atomic details of the transport mechanism through nanopores, as has been shown, e.g. for alpha-hemolysin [10], MscS [11], OmpF [13, 14], and OmpC [15]. A good correspondence between experiment and theory was possible for the temperature-dependent conductance in OmpF and OmpC. Without any fitting parameters the agreement in conductance is within a factor of two for most of the studied temperature range. In many cases the agreement is actually much better as, for example, in the case of OmpC and low salt concentrations [15]. But the simulations cannot only nicely reproduce the experimental results but also yield a full atomistic picture of the underlying processes and interactions. The influence of ion pair forming and breaking can be investigated [13] or the influence of mutations can be predicted [14]. Of course, there are still several limitations to calculating ionic currents using all-atom classical MD. First of all, there are the sampling problems which call for even longer simulation times than currently performed. Furthermore,

standard force fields do not include, among other properties, polarizability effects and temperature dependence.

The second approach concerning the interaction of antibiotics with the inner walls of membrane proteins deals with the calculation of free energy profiles. These energy landscapes give quite detailed information on the interaction between the substrate molecules and the interior of the channel, especially in the constriction zone where it is of paramount importance. Several such simulations have been performed (see, e.g. [21–24, 36]) showing molecular features and insight inaccessible by electrophysiological experiments. Most of these studies employ metadynamics simulations [21–24] to obtain the energy barriers along the diffusion pathway. Using this approach one cannot only determine the energy barriers for wild-type pores by also for mutations that, for example, affect the charge and size at the channel constriction zone. Furthermore the most likely orientation of the substrate in the channel has been predicted and verified optically by fluorescence resonance energy transfer (FRET) between a tryptophan as a donor and a moxifloxacin (an antibiotic) as an acceptor molecule [22].

Missing so far is a combined description of the two aspects above: the theoretical determination of the ionic current in the present of an antibiotic or, even better, while steering an antibiotic through the pore. Such a combined approach is challenging because of the unlike timescales involved in the different transport processes but might be feasible when determining the free energy landscape using non-equilibrium methods, e.g. Crooke's formalism.

Simulations of ionic conduction involving ionic liquids (and/or heavy water) as solvents should be rather straightforward with today's computer power but have not been performed so far. Force fields for several ionic liquids have recently been reported in the literature although they might not be compatible with those usually used in many biological simulations such as CHARMM or AMBER.

4. Conclusions and outlook

As the binding of antibiotic molecules in the channels of interest is significantly weaker than that of preferentially diffusing nutrients in substrate-specific pores, the resolution of conductance measurements has to be significantly increased to be able to resolve the events in all cases. Reducing the size of the lipid patch allows lowering the background capacitance below 2 pF and thus the amplifier becomes the limiting element. Nevertheless molecular diffusion can be too fast to be visible by ion current fluctuations. Subsequently the physical process of diffusion has to be slowed down and conclusions may be taken from extrapolation into the biological parameter regime. A further possibility is to change the solvent and thus to modulate the solute–channel interactions. Ion current fluctuation analysis revealed an exceptionally long residence time for antibiotics in the presence of ionic liquids. This study proves that the ionic liquid BMIM–Cl strongly influences the facilitated transport of solutes through the OmpF channel and gives new insights into the translocation of small molecules through biological nanopores. The latter approach needs

to be explored and offers an enormous potential for using channels as a screening device. In addition, the potential of MD simulations in understanding the underlying transport processes in atomic detail has been outlined. Now that it is possible to almost quantitatively calculate electrophysiological data using molecular-level simulations, one can envisage that using combinations of innovative experiments and simulations can help to create a new understanding and engineering of transport processes through artificial and biological nanopores.

Acknowledgments

Financial support through EU-grant MRTN-CT-2005-019335 (Translocation), DFG Wi 2278/18-1, and KL-1299/6-1 is gratefully acknowledged.

References

- [1] A broad overview of the current state of planar lipid bilayer research in the year 2001 is given in: Tien H T and Ottova-Leitmannova A (ed) 2003 *Planar Lipid Bilayers (BLMs) and Their Applications* (Amsterdam: Elsevier)
- [2] An extensive overview with respect to patch-clamping is given in: Sakmann B and Neher E (ed) 1995 *Single Channel Recording* (New York: Plenum) or Hille B (ed) 1992 *Ionic Channels of Excitable Membranes* (Sunderland, MA: Sinauer Associates)
- [3] Stepwise increase in conductance has been observed after addition of a so-called excitability-induced material (EIM): Bean R C, Shepard W C, Chan H and Eichner J 1969 *J. Gen. Physiol.* **53** 741–57
However the step-wise increase must be treated with caution Blicher A, Wodzinska K, Fidorra M, Winterhalter M and Heimburg M 2009 *Biophys. J.* **96** 4581–91
- [4] Merzlyak P G, Yuldasheva L N, Rodrigues C G, Carneiro C M, Krasilnikov O V and Bezrukov S M 1999 *Biophys. J.* **77** 3023–33
- [5] Alcaraz A, Nestorovich E M, López M L, García-Giménez E, Bezrukov S M and Aguilera V M 2009 *Biophys. J.* **96** 56–66
- [6] Danelon C, Suenaga A, Winterhalter M and Yamato I 2003 *Biophys. Chem.* **104** 591–603
- [7] Schulz R and Kleinekathöfer U 2009 *Biophys. J.* **9** 3116–25
- [8] Saraniti M, Aboud S and Eisenberg R 2006 *Rev. Comput. Chem.* **22** 229–94
- [9] Roux B, Allen T, Berneche S and Im W Q 2004 *Rev. Biophys.* **37** 15–103
- [10] Aksimentiev A and Schulten K 2005 *Biophys. J.* **88** 3745–51
- [11] Sotomayor M, Vasquez V, Perozo E and Schulten K 2007 *Biophys. J.* **92** 886–902
- [12] Cruz-Chu E R, Aksimentiev A and Schulten K 2005 *J. Phys. Chem. C* **113** 1850–62
- [13] Chimerele C, Movileanu L, Pezeshki S, Winterhalter M and Kleinekathöfer U 2008 *Eur. Biophys. J.* **38** 121–5
- [14] Pezeshki S, Chimerele C, Bessenov A, Winterhalter M and Kleinekathöfer U 2009 *Biophys. J.* **97** 1898–906
- [15] Biro I, Pezeshki S, Weingart H, Winterhalter M and Kleinekathöfer U 2010 *Biophys. J.* **98** 1830–9
- [16] Nekolla S, Andersen C and Benz R 1994 *Biophys. J.* **66** 1388–97
- [17] Kasianowicz J J, Burden D L, Han L C, Cheley S and Bayley H 1999 *Biophys. J.* **76** 837–45
- [18] Bezrukov S M and Winterhalter M 2000 *Phys. Rev. Lett.* **85** 202–4
- [19] Winterhalter M, Hilty C, Bezrukov S M, Nardin C, Meier W and Fournier D 2001 *Talanta* **55** 965–71
- [20] Pagès J M, James C E and Winterhalter M 2008 *Nat. Rev. Microbiol.* **6** 893–903
- [21] Danelon C, Nestrovich E M, Winterhalter M, Ceccarelli M and Bezrukov S M 2006 *Biophys. J.* **90** 1617–27
- [22] Mach T, Neves P, Spiga E, Weingart H, Winterhalter M, Ruggerone P, Ceccarelli M and Gameiro P 2008 *J. Am. Chem. Soc.* **130** 13301–9
- [23] Hajjar E, Mahendran K R, Kumar A, Bessonov A, Petrescu M, Weingart H, Ruggerone P, Winterhalter M and Ceccarelli M 2010 *Biophys. J.* **98** 569–75
- [24] Mahendran K R, Hajjar E, Mach T, Lovelle M, Kumar A, Sousa I, Spiga E, Weingart H, Gameiro P, Winterhalter M and Ceccarelli M 2010 *J. Phys. Chem. B* **114** 5170–9
- [25] Mahendran K R, Chimerele C, Mach T and Winterhalter M 2009 *Eur. Biophys. J.* **38** 1141–4
- [26] Kreir M, Farre C, Beckler M, George M and Fertig N 2008 *Lab Chip* **4** 587–95
- [27] Mahendran K R, Kreir M, Weingart H, Fertig N and Winterhalter M 2010 *J. Biomol. Screen.* **15** 302–7
- [28] Jayawardhana D A, Crank J A, Zhao Q, Armstrong D W and Guan X 2009 *Anal. Chem.* **81** 460–4
Zoysa R S, Jayawardhana D A, Zhao Q, Wang D, Armstrong D W and Guan X 2009 *J. Phys. Chem. B* **113** 13332–6
- [29] Li X, Zhao D, Fei Z and Wang L 2006 *Sci. China B* **49** 385–401
- [30] Zhao H 2006 *Chem. Eng. Commun.* **193** 1660–77
Weingaertner H 2008 *Angew Chem. Int. Edn* **47** 654–70
- [31] Montal M and Mueller P 1972 *Proc. Natl. Acad. Sci. USA* **69** 3561–6
- [32] Kawano R, Schibel A, Cauley C and White H 2009 *Langmuir* **25** 1233–7
- [33] Ries L A S, do Amaral F A, Matos K, Martini E M A, de Souza M O and de Souza R F 2008 *Polyhedron* **27** 3287–93
- [34] Humphrey W F, Dalke A and Schulten K 1996 *J. Mol. Graph.* **14** 33–8
- [35] Aksimentiev A 2010 *Nanoscale* **2** 468–83
- [36] Luan B and Aksimentiev A 2008 *Phys. Rev. E* **78** 021912
- [37] Fologea D, Uplinger J, Thomas B, McNabb D S and Li J 2005 *Nano Lett.* **5** 1734–7

Chapter 4.2

Reprinted with permission from American Chemical Society

Modi, N., Singh, P. R., Mahendran, K. R., Schulz, R., Winterhalter, M., & Kleinekathöfer, U. (2011). Probing the Transport of Ionic Liquids in Aqueous Solution through Nanopores. The Journal of Physical Chemistry Letters, 2(18), 2331–2336. doi:10.1021/jz201006b

Copyright © 2011, American Chemical Society

Individual Contribution:

Experimental work on single channel measurements and analysis

Probing the Transport of Ionic Liquids in Aqueous Solution through Nanopores

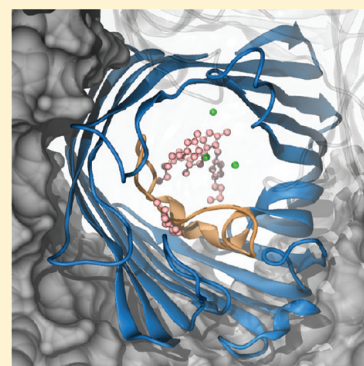
Niraj Modi, Pratik Raj Singh, Kozhinjampara R. Mahendran, Robert Schulz, Mathias Winterhalter, and Ulrich Kleinekathöfer*

School of Engineering and Science, Jacobs University Bremen, Campus Ring 1, 28759 Bremen, Germany

S Supporting Information

ABSTRACT: The temperature-dependent transport of the ionic liquid 1-butyl-3-methylimidazolium chloride (BMIM-Cl) in aqueous solution is studied theoretically and experimentally. Using molecular dynamics simulations and ion-conductance measurements, the transport is examined in bulk as well as through a biological nanopore, that is, OmpF and its mutant D113A. This investigation is motivated by the observation that aqueous solutions of BMIM-Cl drastically reduce the translocation speed of DNA or antibiotics through nanopores in electrophysiological measurements. This makes BMIM-Cl an interesting alternative salt to improve the time resolution. In line with previous investigations of simple salts, the size of the ions and their orientation adds another important degree of freedom to the ion transport, thereby slowing the transport through nanopores. An excellent agreement between theory and conductance measurements is obtained for wild type OmpF and a reasonable agreement for the mutant. Moreover, all-atom simulations allow an atomistic analysis revealing molecular details of the rate-limiting ion interactions with the channel.

SECTION: Biophysical Chemistry



Pure ionic liquids (ILs), usually molten salts with a melting point lower than 100 °C, have become a subject of intense studies in recent years. ILs are characterized by a high ion conductivity, thermal and chemical stability, as well as favorable solvation properties. These characteristics of ILs generated enormous interest, and they can be applied to a large number of useful applications including organic synthesis, catalysis, separation, and electrochemical studies.^{1–5} Moreover, mixtures of water and ILs, that is, ILs in aqueous solution, have been investigated recently,^{6,7} which is actually the subject of our study.

Ion and substrate transport through nanopores is currently an active field of research with exciting biological applications.^{8,9} Concerning the ion transport, most studies, especially including the effect of temperature, have been restricted to simple ions such as KCl, NaCl, or MgCl₂ (see, e.g., refs 10–18). Concerning substrate transport, one investigates, for example, the translocation of antibiotics,¹⁹ DNA,⁹ and peptides²⁰ through nanopores. The translocation of these substrates is experimentally studied using electrophysiology, that is, the use of ion-current measurements as an indirect probe. One of the potential applications of IL solutions is slowing down the kinetics of fast permeation events through nanopores. To this end, de Zoysa et al.²¹ successfully used a 1 M 1-butyl-3-methylimidazolium chloride (BMIM-Cl) (Figure 1a) solution to slow down the DNA translocation in a nanopore. This reduction in speed might help in DNA sequencing by increasing the residence time of DNA in the pore.²¹ Furthermore, we have recently shown that a 1 M BMIM-Cl solution increases the residence time of ampicillin in

the outer membrane porin F (OmpF) pore by a factor of 3 compared with a KCl solution of the same concentration.²² Again, this increase in residence time improved the time resolution to catch fast events of antibiotic translocation through the pore, which is otherwise hard to detect or even undetectable. In the same study, it was found that BMIM-Cl compared with KCl leads to a roughly two-fold reduction in bulk conductivity, whereas the respective OmpF conductance decreases by a factor of ~7.²² This study is devoted to understand the underlying interactions of ILs with the nanopore walls.

The investigated nanopore is the general diffusion porin OmpF, that is, a pore in the outer membrane of the *E. coli* bacterium. (See Figure 1c.) High-resolution crystal structures of OmpF reveal their trimeric organization.^{23,24} The constriction zone contains three positively charged arginine residues R42, R82, and R132 on the one side and two negatively charged residues, namely, aspartic acid D113 and glutamic acid E117, on the other side. (See Figure S1 in the Supporting Information.) This spatial arrangement of positively and negatively charged residues is responsible for a strong transverse electric field inside the pore leading to particular orientations of molecules in this region.^{25–27} The inner loop L3 is a part of the constriction zone and has a large influence on the translocation properties of the pore.

Received: July 22, 2011

Accepted: August 25, 2011

Published: August 25, 2011

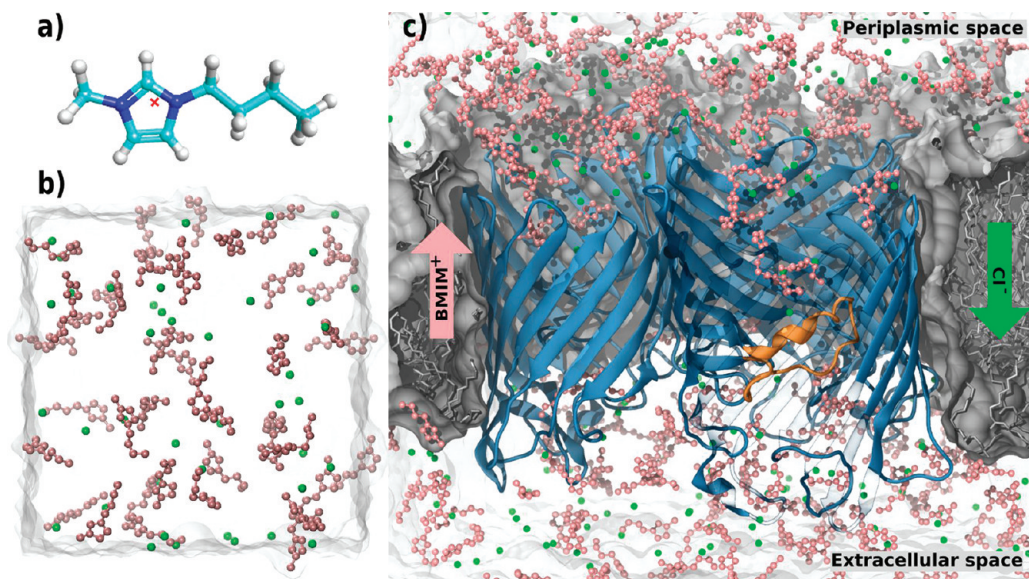


Figure 1. (a) Structure of BMIM^+ (atom colors: C, cyan; N, blue; H, white) including the center of charge indicated by a red cross. (b) Simulation box for the bulk simulations. The Cl^- ions are shown as green spheres and the BMIM^+ ions are shown as pink ball-stick structures. (c) Simulation setup for the pore simulations including OmpF (blue, secondary structure; orange, loop L3) and the membrane (gray surface and stick representation). The arrows indicate the direction of the movement of ions under the effect of a positive applied field (in the same direction as the flow of the BMIM^+ ions). For the sake of visualization, part of the monomer in the front has been removed. The figures were generated using VMD.²⁸

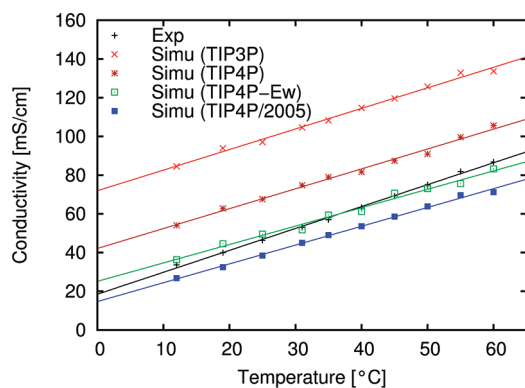


Figure 2. Bulk conductivity versus temperature for different water models compared to experiments.

In this study, we investigated molecular details of BMIM-Cl transport through OmpF. In particular, the behavior and orientation of the bulky ions within the channel and the constriction region are of interest. To this end, we performed applied field MD simulations to model the ion flow of BMIM-Cl through OmpF and to compare the calculated conductance to experimental data.

As a first step in the molecular modeling of BMIM-Cl , we compared theoretical and experimental values for the bulk conductivity in water. The simulations were performed using NAMD2.7²⁹ together with the CHARMM27 force field,³⁰ BMIM force field parameters,³¹ and different water models, for example, TIP3P,³² TIP4P,³³ TIP4P-Ew,³⁴ and TIP4P/2005.³⁵ Details are given in the Supporting Information. (Also see Figure 1b.)

The temperature-dependent bulk conductivity of 1 M BMIM-Cl was calculated for temperatures ranging from 10 to 60 °C using the approach of Aksimentiev and Schulten.¹¹ (Also see the Supporting Information.) As a control of the underlying interactions between

Table 1. Self-Diffusion Coefficient and Bulk Conductivity for Different Water Models Together with Experimental Values at 25 °C

data set	self diffusion [10^{-5} cm ² /s]	bulk conductivity [mS/cm]
experimental	2.27 ³⁶	46.26
TIP3P	5.06 ³⁷	97.07
TIP4P	3.29 ³⁷	67.57
TIP4P-Ew	2.4 ³⁴	49.51
TIP4P/2005	2.08 ³⁵	38.46

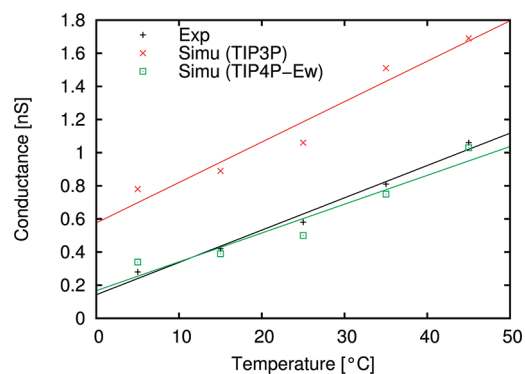


Figure 3. Pore conductance versus temperature for experiment and simulation using two different water models together with linear fits of the data sets.

ions and water, the temperature dependence of the calculated conductivities is compared with the experimental values. (See Figure 2.) As in previous simulations for KCl conductivity, we initially employed the TIP3P water model.^{13,14} Although the slope of the simulation data with the TIP3P water model is very similar to the

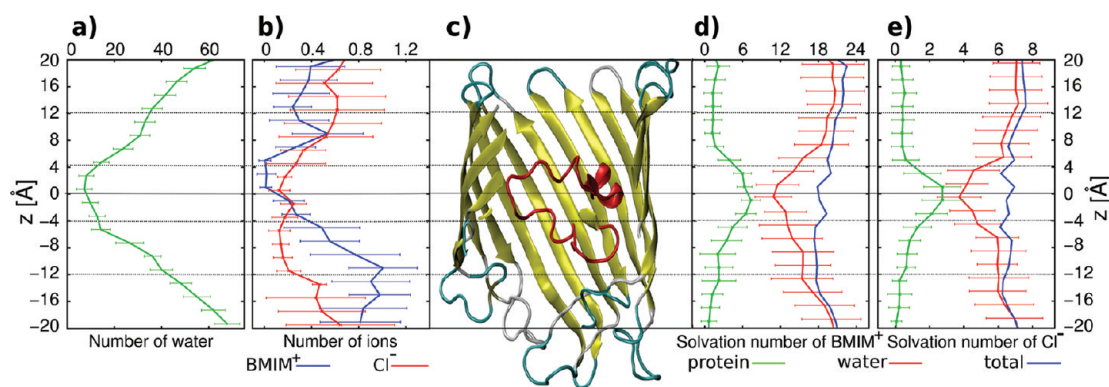


Figure 4. Several ion quantities as a function of the channel coordinate z . (a) number of water molecules; (b) number of ion molecules per species; (c) channel in the same scale as the ordinate; (d) solvation number of the BMIM^+ ions; and (e) solvation number of the Cl^- ions. (See the main text.) The dotted horizontal lines are given to help guiding the eye.

experimental results, a considerable parallel shift is visible. Surprisingly, the ratio between the calculated conductivity at room temperature and its experimental counterpart is almost equal to that of the corresponding self-diffusion constants of water as listed in Table 1. Motivated by the possible connection between conductivity and self diffusion, different water models were probed with self-diffusion constant in decreasing order. (See Table 1.) In conclusion, we found that the conductivity of 1 M $\text{BMIM}\text{-Cl}$ solution is strongly correlated with the self-diffusion constant of the water model and that the best results are obtained for the TIP4P-Ew water model (Figure 2, Table 1). This is not too surprising because both quantities, the conductivity of $\text{BMIM}\text{-Cl}$ and the self-diffusion constant of water, involve the process of moving a molecule, that is, either a BMIM^+ ion or a water molecule, through the surrounding water.

After the validation of the force fields and water models, the transport through OmpF was investigated. We performed 30 ns simulations for different temperatures and using the TIP3P and the TIP4P-Ew water models. (See the Supporting Information.) The current was determined as previously described.^{11,13,14} The applied voltage of 1 V in the simulations is considerably larger than the experimental one to increase the number of passing ions during the simulation time, that is, to improve the statistics. The experimental results of the pore conductance of OmpF using 1 M $\text{BMIM}\text{-Cl}$ solution at different temperatures show a linear dependence as shown in Figure 3. (See the Supporting Information for experimental measurement details.) Similar to the bulk conductivity calculations, the simulations using the TIP3P water model yield a considerably higher conductance, although also an almost linear increase with temperature. Results obtained with the TIP4P-Ew water model are in good quantitative agreement with the experimental results. These results further demonstrate the dependence of such conductance measurements on the water model and their self-diffusion constant. The good agreement between experimental and theoretical conductance can be further exploited to obtain atomic-level details of the transport process of $\text{BMIM}\text{-Cl}$ through the OmpF pore.

In contrast with experiments, the simulations immediately yield the contributions of the individual ion types to the current, that is, BMIM^+ and Cl^- . (See also the Supporting Information movie.) The ratio of the Cl^- to BMIM^+ currents is found to be in the range of 3–5 increasing with temperature in the range from 5 to 45 °C (data not shown). Analysis showed that the mobility of Cl^- ions is influenced more by the increasing temperature than the BMIM^+ ions. This leads to an increased ratio of Cl^- to

BMIM^+ currents at higher temperatures. Furthermore, it is found that, at 25 °C, BMIM^+ ions have an approximately four times higher residence time in the constriction region compared with the Cl^- ions (see also below).

For further analysis of the MD data at 25 °C, the channel was divided into bins of 2 Å width along the channel coordinate z . If the center of mass of the molecule under investigation was within the z range of this bin, the count of the individual quantities was increased. Subsequently, the number of molecules was averaged over the trajectory and are displayed in Figure 4. In fact, the number of water molecules can be used as an estimate for the channel size. As can be clearly seen, the constriction zone extends from roughly -4 to $+4$ Å. (See Figure 4a.) For the analysis of the average ion occupation in the channel, note that the applied positive voltage forces the Cl^- ions down toward negative values of the channel coordinate z (from the periplasmic side of the membrane to the extracellular side) while the BMIM^+ are dragged up toward positive values. Compared with the average water occupation in the channel, the Cl^- ions have a slightly higher average number above the constriction zone and a slightly depleted occupation at negative z values. (See Figure 4b.) This is due to the hindrance caused by the constriction region. Once the narrow part of the pore is passed, the ions are easily dragged away by the external field. As can also be seen in the Supporting Information movie, the effect is much more enhanced for the bulky BMIM^+ ions, which are crowded below the constriction zone.

For the present nonspecific channel, we examined the solvation characteristics of permeating BMIM^+ and Cl^- ions along the channel coordinate z . In general, ion channels regulate the flow of ions across the membrane via substituting the loss of hydration with favorable protein interactions.³⁸ To be able to quantify these, we determined solvation shell definitions of the BMIM^+ and Cl^- ions by calculating radial distribution function (RDF) for the previously described simulation of 1 M $\text{BMIM}\text{-Cl}$ aqueous bulk solution and 4 ns long trajectories. For the BMIM^+ molecule, the center of charge was considered, and a first minimum was found at 4.1 Å, which was subsequently used as radius of the first hydration shell. Similarly for Cl^- , the radius of the first hydration shell was obtained as 3.2 Å. With regard to the protein contacts, only oxygen atoms were considered for the contribution of the protein to the solvation number of BMIM^+ ions and nitrogen atoms for that of Cl^- ions. For the ion–protein contacts, the same distance criteria as

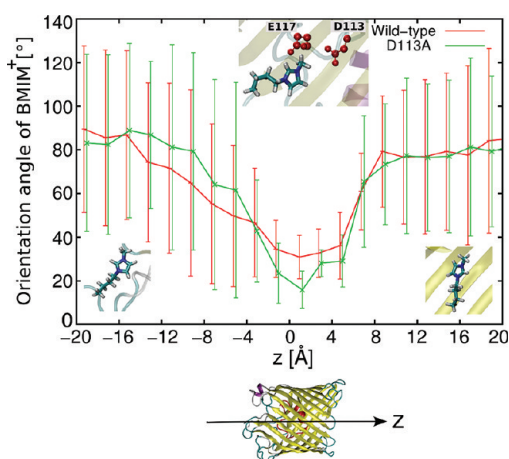


Figure 5. Average orientation of the BMIM⁺ dipole with respect to the channel coordinate Z with error bars showing the standard deviation per bin. Representative orientations of BMIM⁺ ions are shown in the insets for three particular regions of OmpF (center inset includes two important negatively charged residues in constriction region; see the main text).

those for the ion–water contacts were applied. The hydration number of the ions progressively alters in response to the changing environment as they move through the OmpF pore (Figure 4d,e). The hydration number appears to be minimal in the constriction zone with approximately 10 to 11 water molecules around each BMIM⁺ ion and 4 water molecules around each Cl[−] ion. Interestingly, the loss of hydration is compensated by protein contacts in the constriction region. Apparently, the contributions of water and protein contacts complement each other to keep the total solvation number per ion roughly constant throughout the channel. For KCl ions in OmpF, a similar phenomenon was previously observed by Im and Roux.²⁷ In addition, both BMIM⁺ and Cl[−] follow separate pathways over the length of the pore in a screw-like fashion. (See the Supporting Information.)

Compared with the simple potassium and chloride ions, an important feature of the more bulky BMIM⁺ ions is their orientation with respect to the channel. This is a key feature not accessible by experiment but by MD simulations. As described above for the other calculations, the channel was divided into bins of 2 Å width along the channel coordinate z and the quantities were averaged over the full length of a 30 ns trajectory. The orientation angle was measured between the dipole of each BMIM⁺ ion residing in a particular bin and the z axis. As shown in Figure 5, the orientation of the BMIM⁺ ions changes gradually as it passes through the pore. Toward the extracellular ($-20 \leq z \leq -12$ Å) and the periplasmic side ($12 \leq z \leq 20$ Å) of the pore, BMIM⁺ has an average orientation perpendicular to the channel axis with very large values of the standard deviation. This perpendicular direction is due to the charged residues lining the pore walls. (See Figure S2 in the Supporting Information.) These charges create local electric field components perpendicular to the channel axis and the BMIM⁺ ions partially align to them. At the same time, the large standard deviation of the orientation angle toward the extracellular and periplasmic side of the pore shows that the ions have a large flexibility in their movement. The situation is different near the constriction region. The pore diameter is not large enough for BMIM⁺ ions to pass in a perpendicular orientation. Therefore, they progressively start to

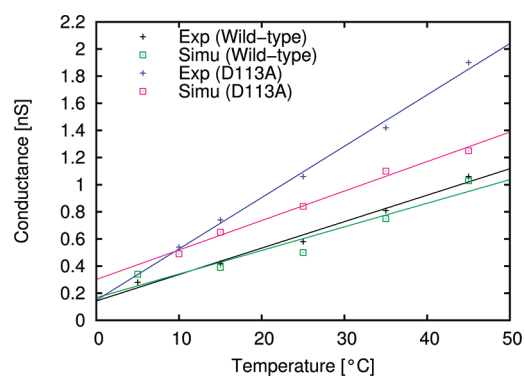


Figure 6. Experimental and calculated pore conductance for the D113A mutant. For comparison, the conductance data for the wild type are shown as well.

change their orientation as they approach the constriction region. There, the BMIM⁺ ions align almost parallel to the channel axis. In terms of the angle between dipole moment and channel axis, this leads to values around 30°. As shown in the middle inset of Figure 5, the positively charged headgroup, that is, imidazole ring, of the BMIM⁺ ion tends to tilt toward negatively charged residues in the constriction region, namely, D113 and E117. This leads to an average angle of the BMIM⁺ dipole away from the expected 0°. Probably more important than the average angle is the relatively small standard deviation in the constriction zone. Although not directly visible in Figure 5 (but, e.g., in the Supporting Information movie), the BMIM⁺ ions have to pass the constriction zone with a certain directionality, that is, the imidazole ring first. This shows that the ions first have to acquire a certain orientation before they can actually pass this region. On average, this leads to a prolongation of the passage time or a decrease in the current produced by the BMIM⁺ ions. Figure 5 shows a second curve, the orientation of the BMIM⁺ ions through the OmpF mutant D113A, where a negatively charged aspartate residue in the constriction zone was mutated into a neutral alanine. The same system setup as that for the wild type OmpF simulations was used with the TIP4P-Ew water model; then, the D113 residue was mutated. Subsequently, the system was equilibrated for 5 ns, followed by an applied-field simulations for 10 ns. Because of the removal of a negative charge in the constriction zone, one may expect a change in the average orientation of the BMIM⁺ dipole in this region. This can be attributed to the reduced electrostatic force experienced by the positively charged imidazole ring leading to a less pronounced tilting of the BMIM⁺ head. Indeed, the average angle in the mutant is found to be $\sim 15^\circ$ compared with roughly 30° in wild type. Farther away from the constriction zone, the average orientation and its standard deviation are rather similar to the wild type data. This is reassuring because it shows that these two independent simulations yield very similar results away from the constriction zone, as to be expected.

In Figure 6, the temperature-dependent conductance of the D113A mutant from electrophysiology and MD simulations is displayed. At the lower considered temperatures, the agreement between both approaches is good, but it is obvious that the experimental and the theoretical curves have different slopes. The curve from the simulation is parallel shifted from the wild type results to larger conductance values. In the case of the experiments, there is a considerable change in slope. Because of

the very good agreement between theory and experiment for the wild type OmpF, these data are somewhat surprising. Although the results are within the range of expected agreement between experiments, it is obvious that some contribution is neglected in the mutant. Nevertheless, the structure of the mutant was quite stable in the simulations. Furthermore, previous studies of the conductance of simple ions provided good agreement with experiments.^{13,14} The ratio of Cl⁻ to BMIM⁺ currents was found to be in the range of 5–8 increasing with temperature. Compared with the ratio of 3–5 for the wild type, it was observed that mainly the Cl⁻ ions are responsible for the larger conductance of the D113A mutant because the contributions from the BMIM⁺ ions were roughly the same as those for the wild type.

In conclusion, we have experimentally measured the temperature-dependent conductance of aqueous BMIM-Cl solution through OmpF trimer and also modeled it using MD simulations. An excellent agreement is obtained between electrophysiology and simulations of wild type OmpF and a reasonable agreement for the D113A mutant. In addition to the experimental findings, the simulations yield a molecular-level picture of the ion transport. In particular, the kinetic simulations reveal the rate-limiting interactions of the ions with the channel wall. As an important issue of the transport process, we have calculated the orientation of the BMIM⁺ ions. It is really astonishing that one can see the realignment of the bulky ions within the time scale of the applied-field MD simulations. The necessity for the correct orientation of BMIM⁺ near the constriction region may serve as a rate-limiting step of the passage, thereby slowing down the kinetics of antibiotic translocation through OmpF. This probably allows us to observe an increased residence time of ampicillin in OmpF with BMIM-Cl compared with KCl, as shown in ref 22. For the translocation of substrates such as antibiotic molecules, the translocation time is too long to be observed directly in standard MD simulations. Hence, one needs to go to more indirect schemes as the calculation of the potential of mean force or steered MD simulations to understand these processes theoretically. Nevertheless, insights from the present study can be further exploited to understand antibiotic translocation processes and to investigate other ILs for similar electrophysiological measurements through nanopores.

■ ASSOCIATED CONTENT

S Supporting Information. Experimental and computational details and movie of the ion transport simulations. This material is available free of charge via the Internet at <http://pubs.acs.org>.

■ AUTHOR INFORMATION

Corresponding Author

*E-mail: u.kleinekathoef@jacobs-university.de.

■ ACKNOWLEDGMENT

This work has been supported by grants KL 1299/6-1 and WI 2278/18-1 of the Deutsche Forschungsgemeinschaft (DFG).

■ REFERENCES

- (1) Welton, T. Room-Temperature Ionic Liquids. Solvents for Synthesis and Catalysis. *Chem. Rev.* **1999**, *99*, 2071–2083.
- (2) Rogers, R.; Seddon, K. Ionic Liquids - Solvents of the Future? *Science* **2003**, *302*, 792–793
- (3) Izgorodina, E. I. Towards Large-Scale, Fully Ab Initio Calculations of Ionic Liquids. *Phys. Chem. Chem. Phys.* **2011**, *13*, 4189–4197.
- (4) Galinski, M.; Lewandowski, A.; Stepniak, I. Ionic Liquids as Electrolytes. *Electrochim. Acta* **2006**, *51*, 5567–5580.
- (5) Anderson, J.; Armstrong, D.; Wei, G. Ionic Liquids in Analytical Chemistry. *Anal. Chem.* **2006**, *78*, 2892–2902.
- (6) Heintz, A.; Ludwig, R.; Schmidt, E. Limiting Diffusion Coefficients of Ionic Liquids in Water and Methanol: A Combined Experimental and Molecular Dynamics Study. *Phys. Chem. Chem. Phys.* **2011**, *13*, 3268–3273.
- (7) Mendez-Morales, T.; Carrete, J.; Cabeza, O.; Gallego, L. J.; Varela, L. M. Molecular Dynamics Simulation of the Structure and Dynamics of Water-1-Alkyl-3-methylimidazolium Ionic Liquid Mixtures. *J. Phys. Chem. B* **2011**, *115*, 6995–7008.
- (8) Albrecht, T.; Edel, J. B.; Winterhalter, M. New Developments in Nanopore Research—from Fundamentals to Applications. *J. Phys.: Condens. Matter* **2010**, *22*, 450301.
- (9) Aksimentiev, A. Deciphering Ionic Current Signatures of DNA Transport through a Nanopore. *Nanoscale* **2010**, *2*, 468–473.
- (10) Roux, B.; Allen, T.; Berneche, S.; Im, W. Theoretical and Computational Models of Biological Ion Channels. *Q. Rev. Biophys.* **2004**, *37*, 15–103.
- (11) Aksimentiev, A.; Schulten, K. Imaging Alpha-Hemolysin with Molecular Dynamics: Ionic Conductance, Osmotic Permeability, and the Electrostatic Potential Map. *Biophys. J.* **2005**, *88*, 3745–3751.
- (12) Miedema, H.; Vroenenraets, M.; Wierenga, J.; Meijberg, W.; Robillard, G.; Eisenberg, B. A Biological Porin Engineered into a Molecular, Nanofluidic Diode. *Nano Lett.* **2007**, *7*, 2886–2891.
- (13) Pezeshki, S.; Chimere, C.; Bessenov, A.; Winterhalter, M.; Kleinekathöfer, U. Understanding Ion Conductance on a Molecular Level: An All-Atom Modeling of the Bacterial Porin OmpF. *Biophys. J.* **2009**, *97*, 1898–1906.
- (14) Biro, I.; Pezeshki, S.; Weingart, H.; Winterhalter, M.; Kleinekathöfer, U. Comparing the Temperature-Dependent Conductance of the Two Structurally Similar *E. coli* Porins OmpC and OmpF. *Biophys. J.* **2010**, *98*, 1830–1839.
- (15) Lopez, M. L.; Aguilera-Arzo, M.; Aguilera, V. M.; Alcaraz, A. Ion Selectivity of a Biological Channel at High Concentration Ratio: Insights on Small Ion Diffusion and Binding. *J. Phys. Chem. B* **2009**, *113*, 8745–8751.
- (16) Cruz-Chu, E. R.; Aksimentiev, A.; Schulten, K. Ionic Current Rectification through Silica Nanopores. *J. Phys. Chem. C* **2009**, *113*, 1850–1862.
- (17) Farauto, J.; Calero, C.; Aguilera-Arzo, M. Ionic Partition and Transport in Multi-ionic Channels: A Molecular Dynamics Simulation Study of the OmpF Bacterial Porin. *Biophys. J.* **2010**, *99*, 2107–2115.
- (18) Chimere, C.; Movileanu, L.; Pezeshki, S.; Winterhalter, M.; Kleinekathöfer, U. Transport at the Nanoscale: Temperature Dependence of Ion Conductance. *Eur. Biophys. J.* **2008**, *38*, 121–125.
- (19) Pages, J. M.; James, C. E.; Winterhalter, M. The Porin and the Permeating Antibiotic: A Selective Diffusion Barrier in Gram-Negative Bacteria. *Nature Rev. Microbiol.* **2008**, *6*, 893–903.
- (20) Romero-Ruiz, M.; Mahendran, K. R.; Eckert, R.; Winterhalter, M.; Nussberger, S. Interactions of Mitochondrial Presequence Peptides with the Mitochondrial Outer Membrane Preprotein Translocase TOM. *Biophys. J.* **2010**, *99*, 774–781.
- (21) de Zoysa, R.; Jayawardhana, D.; Zhao, Q.; Wang, D.; Armstrong, D.; Guan, X. Slowing DNA Translocation through Nanopores Using a Solution Containing Organic Salts. *J. Phys. Chem. B* **2009**, *113*, 13332–13336.
- (22) Mahendran, K. R.; Singh, P. R.; Arning, J.; Stolte, S.; Kleinekathöfer, U.; Winterhalter, M. Permeation through Nanochannels: Revealing Fast Kinetics. *J. Phys.: Condens. Matter* **2010**, *22*, 454131.
- (23) Cowan, S. W.; Schirmer, T.; Rummel, G.; Steiert, M.; Ghosh, R.; Pauptit, R. A.; Jansonius, J. N.; Rosenbusch, J. P. Crystal Structures Explain Functional Properties of Two *E. coli* Porins. *Nature* **1992**, *358*, 727–733.

- (24) Cowan, S. W.; Garavito, R. M.; Jansonius, J. N.; Jenkins, J. A.; Karlsson, R.; Konig, N.; Pai, E. F.; Pauptit, R. A.; Rizkallah, P. J.; Rosenbusch, J. P. The Structure of OmpF Porin in a Tetragonal Crystal Form. *Structure* **1995**, *3*, 1041–1050.
- (25) Tieleman, D. P.; Berendsen, H. J. A Molecular Dynamics Study of the Pores Formed by *Escherichia coli* OmpF Porin in a Fully Hydrated Palmitoylcholine Bilayer. *Biophys. J.* **1998**, *74*, 2786–2791.
- (26) Robertson, K. M.; Tieleman, D. P. Orientation and Interactions of Dipolar Molecules during Transport through OmpF Porin. *FEBS Lett.* **2002**, *528*, 53–57.
- (27) Im, W.; Roux, B. Ions and Counterions in a Biological Channel: A Molecular Dynamics Simulation of OmpF Porin from *Escherichia coli* in an Explicit Membrane with 1 M KCl Aqueous Salt Solution. *J. Mol. Biol.* **2002**, *319*, 1177–1197.
- (28) Humphrey, W. F.; Dalke, A.; Schulten, K. VMD – Visual Molecular Dynamics. *J. Mol. Graph.* **1996**, *14*, 33–38.
- (29) Phillips, J. C.; Braun, R.; Wang, W.; Gumbart, J.; Tajkhorshid, E.; Villa, E.; Chipot, C.; Skeel, R. D.; Kale, L.; Schulten, K. Scalable Molecular Dynamics with NAMD. *J. Comput. Chem.* **2005**, *26*, 1781–1802.
- (30) MacKerell, A. D., Jr.; Bashford, D.; Bellott, M.; Dunbrack, R. L., Jr.; Evanseck, J. D.; Field, M. J.; Fischer, S.; Gao, J.; Guo, H.; Ha, S.; et al. All-Atom Empirical Potential for Molecular Modeling and Dynamics Studies of Proteins. *J. Phys. Chem. B* **1998**, *102*, 3586–3616.
- (31) Morrow, T. I.; Maginn, E. J. Molecular Dynamics Study of the Ionic Liquid 1-*n*-Butyl-3-methylimidazolium Hexafluorophosphate. *J. Phys. Chem. B* **2002**, *106*, 12807–12813.
- (32) Jorgensen, W. L.; Chandrasekhar, J.; Madura, J. D.; Impey, R. W.; Klein, M. L. Comparison of Simple Potential Functions for Simulating Liquid Water. *J. Chem. Phys.* **1983**, *79*, 926–935.
- (33) Jorgensen, W.; Madura, J. Temperature and Size Dependence for Monte-Carlo Simulations of TIP4P Water. *Mol. Phys.* **1985**, *56*, 1381–1392.
- (34) Horn, H.; Swope, W.; Pitner, J.; Madura, J.; Dick, T.; Hura, G.; Head-Gordon, T. Development of an Improved Four-site Water Model for Biomolecular Simulations: TIP4P-Ew. *J. Chem. Phys.* **2004**, *120*, 9665–9678.
- (35) Abascal, J.; Vega, C. A General Purpose Model for the Condensed Phases of Water: TIP4P/2005. *J. Chem. Phys.* **2005**, *123*, 234505.
- (36) Longworth, L. The Mutual Diffusion of Light and Heavy Water. *J. Phys. Chem.* **1960**, *64*, 1914–1917.
- (37) Mahoney, M.; Jorgensen, W. Diffusion Constant of the TIP5P Model of Liquid Water. *J. Chem. Phys.* **2001**, *114*, 363–366.
- (38) Alberts, B.; Johnson, A.; Lewis, J.; Raff, M.; Roberts, K.; Walter, P. *Molecular Biology of the Cell*, 4th ed.; Garland Science: New York, 2002.

Chapter 4.3

Combing the effect of temperature and Ionic liquid in antibiotic permeation

We studied the conductance of ionic liquid in different OmpF mutants. The temperature-dependent transport of the ionic liquid 1-butyl-3-methylimidazolium chloride (BMIM-Cl) in OmpF and OmpF D113A mutant has been studied both theoretically and experimentally. An excellent agreement between applied field molecular dynamics simulation and conductance measurements is obtained for wild type OmpF and a reasonable agreement was obtained for the mutant D113A pore. Moreover, all-atom simulations depicted an atomistic analysis revealing molecular details of the rate-limiting ion interactions of the bulky cation with the OmpF channel. We performed conductance measurements on different other OmpF mutant in presence of BMIM Cl electrolyte as shown below in Table 1.

Table 1: Experimental and Simulation conductance of OmpF mutants in KCl and Ionic Liquid

Mutant	Mutated residues	KCL		Ionic Liquid	
		Experiment[nS]	Simulation[nS]	Experiment[nS]	Simulation[nS]
Wild Type	-----	4.0	3.0	0.6	0.5
D113A	Negative neutralized	3.9	NA	1.0	0.8
R132A	Positive Neutralized	4.0	NA	0.3	NA
D113N, E117Q	Two negative Neutralized	1.8	1.9	1.2	NA
R132A, R42A, R82A	Three Positive Neutralized	4.2	4.7	NA	NA

As mentioned earlier, the selectivity of the OmpF channel changes to anion selective in presence of the bulky BMIM Cl electrolyte. The movement of chloride ions dominates the ion conductance of the channel. When the negatively charged residues, D113 and E117, are neutralized inside the pore lumen, we observe an increased conductance in the OmpF mutant channel, which could be due to reduced electrostatic repulsion for the chloride ion. Similarly, when the positive charged residue R132 was neutralized, we observe a reduced conductance. The changes in conductance of ionic liquid at different mutants are very interesting and for better reasoning, MD simulation needs to be performed to get an insight on the transport mechanisms.

Ampicillin translocation through OmpF in Ionic Liquid

The interaction of ampicillin with OmpF in presence of 1M KCl and 1M BMIM Cl electrolyte solution has been previously shown. The kinetics of such translocation has been studied and the results show that the resident time of ampicillin inside the pore to be around 300 μ s for 1M KCl and 900 μ s for 1M BMIM Cl. The increase in ampicillin residence time inside the channel in presence of BMIM Cl could be due to the increased viscosity of the solution and the fact that the bulky cation needs to position itself in a defined orientation inside the channel which could hinder/slow ampicillin interaction. Another study by Mahendran et al. has shown that ampicillin translocation can be slowed down by lowering the temperature of the system. Here, we combined the two approaches and study the change in the ampicillin kinetics with the OmpF WT channel.

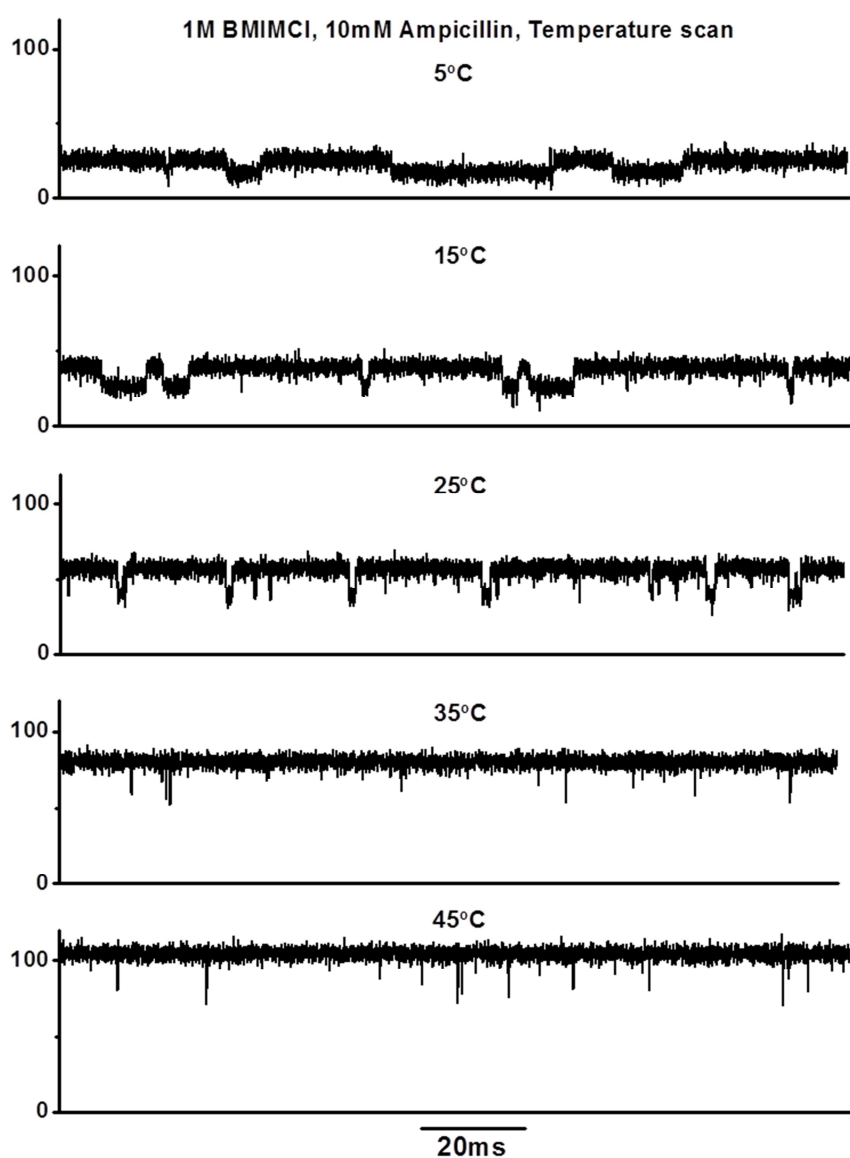


Figure 1: Ampicillin interaction with OmpF channel at different temperatures

Figure 1 shows the ion-current fluctuations of ampicillin with the OmpF channel at different temperature using 1M BMIM CL electrolyte solution. The residence time of ampicillin at different temperature was calculated and compared in presence of 1M KCl and 1M BMIM Cl solution as shown in **Figure 2**. Combining two approaches, we have been able to successfully slow down the ampicillin residence time from 300 μ s to 8ms at 5 $^{\circ}$ C using 1M BMIM Cl ionic liquid solution.

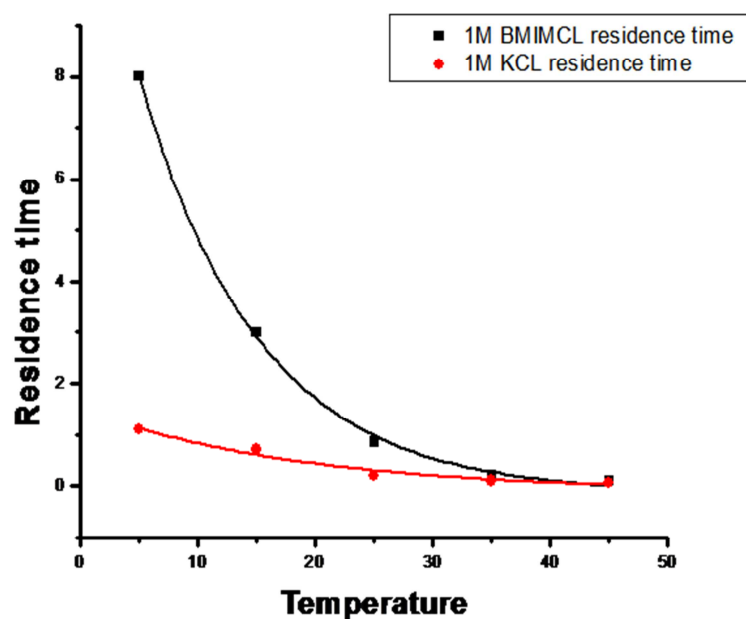


Figure 2: Residence time of ampicillin in OmpF channel using potassium chloride and ionic liquid BMIMCl

The interaction of ampicillin with the OmpF channel at different temperatures can be hypothesized to follow an Arrhenius behavior. Using the ampicillin residence time inside the channel, one can obtain the dissociation rate (K_d) of ampicillin inside the channel. The change of dissociation rate constant with changing temperature has been plotted following the Arrhenius equation as shown in **Figure 3**. The natural logarithm of dissociation rate follows a linear trend with $1/\text{Temperature}$, whose slope multiplied by the ideal gas constant gives us the E_a (effective energy barrier). As seen from the figure, the energy barrier for ampicillin permeation is higher in ionic liquid solution, 20 kcal/mol, compared to potassium chloride solution with energy barrier of around 14 kcal/mol.

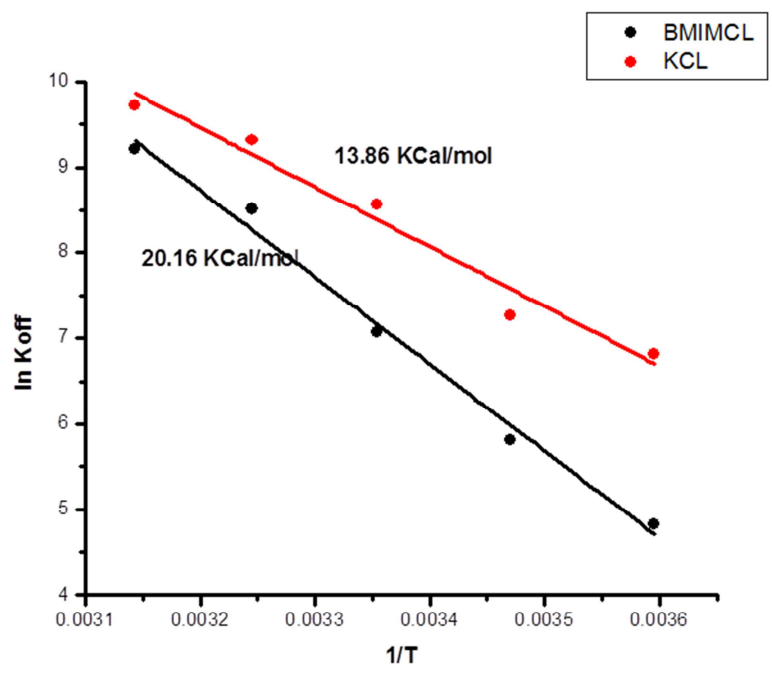


Figure 3: Energy barrier of ampicillin interaction with the OmpF channel in presence of KCL and BMIMCL

Chapter 5

Antibiotic interaction with the outer-
membrane porins of *Enterobacter*
aerogenes

This chapter consists of work performed under the European-IMI Translocation project. The chapter consists of a written manuscript that has not been submitted yet. In this publication, we characterize the three major porins from *Enterobacter aerogenes*, Omp35, Omp36 and Omp37. The interaction and kinetics of β -lactam antibiotics such as penicillins, carbapenems and cephalosporins with the three major porins have been studied using single channel electrophysiology. Comparative study on *in vitro* and *in vivo* experiments was performed. Antibiotic sensitivity conferred by Omp35, Omp36 and Omp37 was obtained using Minimum Inhibitory Concentration (MIC) assay and antibiotic killing rates. Our data shows a strong correlation between the *in vitro* single channel electrophysiology data with the *in vivo* biological assays.

Chapter 5.1

Manuscript in preparation

Individual Contribution:

Biophysical characterization, Single channel measurements and analysis, Composition of manuscript

Antibiotics interaction with the outer membrane porins of *Enterobacter aerogenes*

***Pratik Raj Singh*¹, Muriel Masi², Jean-Marie Pagès², Mathias Winterhalter¹**

¹ Department of Biophysics, Jacobs University Bremen, Bremen 28759, Germany

² UMR-MD1, Aix-Marseille Université IRBA, Faculté de Médecine, 27 Bd Jean Moulin, 13385
Marseille Cedex 05, France

Abstract

The permeation of water soluble molecules across the cell membrane is controlled by channel forming proteins present in the outer membrane of Gram-negative bacteria called porins. An adequate method to study properties of such channels is electrophysiology and in particular analyzing the ion current fluctuation in the presence of permeating solutes provides information on possible interactions with the channel surface. The major focus of this work is to characterize the interactions of several antibiotics through the *Enterobacter aerogenes* outer membrane porins. The outer membrane of *Enterobacter aerogenes* contain three major diffusion porins, Omp35, Omp36 and Omp37. Using single channel electrophysiology, interaction of β -lactam antibiotics such as penicillins, carbapenems and cephalosporins with each of the three different porins were measured and the kinetic rates of antibiotics interactions with the pore was obtained. In-vivo assays such as Minimum Inhibitory Concentration (MIC) assays and killing rates of antibiotics were performed to compare with the *in vitro* electrophysiology results.

Introduction

The outer-membrane of Gram-negative bacteria plays a major role in protecting the bacterial from various hostile environments yet ensuring a selective permeation of various essential nutrients into the cell cytoplasm [1–4]. Acting as a first line of defense, the hydrophobic asymmetric lipid bilayer is composed of Lipopolysaccharides in the outer-leaflet and phospholipids in the inner leaflet [5,6]. The selective exchange of hydrophilic solutes such as sugars and amino acids are modulated by the presence of water-filled channels in the outer-membrane called porins [7–9]. Additionally, various clinical and electrophysiological studies have shown porins to be a major pathway of several hydrophilic antibiotics such as β -lactams and fluoroquinolones [1,10–12].

In the outer-membrane of *Enterobacter aerogenes*, three major porins have been identified; Omp35, Omp36 and Omp37 [10,13]. As an opportunistic pathogen and a major causative agent of respiratory tract nosocomial infections, *Enterobacter aerogenes* generally exhibit high resistance to various antibiotics. The basis of multidrug resistance of *Enterobacter aerogenes* against various antibiotics was the high permeability barrier induced by down-regulation or mutations of these outer-membrane porins [2,13–15]. For instance, resistance to cefipime and cefpirome in *Enterobacter aerogenes* associated with mutations in Omp36 porin has been reported [14]. Similarly, resistance to carbapenems has been associated due to the loss of major porins Omp35 and Omp36 [16]. With increasing antibiotic resistance in *Enterobacter* species, the study of interaction of antibiotics with bacterial porins is important to understand the relationship between the structural properties of the protein and the uptake of these drugs.

We are interested in characterizing the three major proteins in *Enterobacter aerogenes* and obtaining detailed kinetics on the transport of various β -lactam antibiotics using single channel electrophysiology and biological assays such as Minimum Inhibitory Concentration (MIC) assay and antibiotic killing rates. The Omp35/Omp36 porins of *Enterobacter* have a high homology to the OmpF/OmpC porin from *E. coli* and OmpK35/OmpK36 from *Klebsiella pneumonia* [2,16]. The Omp35/36 porin is a trimer composed of 16 stranded β -barrels. The sequence homology also shows a conserved L3 loop in Omp35/Omp36 porins compared to the *E. coli* OmpF/OmpC suggesting common functional organization of the constriction region [14]. Similar to *E. coli*, the Omp35 porins is expressed at low osmolarity conditions whereas Omp36 porin is expressed at high-osmolarity conditions [13]. However, the Omp37 porin is known to be a quiescent pore and the functional activity of the pore is still

not know. Using single channel reconstitution of these purified channels in the lipid bilayer, important biophysical information such as conductance, selectivity and size of the channel can be obtained. Similarly, ion current fluctuations in presence of antibiotics can be used to obtain detailed kinetics interactions of the channel with the antibiotic. In this study, we show that all three outer-membrane porins provide a pathway for the permeation of hydrophilic β -lactam antibiotics. The kinetics of antibiotics interaction with the pores obtained using electrophysiology were compared with the MIC and antibiotic killing rates obtained *in vivo*, which showed a high degree of correlation.

Materials and Methods

Bacterial strains and media

Cloning was performed using *E. coli* JM109. Protein expression for purification was performed in porin-null *E. coli* BL21(DE3)omp8 (Δ lamB, ompF::Tn5, Δ OmpA, Δ OmpC). Bacteria were grown in Luria bertani (LB). Transformants were selected on LB-agar containing ampicillin, 100 μ g/ml.

Cloning of OMP genes and overexpression

The omp35, omp36 and omp37 genes were amplified, including their signal peptide sequences, from *E. aerogenes* ATCC15038 using PCR. Purified PCR products were cloned into the expression vector pColdIV (Takara) using the InFusion technique (Clontech). Plasmid constructs were confirmed by sequencing (Cogenics), then transformed into BL21(DE3)omp8. Transformants were grown to early exponential phase (OD₆₀₀ 0.4) in LB at 37°C and induced with 1 mM IPTG for 24 hours at 15°C. Expression was confirmed by SDS page and immunodetection.

Outer-membrane extraction

Induced cultures (1L) were harvested by centrifugation (10,000 x g, 20 min, 4°C). Bacterial cells were suspended in 50 mM sodium phosphate buffer (NaPi) pH 7.4 supplemented with 1 mM Pefabloc and submitted to pressure disruption by two passage through a cell disrupter. Total membranes were collected by ultracentrifugation (100,000 x g, 60 min, 4°C). Inner membrane proteins were solubilized with sodium lauryl sarcosinate, 0.15% w/v in NaPi buffer (50 mM, pH 7.4) for 30 min at room temperature. Outer membrane proteins were harvested by ultracentrifugation (100,000 x g, 60 min, 4°C).

Purification of porins

OM extracts were successively washed with 0.5% and 1% octyl-POE in NaPi (50 mM, pH 7.4). Omp36 was extracted by solubilization from OM preparations using 2% octyl-POE in the presence of 1 M NaCl at 37°C for 1 h with constant stirring. Insolubilized proteins were removed by ultracentrifugation (100,000 x g, 60 min, 4°C). Omp35 was by two rounds solubilization from OM preparations using 2% dodecyl-maltoside in the presence of 1 M NaCl. Supernatants were pooled and concentrated using Vivaspin 20 30K filters and NaCl was removed using Hi-Trap Desalting columns (GE Healthcare). Omp36 and Omp37 were purified using a Resource Q ion exchange column (GE healthcare). The column was equilibrated with NaPi, pH 7.4 containing 1.2% POE and 10 mM NaCl. Extracts were loaded at a flow rate of 2 ml/min, monitoring conductivity and OD at 280 nm at all times using Akta Explorer 10 apparatus. Omp36 and Omp35 were eluted from the column using a linear gradient (12 CV) from 10mM to 1M NaCl. Fractions containing Omp36 or Omp35 were verified by SDS-page.

Antibiotic susceptibility assays (MIC assay)

E. coli BZB1107 cultures harboring pTrc99A (empty vector) or recombinant plasmids with *omp35*, *omp36* or *omp37* were grown overnight in Muller Hinton II (MHII) broth in the presence of the appropriate antibiotic for plasmid maintenance (Amp, 100 µg/ml). The next morning, cells were diluted to 1/100 in fresh MHII medium in the presence of Amp and IPTG (100 µM) for protein induction and grown to an OD₆₀₀ of 0.4.

2-fold dilutions series of each antibiotic were prepared in 96-wells microplates and added to 200 µl aliquots of bacterial suspensions containing 2×10^5 cells in MHII. MICs were performed in the presence of IPTG (100 µM) to induce porin expression and β-lactamase quenchers tazobactam and clavulanic acid (4 µg/ml each), in the absence of ampicillin. The MIC was determined as the lowest concentration of each compound at which no visible growth was observed after 18 h of incubation at 37°C and were expressed in µg/ml. Each test was performed triplicate.

Antibiotic killing assays

E. coli BZB1107 cultures harboring pTrc99A (empty vector) or recombinant plasmids with *omp35*, *omp36* or *omp37* were grown as for MIC assays. Bacteria were induced and diluted in MHII to an OD₆₀₀ of 0.01 (~ 10⁷ cells/ml), then exposed to drugs added at a final concentration of × 2 MIC of bacteria expressing Omp35. 10-fold dilution series of exposed bacterial cultures were prepared every 15-30 min time for 90-180 min after drug addition. 10 µl of chosen dilutions were spread onto individual 37 mm-Petri dishes, with each containing 3 ml of MH-Amp-Agar. Plates were incubated at 37°C overnight. Dilutions that yielded between 20-100 colonies were counted for each time point, CFU/ml were calculated and plotted as the percentage decrease in CFU/ml compared to time 0. All experiments were performed in triplicate.

Single Channel electrophysiology

Montal and Muller technique was used to form artificial phospholipid bilayer using DphPC lipid (Avanti polar lipids) [17]. Reconstitution of protein in a phospholipid bilayer was performed as described previously [18]. A Teflon cell with an aperture of around 50-100 µm diameter was positioned between the two chambers of the cuvette. The first step was to prepaint the aperture with 1% hexadecane in hexane solution for formation of a stable bilayer. 1 M KCl, 10 mM MES, pH 6 was used as the electrolyte solution and added to both sides of the chamber. Ion current was detected by placing standard silver-silver chloride electrodes from WPI (World Precision Instruments) to each side of the chamber. Small amount of protein was adding to the *cis*-side of the chamber (side connected to ground electrode) and spontaneous channel insertion was usually obtained while stirring under applied voltage. After a successful single channel reconstitution, the *cis* side of the chamber was carefully diluted to remove remaining porins. Conductance measurements were performed using an Axopatch 200B amplifier (Molecular devices) in the voltage clamp mode. Signals were filtered by an on board low pass Bessel filter at 10 kHz and recorded with a sampling frequency of 50 kHz. Single channel analysis was used to determine the antibiotic binding kinetics. In a single-channel measurement the usual measured quantities are the duration of closed levels residence time (τ_c) and the number of blockage events per second per monomer (v_m). The rate constants of association k_{on} can be derived using the number of blockage events, $k_{on} = v_m / 3[c]$, where c is the antibiotic concentration. The rate constants of dissociation (k_{off}) were determined by averaging the $1/\tau_c$ values recorded over the whole concentration range [19].

Results

Characterization of OMPs from *Enterobacter aerogenes*

Purified Omp35, Omp36 and Omp37 proteins were reconstituted in artificial lipid membrane respectively. Successful reconstitution of porin was determined when ion current through the channel was observed in application of transmembrane voltage. Single channel conductance of all three major proteins at 1 M KCl, 10 mM MES, pH 6.0 was determined and is shown in **Table 1**. As expected, the conductance of Omp35 was related to its OmpF (4 nS in 1 M KCl) *E. coli* homologue representing a channel with a bigger pore opening [20]. Similarly, Omp36 also had a similar conductance with the OmpC *E. coli* homologue. The selectivity of both Omp35 and Omp36 has been measured before showing both of them to be cation-selective [13]. Interestingly, the quiescent Omp37 porin also had reasonably high conductance/pore size which could facilitate the permeation of large hydrophilic molecules similar to OmpF and OmpC.

Table 1: Single Channel conductance of OMPs of Enterobacter aerogenes

Porins	Conductance[nS]
Omp35	4.5±0.2
Omp36	3.0±0.1
Omp37	2.6±0.2

Each of the three outer-membrane channel has its own channel characteristics as shown in **Figure 1**. The Omp35 channel had a subtle change in the conductance with application of transmembrane voltage. The constant variation of channel conductance in two states could represent the constant movements of the loops. Similarly, Omp37 channel had a strong sub-conductance gating events present in the channel which also could be due to the movement of loops inside the channel. However, Omp36 channel was rather silent with small infrequent gating events observed.

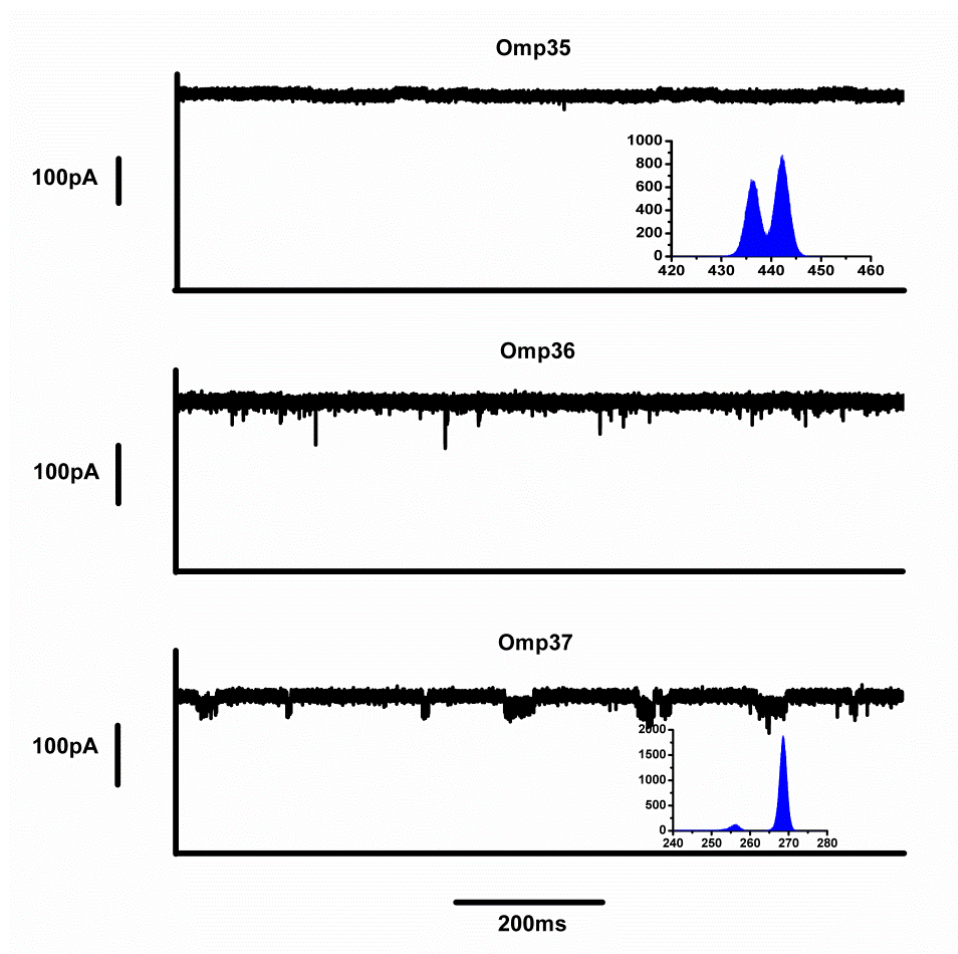


Figure 1: Single Channel characteristic of OMPs from Enterobacter aerogenes at 1 M KCl, 10 mM MES, pH 6.0

Interaction of Antibiotics

Different classes of hydrophilic β -lactam antibiotics such as penicillins, cephalosporins and carbapenems were selected to study the antibiotic-pore interactions. Interaction of antibiotic with the pore was represented by the transient blocking of ion current through the pore in presence of antibiotics. Interaction of antibiotics through the channel was usually observed in both positive and negative applied transmembrane potential. Also, increasing the concentration of antibiotics increased the interaction of antibiotics with the channel. **Table 2** shows the kinetic on-rates of different β -lactams with the three major OMPs.

Table 2: Association rates of antibiotic interactions with OMPs from *Enterobacter aerogenes*. Kinetics is measured at 1M KCl, pH 6.0 at either +100mV or -100mV applied potential. Red fonts indicate preferred pathway.

Antibiotics		K_{on} [$M^{-1}s^{-1}$]		
		Omp35	Omp36	Omp37
Carbapenems	Ertapenem	49000 ± 5000	7000 ± 500	1700 ± 2000
	Imipenem	1200 ± 100	2000 ± 200	1150 ± 100
	Meropenem	<i>Short events</i>	<i>Short events</i>	<i>Short events</i>
Cephalosporins	Cefepime	<i>Short events</i>	4400 ± 400	21000 ± 2000
	Cefotaxime	1750 ± 2000	9000 ± 1000	4000 ± 400
	Ceftobiprole	<i>Short events</i>	95000 ± 5000	60000 ± 5000
	Ceftazidime	900 ± 100	<i>No interaction</i>	2000 ± 200
Penicillins	Ticarcillin	17000 ± 1500	400 ± 50	150 ± 50
	Piperacillin	<i>No interaction</i>	<i>No interaction</i>	<i>No interaction</i>

The association rates of different antibiotics with the OMPs were compared to deduce the selective preference of the antibiotic pathway through the porins. In some antibiotics, such as meropenem and cefepime, association rates could not be analyzed using single channel analysis measurements as the interactions observed were very short ion fluctuation events which were not properly resolved by the instrument. However, power spectrum analysis showed an increased noise with increasing antibiotics concentration (**Supplementary Figure 1**), hinting that the molecules could be translocating through the channel very fast which was not resolved by our current instrumentation.

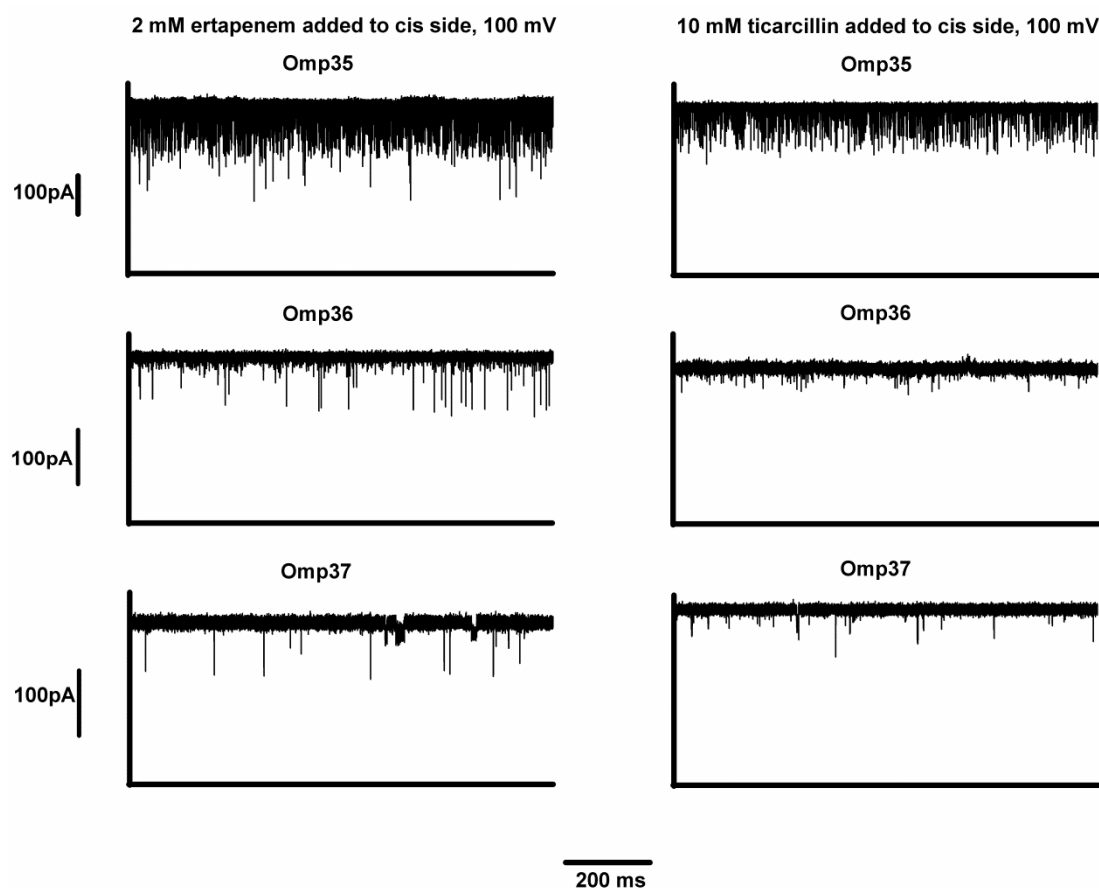


Figure 2: Ertapenem and ticarcillin interaction with OMPs of *Enterobacter aerogenes*. Experiment conditions: 1 M KCl, 10 mM MES, pH 6.0

The association rates in our results indicate that ertapenem and ticarcillin have a strong interaction with the Omp35 porin as shown in **Figure 2**. Similarly, cefotaxime and ceftobiprole have a stronger effect with Omp36 porins and cefepime has a strong interaction with the Omp37 porins. For other antibiotics such as imipenem and ceftazidime, there was no major difference in the association rates with all the three different OMPs. However, the interaction observed using *in vitro* single channel experiments does not imply successful translocation. *In vivo* MIC assays and antibiotics killing rates were performed to obtain further information on antibiotic permeation through the OMPs of *Enterobacter aerogenes*.

MIC assay

Minimum inhibitory concentration of antibiotics in presence of highly expressed Outer membrane *Enterobacter aerogenes* porins in porin null *E. coli* was measured as shown in Table 3.

Table 3: Minimum Inhibitory concentration of *E. coli* BZB1107 in empty and over expressed OMPs

	BZB1107 pTrc99A			
	Empty [$\mu\text{g/mL}$]	<i>omp35</i> [$\mu\text{g/mL}$]	<i>omp36</i> [$\mu\text{g/mL}$]	<i>omp37</i> [$\mu\text{g/mL}$]
Imipenem	0,5	0,125	0,125	0,125
Ertapenem	2	0,5	0,5	0,5
Meropenem	0,5	0,125	0,125	0,125
Cefepime	2	0,25	0,25	0,25
Ceftazidime	1	0,5	0,5	0,5
Aztreonam	0,25	0,25	0,25	0,25
Cefoxitin	16	16	16	16
Ceftriaxone	0,125	0,125	0,125	0,125
Piperacillin	64	1-0,5	2	2-1
Ticarcillin	>1024	16	512	256
Ceftarolin	2	0,063	0,125	0,125
Chloramphenicol	4	4	4	4

The minimum inhibitory concentration of antibiotics in presence of over expressed porins and in porin null strains determines the ability of antibiotics to translocate through the porins. There is a decrease in the MIC values (ranging from 4 to 8 folds) of imipenem, etrapenem, meropenem, cefepime, ceftazidime and ceftarolin from porin null strain compared to all the three over expressed OMPs. This shows that all the three OMPs in the *Enterobacter aerogenes* are involved in the susceptibility of these β -lactam antibiotics. Similar antibiotic interactions have been observed in *in vitro* single channel electrophysiology experiments in presence of these antibiotics. However, ticarcillin only showed a strong decrease in MIC in presence of over expressed Omp35 porin, whereas other antibiotics such as azteronam, cefoxitin, ceftriaxone and chloramphenicol did not show any changes in the MIC values.

Antibiotic Killing rates

The changes in MIC values of different antibiotics obtained in overexpressed OMPs do not give us the kinetics of antibiotic translocation into the bacteria. The efficacy of different

antibiotics in presence of over expressed porins were measured by exposing the bacterial cultures to double their inhibitory concentration of antibiotics and counting the percentage decrease in the colony forming units over time. This gives us a value to compare the rate of antibiotic entry in each of the three different porins (where MIC values were similar). We selected the antibiotics that showed susceptibility in presence of the over expressed porins for our antibiotics killing rates. First we selected two cephalosporins, cefepime and ceftaroline (similar to ceftobiprole both are 5th generation cephalosporins) and measured the antibiotic killing rate as shown in **Figure 3**.

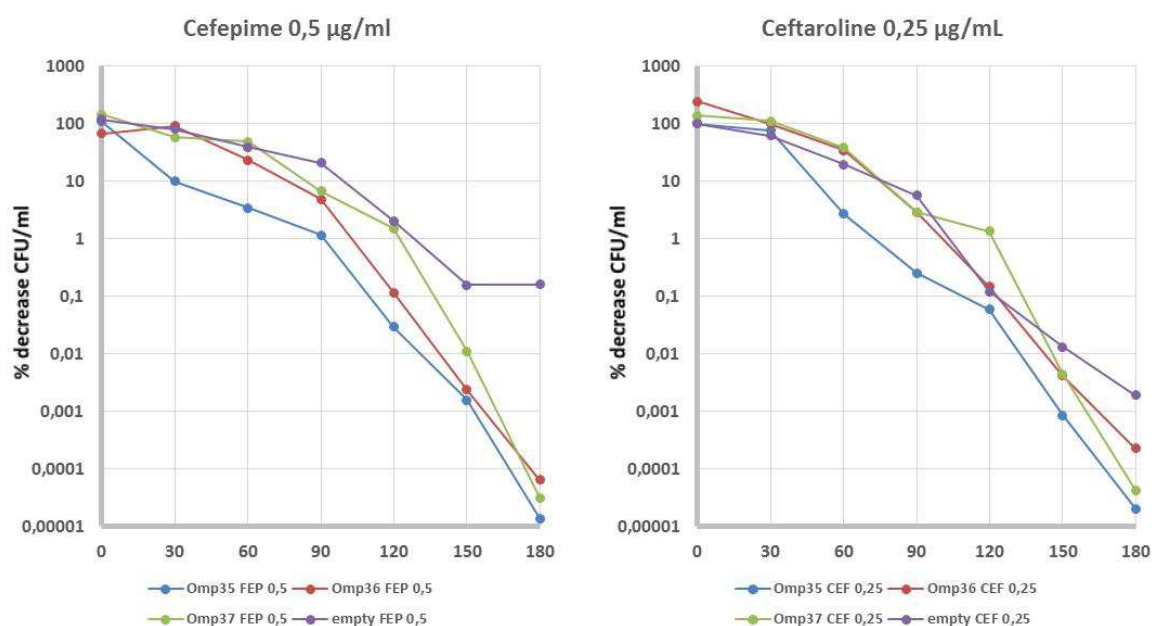


Figure 3: Antibiotic killing rates for cefepime and ceftaroline

In both the cases, we observe that there is no drastic change in the antibiotic killing rate of *E. coli* containing both over expressed porins and empty vectors. This indicates that there are other mechanism or other porins present in the bacteria that could facilitate the translocation of both the cephalosporins. Thus, we cannot directly correlate the results obtained using single channel electrophysiology and antibiotic killing rates.

In the next experiment, we selected three carbapenems; imipenem, meropenem and ertapenem, and measured their killing rates as shown in **Figure 4**. Here, we observe that *E. coli* with no over expressed porins (empty) still survive in the presence of these carbapenems. In all three carbapenems, Omp35 seems to be more effective for permeation of antibiotics. *In vitro* electrophysiology experiment show that ertapenem has a higher association rate in Omp35 porin compared to the other two porins. However, in case of imipenem, the association rates of antibiotics are very similar in all three cases and does not compare well

with the *in vivo* data. This could be due to the fact that all interacting events that we observe *in vitro* are not actual translocation events and only binding with the channel.

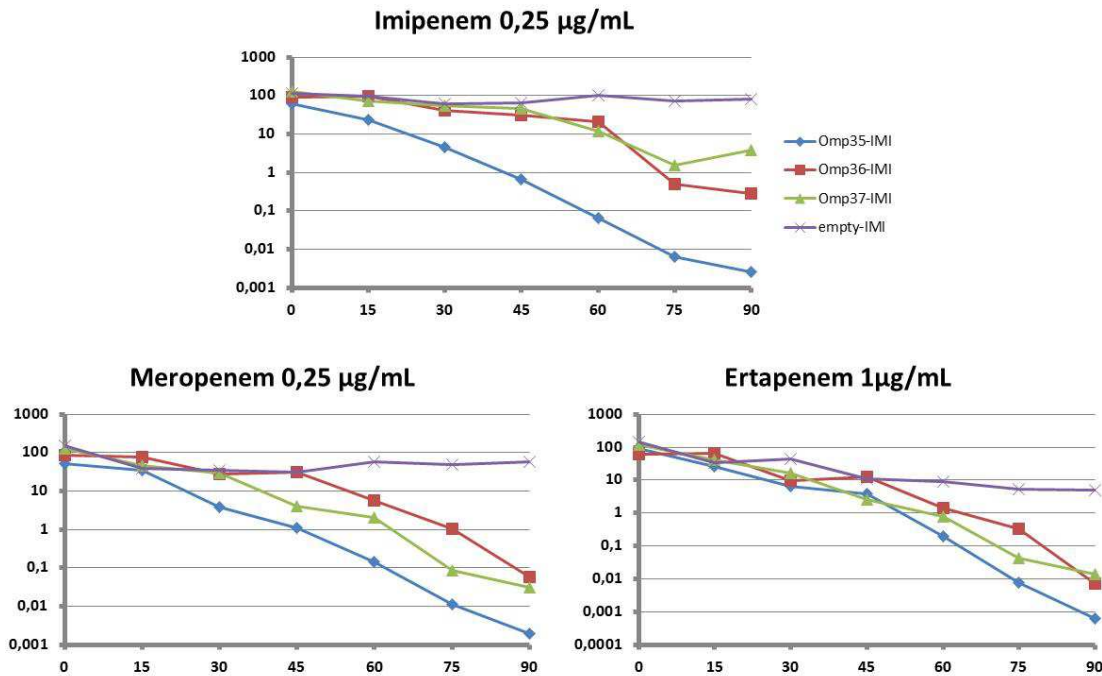


Figure 4: Antibiotic killing rates for carbapenems

Finally, we performed similar experiments with ticarcillin, where we compared *in vivo* experiment with *in vitro*. The results show an astounding similarity, where we only observe antibiotic killing in presence of over expressed Omp35 porin. In empty vector and over expressed Omp36 and Omp37, we observed no decrease in the colony forming units (Figure 5). Similar results have been obtained in MIC assay and electrophysiology experiments.

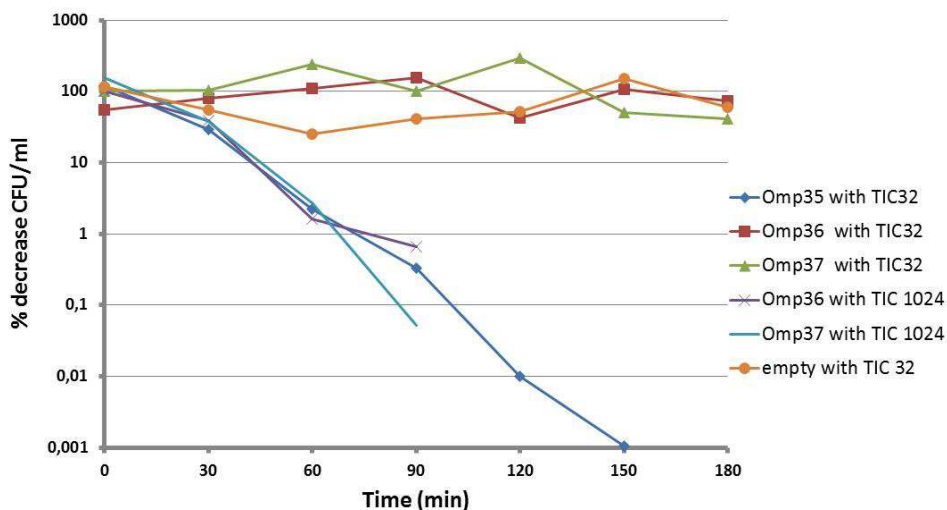


Figure 5: Antibiotic killing rates for ticarcillin

Discussion

In this study we focus on the role of *Enterobacter aerogenes* OMPs in the permeation of hydrophilic β -lactam antibiotics. Three major porins, Omp35, Omp36 and Omp37 are present in *Enterobacter aerogenes* and regulation and expression of these OMPs varies depending on several external conditions of the bacteria such as osmolarity, temperature and the growth mediums [10,15]. Additionally, regulations of these pores also occur in response to antibiotic stress where the bacteria reduce its outer-membrane permeability to gain resistance [14,16]. For example, *Enterobacter aerogenes* clinical strains with imipenem resistance showed decreased outer membrane permeability with lower porin expression [21]. Similar behavior has been observed in *Klebsiella pneumoniae* where resistance to ertapenem antibiotic was obtained by loss of OmpK36 porin [22]. Since different environmental and external factors alter the expression level of different OMPs in the outer membrane of *Enterobacter aerogenes*, it is very important to study, understand and compare the molecular details of antibiotic permeation with all the three major OMPs.

In vitro single channel electrophysiology and *in vivo* MIC and antibiotic killing rates have been performed to reveal the interactions of clinically relevant β -lactam antibiotics with the porins. Similar studies have been carried out on porins from *E. coli* and *Providencia stuartii* [23–25]. Using ion-current fluctuation analysis, we can measure two kinetics parameters, number of events of interaction and the time of interaction (residence time). Using these values, and assuming the antibiotic-pore interaction similar to enzyme-substrate complex, one can measure the kinetic rate of association (k_{on}) and rate of dissociation (k_{off}). In almost all the measurements, the residence time of antibiotics inside the channel was 100 μ s or lower, which is close to the instruments time resolution limit. However, sharp differences were observed with the kinetic on-rate or association rate of antibiotics with the channel. Experimental values obtained for k_{on} and k_{off} with respect to the concentration gradient of antibiotics used in our experiment (μ M to mM) yields $k_{off} \gg k_{on} \Delta[c]$. This simplifies the flux measured, $J = k_{on} \Delta[c]/2$, such that increasing the on-rate directly results in the increase in translocation of antibiotics [26]. Thus, in our experiments, we use the kinetic on-rate (association rate) to compare the permeability of different antibiotics with the three different outer-membrane porins. Similarly, over expression of OMPs of *Enterobacter aerogenes* in *E. coli* BZB1107 was performed to obtain MIC and antibiotic killing rates of antibiotics.

Comparative studies show that ticarcillin has a very strong correlation with *in vitro* and *in vivo* experiments. Electrophysiology experiments showed a very high association rate of ticarcillin with Omp35 ($17000 \text{ M}^{-1}\text{s}^{-1}$) compared to the Omp36 and Omp37 porins, while MIC assay showed a strong decrease only in the presence of over-expressed Omp35 porin. Antibiotic killing rate performed indicate a rapid decrease in colony forming units in over expressed Omp35 porins while the others had no effects on bacterial survival. This indicates that ticarcillin favor the pathway of Omp35 porin compared to Omp36 and Omp37 porins. In contrast, piperacillin did not show any interaction with the porins during electrophysiology measurements. The presence of bulky side chains of the piperacillin molecule could be the reason of such reduced/no interaction [27].

However, no correlation was observed with *in vivo* and *in vitro* experiments with respect to the cephalosporins. The antibiotics killing rates performed with cephalosporins; cefepime and ceftaroline, indicate that the empty *E. coli* BZB1107 also show similar decrease in colony forming rate compared to *E. coli* BZB1107 with over expressed OMPs. This point out that there could be another permeation pathway of these cephalosporins through the outer membrane and thus our result based on these measurements is not optimized to perform comparative studies. The experiment needs to be repeated in a different *E. coli* strain such that no cephalosporin effect can be observed in presence of empty vector.

In contrast, *in vivo* MIC and antibiotic killing rates performed on carbapenems implies, Omp35 to be the favorable porin for antibiotic permeation. While, electrophysiology experiments revealed Omp35 ($49000 \text{ M}^{-1}\text{s}^{-1}$) having a strong interaction to ertapenem; imipenem on the other hand showed no distinct differences between the OMPs. Two major drawback of the single channel electrophysiology technique includes, *i*) not being able to distinguish binding from translocation; which could be the case in imipenem where all current fluctuation events are not actual translocation events, and *ii*) not being able to resolve fast translocation events; such as for cefepime and meropenem where determining kinetic constants were not possible due to temporal resolution of the instrument. Improving the technique for better time resolution and performing liposome swelling assays to distinguish translocation should be considered for the next steps.

The permeability of different antibiotic molecules is usually based on their chemical and physical properties such as size, charge and hydrophobicity [10,28,29]. Previous studies indicate that the rate of permeation of zwitterionic antibiotics is higher through general diffusion porins as opposed to the anionic antibiotics [30]. However, in our experiments we

observed that negatively charged antibiotics such as ticarcillin and ertapenem have a stronger interaction with the Omp35 porin compared to the zwitterionic imipenem. Similar results are obtained for Omp36 porin with negatively charged cefotaxime and Omp37 with negatively charged cefepime. The exact reason for such interactions is unclear and to have a better understanding of the atomistic detail of antibiotic-porin interaction, we must further our research using molecular dynamics simulations.

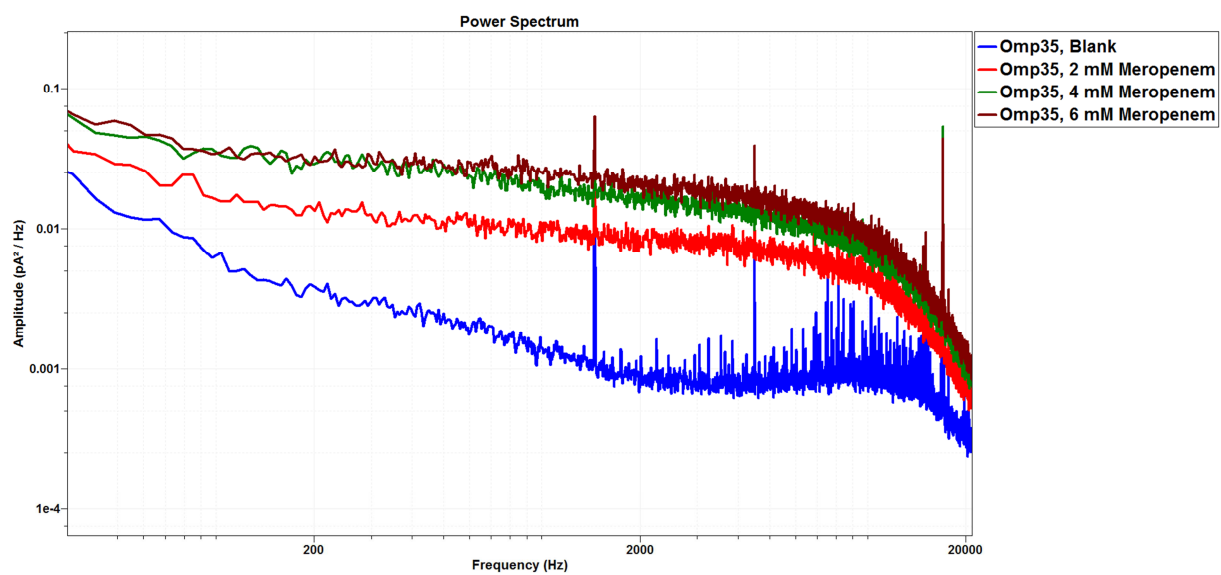
References:

- [1] R.E. Hancock, The bacterial outer membrane as a drug barrier., *Trends Microbiol.* 5 (1997) 37–42. doi:10.1016/S0966-842X(97)81773-8.
- [2] H. Nikaido, Molecular basis of bacterial outer membrane permeability revisited., *Microbiol. Mol. Biol. Rev.* 67 (2003) 593–656.
- [3] R. Benz, K. Bauer, Permeation of hydrophilic molecules through the outer membrane of gram-negative bacteria. Review on bacterial porins., *Eur. J. Biochem.* 176 (1988) 1–19.
- [4] R. Benz, *Bacterial Cell Wall*, Elsevier, 1994. doi:10.1016/S0167-7306(08)60422-6.
- [5] T.J. Silhavy, D. Kahne, S. Walker, The bacterial cell envelope., *Cold Spring Harb. Perspect. Biol.* 2 (2010) a000414. doi:10.1101/cshperspect.a000414.
- [6] A.H. Delcour, Outer Membrane Permeability and Antibiotic Resistance, *Biochim Biophys Acta.* 1794 (2009) 808–816. doi:10.1016/j.bbapap.2008.11.005.
- [7] A.H. Delcour, Solute uptake through general porins., *Front. Biosci.* 8 (2003) d1055–71.
- [8] R. Benz, ed., *Bacterial and Eukaryotic Porins*, Wiley-VCH Verlag GmbH & Co. KGaA, Weinheim, FRG, 2004. doi:10.1002/3527603875.
- [9] G.E. Schulz, Bacterial porins: structure and function, *Curr. Opin. Cell Biol.* 5 (1993) 701–707. doi:10.1016/0955-0674(93)90143-E.
- [10] C.E. James, K.R. Mahendran, A. Molitor, J.-M. Bolla, A.N. Bessonov, M. Winterhalter, et al., How beta-lactam antibiotics enter bacteria: a dialogue with the porins., *PLoS One.* 4 (2009) e5453. doi:10.1371/journal.pone.0005453.
- [11] Y. Kobayashi, I. Takahashi, T. Nakae, Diffusion of beta-lactam antibiotics through liposome membranes containing purified porins., *Antimicrob. Agents Chemother.* 22 (1982) 775–80.

- [12] H. Nikaido, Prevention of drug access to bacterial targets: permeability barriers and active efflux., *Science*. 264 (1994) 382–388. doi:10.1126/science.8153625.
- [13] C. Bornet, N. Saint, L. Fetnaci, M. Dupont, A. Davin-Régli, C. Bollet, et al., Omp35, a new *Enterobacter aerogenes* porin involved in selective susceptibility to cephalosporins., *Antimicrob. Agents Chemother.* 48 (2004) 2153–8. doi:10.1128/AAC.48.6.2153-2158.2004.
- [14] A. Thiolas, C. Bornet, A. Davin-Régli, J.M. Pagès, C. Bollet, Resistance to imipenem, cefepime, and ceftazidime associated with mutation in Omp36 osmoporin of *Enterobacter aerogenes*, *Biochem. Biophys. Res. Commun.* 317 (2004) 851–856. doi:10.1016/j.bbrc.2004.03.130.
- [15] R.N. Charrel, J.M. Pagès, P. De Micco, M. Mallea, Prevalence of outer membrane porin alteration in beta-lactam-antibiotic-resistant *Enterobacter aerogenes*., *Antimicrob. Agents Chemother.* 40 (1996) 2854–8.
- [16] H. Yigit, G.J. Anderson, J.W. Biddle, C.D. Steward, J.K. Rasheed, L.L. Valera, et al., Carbapenem resistance in a clinical isolate of *Enterobacter aerogenes* is associated with decreased expression of OmpF and OmpC porin analogs., *Antimicrob. Agents Chemother.* 46 (2002) 3817–3822. doi:10.1128/AAC.46.12.3817-3822.2002.
- [17] M. Montal, P. Mueller, Formation of bimolecular membranes from lipid monolayers and a study of their electrical properties., *Proc. Natl. Acad. Sci. U. S. A.* 69 (1972) 3561–3566. doi:10.1073/pnas.69.12.3561.
- [18] P.R. Singh, I. Bárcena-Urbarri, N. Modi, U. Kleinekathöfer, R. Benz, M. Winterhalter, et al., Pulling peptides across nanochannels: resolving peptide binding and translocation through the hetero-oligomeric channel from *Nocardia farcinica*., *ACS Nano*. 6 (2012) 10699–707. doi:10.1021/nn303900y.
- [19] E.M. Nestorovich, C. Danelon, M. Winterhalter, S.M. Bezrukov, Designed to penetrate: time-resolved interaction of single antibiotic molecules with bacterial pores., *Proc. Natl. Acad. Sci. U. S. A.* 99 (2002) 9789–94. doi:10.1073/pnas.152206799.
- [20] C. Danelon, A. Suenaga, M. Winterhalter, I. Yamato, Molecular origin of the cation selectivity in OmpF porin: Single channel conductances vs. free energy calculation, *Biophys. Chem.* 104 (2003) 591–603. doi:10.1016/S0301-4622(03)00062-0.
- [21] C. Bornet, A. Davin-Régli, C. Bosi, J.M. Pages, C. Bollet, Imipenem resistance of *enterobacter aerogenes* mediated by outer membrane permeability., 2000.
- [22] G.A. Jacoby, D.M. Mills, N. Chow, Role of β -Lactamases and Porins in Resistance to Ertapenem and Other β -Lactams in *Klebsiella pneumoniae*, *Antimicrob. Agents Chemother.* 48 (2004) 3203–3206. doi:10.1128/AAC.48.8.3203-3206.2004.
- [23] E. Hajjar, K.R. Mahendran, A. Kumar, A. Bessonov, M. Petrescu, H. Weingart, et al., Bridging timescales and length scales: from macroscopic flux to the molecular mechanism of antibiotic diffusion through porins., *Biophys. J.* 98 (2010) 569–75. doi:10.1016/j.bpj.2009.10.045.

- [24] E. Hajjar, A. Bessonov, A. Molitor, A. Kumar, K.R. Mahendran, M. Winterhalter, et al., Toward screening for antibiotics with enhanced permeation properties through bacterial porins., *Biochemistry*. 49 (2010) 6928–35. doi:10.1021/bi100845x.
- [25] Q.-T. Tran, K.R. Mahendran, E. Hajjar, M. Ceccarelli, A. Davin-Regli, M. Winterhalter, et al., Implication of porins in beta-lactam resistance of *Providencia stuartii*., *J. Biol. Chem.* 285 (2010) 32273–81. doi:10.1074/jbc.M110.143305.
- [26] H. Weingart, M. Petrescu, M. Winterhalter, Biophysical characterization of in- and efflux in Gram-negative bacteria., *Curr. Drug Targets*. 9 (2008) 789–96.
- [27] C. Danelon, E.M. Nestorovich, M. Winterhalter, M. Ceccarelli, S.M. Bezrukov, Interaction of zwitterionic penicillins with the OmpF channel facilitates their translocation., *Biophys. J.* 90 (2006) 1617–1627. doi:10.1529/biophysj.105.075192.
- [28] H. Nikaido, Prevention of drug access to bacterial targets: permeability barriers and active efflux., *Science*. 264 (1994) 382–8.
- [29] H. Nikaido, E.Y. Rosenberg, Effect on solute size on diffusion rates through the transmembrane pores of the outer membrane of *Escherichia coli*., *J. Gen. Physiol.* 77 (1981) 121–35.
- [30] F. Yoshimura, H. Nikaido, Diffusion of beta-lactam antibiotics through the porin channels of *Escherichia coli* K-12., *Antimicrob. Agents Chemother.* 27 (1985) 84–92.

Supplementary Figure 1: Power spectrum density of meropenem interaction with Omp35 porin



Chapter 6

Summary and future outlooks

Summary of the thesis

Porins play an intrinsic role in the transport of essential hydrophilic nutrients into the cell cytoplasm, which is hijacked by the antibiotics as a pathway to diffuse into the cell. However, under antibiotic stress, bacteria are able to obtain resistance by altering its permeability by either lowering the expression of porins or mutating some important residues of the porin. Structural and functional features of porins play an important role in determining the translocation of antibiotics through the porin. In this thesis, we have investigated antibiotic permeation through the outer-membrane porins of Gram-positive and Gram-negative bacteria. Using interdisciplinary approaches such as electrophysiology, molecular dynamics and *in vivo* assays we have been able to obtain significant knowledge on how the antibiotic molecule utilize the porins to penetrate the hydrophobic cell envelope. To summarize, we have listed some of our key outcome,

1. We report the first study of antibiotic interaction through the outer-membrane of Gram-positive bacterial porins using single channel electrophysiology. Strong interaction of positively charged antibiotics such as amikacin and kanamycin was observed with the channel, which we assume to be present due to many negatively charged residues inside the *Nocardia farcinica* porin that could be acting as an affinity site. The significance of affinity site/charged residues inside the channel was verified by performing mutational studies, where we mutated 24 negatively charged residue inside the channel to neutral residues. As expected, the mutant pore later showed a lower association rate and flux of the positive charged antibiotic through the channel.
2. An interesting example of a negatively charged antibiotics, ertapenem showing strong interaction with the negatively charged *Nocardia farcinica* porin was also observed. Experimentally we showed that the interaction in this case was not due to charge but rather hydrophobic interactions present with the antibiotic and the pore. Nonetheless, could the presence of negatively charged residue inside the channel hinder the flux of such negatively charged molecule? Using the mutant porin we were able to obtain the depleted kinetics and flux of ertapenem in the wide type porins compared to the mutant porin. Affinity sites of the antibiotic with the channel is not charge-specific, however the presence of charge in the pathway can alter the diffusion of antibiotics through the channel.
3. The presence of ions in the buffer solution or the physiological solution can alter the basis of permeation. Using only an additional magnesium ion in the solution, we

observe the change in kinetics of enrofloxacin interaction with the *E. coli* OmpF porin. Interdisciplinary approach using molecular dynamics simulation show that the presence of magnesium inside the channel reverses the charge inside the pore lumen making it more favorable for enrofloxacin to permeate into the channel.

4. We report a simple solution to a problem of temporal limitation of the instrument. Using bulky salt solutions such as ionic liquids, we were able to slow the permeation of ampicillin through the OmpF channel, hence increasing the time resolution. Combining existing techniques such as lowering the temperature, we were able to slow down permeation as much as 20 times.
5. Finally, we performed a comparative study on antibiotic permeation through the outer-membrane of *Enterobacter aerogenes*. The kinetics of various β -lactam antibiotics with the three major porins Omp35, Omp36 and Omp37 were obtained and compared with in-vivo assay. The preferred porin pathway of different antibiotics were analyzed, however atomistic detail of interaction can only be obtained using molecular dynamics simulations. The limiting step is the crystal structure of the protein which is still not obtained.

Future outlook

Nocardia farcinica: Tool for DNA sequencing

The bloom of nanopore based DNA sequencing started in the 1990s [1]. This technique follows the coulter counter principle, where the analyte to be detected hinders the flow of the ions through the nanopore hence disrupting the ion current [2]. The characteristic change in the ion current in presence of the analyte can be used to characterize the molecule. For instance, the differences in the ion current shifts observed with the passage of different nucleotides, A, T, G and C, can be used to distinguish each of them. Currently single molecule sequencing using nanopore utilizes two different approaches to obtain such nanometer sized pores; *i*) biological nanopore such as protein channels and *ii*) solid state nanopore formed by drilling a hole into a solid substrate [3,4]. Both these biological nanopores and solid state nanopore have advantages and disadvantages. Solid state nanopores are usually easy to tune based on size, selectivity, dimensions, and structure. Solid state

nanopores are easy to handle and are highly stable compared to biological nanopores [5]. However, the atomic level precisions obtained in modifying biological nanopores are incomparable to the modification performed on solid state nanopores [6,7]. Even though the results obtained from biological nanopores are precise and reproducible, currently only two biological nanopores, MspA porin from *Mycobacterium smegmatis* and α -hemolysin toxin from *Staphylococcus aureus*, exists that is used for DNA sequencing. We introduce a possible new porin from *Nocardia farcinica*, with homology to MspA, which can be a new biological pore for DNA sequencing [8,9].

The biological nanopore suitable for DNA sequencing should have a pore constriction of size larger than the hydrodynamic radii of the DNA molecule. The constriction region of the pore should be as narrow as possible to distinguish individual DNA bases. The pore should be robust and should not gate at higher voltages. Most of the Gram-negative beta-barrel porins have small pore sizes that have high intrinsic gating making them an unsuitable candidate. The porin from *Nocardia farcinica* satisfies most of the required characteristics making it a promising new candidate for DNA sequencing. However, the major drawback of this porin is its gating behavior. Similar to the wild type MspA channel, *Nocardia farcinica* porins also gates rapidly in application of positive potentials [10,11]. Thus, modification of amino acid sequences in loops of the protein to reduce channel gating is the first task at hand. We have performed several mutations and screened them based on their gating behavior; however we have not been successful so far. The future task would be to perform In-vitro Transcription Translation (IVTT) method to generate a larger pool of mutant and screen them to obtain a highly stable channel. We would also like to obtain a crystal structure of the channel so that modification of the channel would be feasible.

References

- [1] H. Bayley, L. Jayasinghe, Functional engineered channels and pores (Review)., *Mol. Membr. Biol.* 21 (n.d.) 209–20. doi:10.1080/09687680410001716853.
- [2] M. GRAHAM, The Coulter principle: foundation of an industry, *J. Assoc. Lab. Autom.* 8 (2003) 72–81. doi:10.1016/S1535-5535(03)00023-6.
- [3] M. Wanunu, Nanopores: A journey towards DNA sequencing., *Phys. Life Rev.* 9 (2012) 125–58. doi:10.1016/j.pprev.2012.05.010.

- [4] I.M. Derrington, T.Z. Butler, M.D. Collins, E. Manrao, M. Pavlenok, M. Niederweis, et al., Nanopore DNA sequencing with MspA., *Proc. Natl. Acad. Sci. U. S. A.* 107 (2010) 16060–16065. doi:10.1073/pnas.1001831107.
- [5] S.W. Kowalczyk, A.Y. Grosberg, Y. Rabin, C. Dekker, Modeling the conductance and DNA blockade of solid-state nanopores., *Nanotechnology.* 22 (2011) 315101. doi:10.1088/0957-4484/23/8/088002.
- [6] L.Q. Gu, O. Braha, S. Conlan, S. Cheley, H. Bayley, Stochastic sensing of organic analytes by a pore-forming protein containing a molecular adapter., *Nature.* 398 (1999) 686–690. doi:10.1038/19491.
- [7] N. Ashkenasy, J. Sánchez-Quesada, H. Bayley, M.R. Ghadiri, Recognizing a single base in an individual DNA strand: A step toward DNA sequencing in nanopores, *Angew. Chemie - Int. Ed.* 44 (2005) 1401–1404. doi:10.1002/anie.200462114.
- [8] C. Kläckta, P. Knörzer, F. Riess, R. Benz, Hetero-oligomeric cell wall channels (porins) of *Nocardia farcinica*, *Biochim. Biophys. Acta - Biomembr.* 1808 (2011) 1601–1610. doi:10.1016/j.bbamem.2010.11.011.
- [9] P.R. Singh, I. Bárcena-Uribarri, N. Modi, U. Kleinekathöfer, R. Benz, M. Winterhalter, et al., Pulling peptides across nanochannels: resolving peptide binding and translocation through the hetero-oligomeric channel from *Nocardia farcinica*., *ACS Nano.* 6 (2012) 10699–707. doi:10.1021/nn303900y.
- [10] E.A. Manrao, I.M. Derrington, A.H. Laszlo, K.W. Langford, M.K. Hopper, N. Gillgren, et al., Reading DNA at single-nucleotide resolution with a mutant MspA nanopore and phi29 DNA polymerase, *Nat. Biotechnol.* 30 (2012) 349–353. doi:10.1038/nbt.2171.
- [11] J. Huff, M. Pavlenok, S. Sukumaran, M. Niederweis, Functions of the periplasmic loop of the porin MspA from *Mycobacterium smegmatis*., *J. Biol. Chem.* 284 (2009) 10223–10231. doi:10.1074/jbc.M808599200.